Towards the Development of an Adaptive Compression System

by

Mahan Rahimi

B.Sc., Azad University, Science and Research Branch, 2009

Thesis Submitted in Partial Fulfillment of the
Requirements for the Degree of
Master of Applied Science

in the
School of Engineering Science
Faculty of Applied Sciences

SIMON FRASER UNIVERSITY

Fall 2016

Approval

Name:	**Mahan Rahimi**
Degree:	**Master of Applied Science**
Title:	***Towards the Development of an Adaptive Compression System***
Examining Committee:	**Chair:** Mr. Steve Whitmore Senior Lecturer

Dr. Carlo Menon, P.Eng.
Senior Supervisor
Professor

Dr. Andrew Blaber
Supervisor
Professor

Dr. Kouhyar Tavakolian
Supervisor
Assistant Professor
University of North Dakota

Dr. Victoria Claydon
Internal Examiner
Associate Professor
Department of Biomedical Physiology and Kinesiology

Date Defended/Approved: November 16th, 2016

Ethics Statement

The author, whose name appears on the title page of this work, has obtained, for the research described in this work, either:

a. human research ethics approval from the Simon Fraser University Office of Research Ethics

or

b. advance approval of the animal care protocol from the University Animal Care Committee of Simon Fraser University

or has conducted the research

c. as a co-investigator, collaborator, or research assistant in a research project approved in advance.

A copy of the approval letter has been filed with the Theses Office of the University Library at the time of submission of this thesis or project.

The original application for approval and letter of approval are filed with the relevant offices. Inquiries may be directed to those authorities.

Simon Fraser University Library
Burnaby, British Columbia, Canada

Update Spring 2016

Abstract

Regarded as the mainstay for treatment of venous insufficiency and the associated complications, compression therapy aims at assisting with venous return through the exertion of external pressure on the limbs. Compression is achieved by medical bandages and stockings, which hold promise only during supine and walking conditions, or mechanical pumps, which are usually bulky and limited to non-ambulatory use. Hence, the purpose of this study was to develop an improved compression system that eliminates the flaws of the existing products. To attain this goal, a motorized compression bandage was designed that takes advantage of force-sensing resistors (FSRs®) to exert reproducible, controlled pressure on the lower extremities. The performance of the device in enhancing venous return was explored in a pilot experiment, wherein graded lower body negative pressure (LBNP) was employed as a surrogate of standing erect. The results revealed a significant reduction in the mean cardiovascular changes to LBNP.

Keywords: venous insufficiency; compression therapy; adaptive compression system; force-sensing resistor; lower body negative pressure

In dedication to my dearest family;
my mother, Hamideh,
my father, Mahmoud,
my brother, Rahan,
my grandmother, Maman Shamsi,
and my aunt, Azhideh,
for their unconditional love and support!

Acknowledgements

First and foremost, I would like to express my heartfelt thanks to my senior supervisor, Dr. Carlo Menon, for his full support and incredible patience throughout my research. His help has been invaluable to me on both an academic and a personal level, for which I am truly grateful. Without the shadow of a doubt the friendly environment of the MENRVA Research Group, wherein I had a chance to work, is the result of Dr. Menon's great management skills.

I wish to offer my deepest gratitude to my supervisor, Dr. Andrew Blaber, whose vast knowledge, understanding, and expertise considerably added to my graduate experience. His office door was always open to me whenever I ran into a problem in my research. I would not have been abled to finish this thesis without Dr. Blaber's great encouragement, such as his motivational words on the history of creating the WD-40 spray after the 40th attempt!

I am extremely thankful to the past and present members of the MENRVA Research Group, and my fellow graduate students at the Simon Fraser University for their selfless support throughout my study. They were always there to take time out of their busy schedules and lend me a hand in any possible way; from giving technical advice to volunteering for lengthy experiments. The friendships we developed will last a lifetime and I will always appreciate the goodwill we share.

I take this opportunity to extend my sincere appreciation to Dr. Kouhyar Tavakolian for serving on my committee and teaching me how to run the human experiments; Mr. Malcom Tremblay for his tremendous assistance with data collection; Dr. Farzad Khosrow-Khavar for his generous help in processing the seismocardiography signals; Mr. Abdollah Safari and Mr. Ian Bercovitz for statistical consulting on the project; Dr. Victoria Claydon for her helpful scientific advice; and the Heart Force Medical Inc. for kindly providing me with the instruments required to record seismocardiograms.

And last but not least, I would like to express my eternal recognition towards my parents and my brother for their unwavering love through my entire life. Without them I would be nothing.

Table of Contents

List of Tables

List of Figures

List of Acronyms

AC	Aortic Valve Closure
ACS	Adaptive Compression System
ANOVA	Analysis of Variance
AO	Aortic Valve Opening
AVCG	Adjustable Velcro™ Compression Garment
AVP	Ambulatory Venous Pressure
CHP	Capillary Hydrostatic Pressure
CO	Cardiac Output
COP	Capillary Osmotic Pressure
CVD	Chronic Venous Disease
CVI	Chronic Venous Insufficiency
CVP	Central Venous Pressure
DBP	Diastolic Blood Pressure
DSI	Dynamic Stiffness Index
DVT	Deep Vein Thrombosis
ECG	Electrocardiogram
FS	Full Scale
FSR®	Force-sensing Resistor
HPG	Hydrostatic Pressure Gradient
HR	Heart Rate
IFHP	Interstitial Fluid Hydrostatic Pressure
IFOP	Interstitial Fluid Osmotic Pressure
IPC	Intermittent Pneumatic Compression
LBNP	Lower Body Negative Pressure
LVET	Left Ventricular Ejection Time
MAP	Mean Arterial Pressure
NASG	Non-Pneumatic Anti-Shock Garment
OH	Orthostatic Hypotension
OI	Orthostatic Intolerance
OPG	Osmotic Pressure Gradient
PP	Pulse Pressure
RT	Recovery Time

SBP	Systolic Blood Pressure
SCG	Seismocardiogram
SCI	Spinal Cord Injury
SD	Standard Deviation
SEM	Standard Error of the Mean
SSI	Static Stiffness Index
SV	Stroke Volume
SVR	Systemic Vascular Resistance
TPR	Total Peripheral Resistance
WUWHS	World Union of Wound Healing Societies

Chapter 1. **Introduction**

1.1. Motivation

Compression therapy, or exertion of external pressure on the limbs, provides a means to manage a variety of conditions in different medical and non-medical fields, including, but not limited to, orthostatic[1] intolerance (OI) [1, 2], hemorrhage [3, 4], burn scars [5, 6], post-surgical operation [7, 8, 9], athletic enhancement [10, 11, 12], and aviation and post-spaceflight complications [13, 14, 15]. In addition to the foregoing, leg venous insufficiency is one of the most common indications for compression therapy [16]. Venous insufficiency, which is a high-prevalence medical condition among the adult population, especially the elderly, pregnant women and spinal cord injury (SCI) patients, is characterized by retrograde blood flow in the lower extremities, and occurs due to poor blood circulation and elevated venous pressure in the lower limbs [17]. It can be accompanied with troublesome and unpleasant complications that negatively affect the quality of life, including varicose veins, excessive leg swelling, heaviness in the legs, pain, skin changes, and hypotension-induced fainting to name a few [18].

The efficacious role of compression therapy in management of venous disorders and its sequelae has been the subject of numerous studies [19, 20, 21, 22]. It has been illustrated that applying an external pressure on the lower limbs assists with fluid volume control and blood circulation in the legs by impacting the arterial, venous, and lymphatic function [22, 23]. Bandages, stockings, and mechanical pumps are among the popular remedies to tackle venous insufficiency. Although being used extensively, compression devices, in their current form, have some drawbacks and limitations. Mechanical pumps are usually bulky and do not allow for ambulatory use [16]. Bandages do not serve to sustain pressure over time, necessitating frequent re-applications, and putting them on correctly is highly clinician dependent [20]. Compression

[1] relating to or caused by an upright posture

hosiery, whose efficacy has been proven to change with anthropometric variables, are difficult to don, and neither these products nor medical wraps are beneficial during passive orthostasis [1]. Also, exertion of recommended pressure levels and their sustenance is of utmost importance for successful treatment, entailing the need for monitoring and controlling the pressure beneath the compression garments [24]. However, sub-bandage pressure, which is determined by garment properties, geometry of the limb, skill of the operator, and physical activities and posture of the user [20, 25], generally is not measured by the clinicians. The health care practitioners count on their own experience while applying compression bandages, and the manufacturers' listed class of compression when prescribing compression hosiery [26, 27]. After the recipients of compression products are discharged from medical centers, it is not feasible to continuously assess the changes in sub-bandage pressure that might occur due to movements and changing physiological conditions of the lower extremities, such as swelling reduction. The shortcomings of the existing compression systems attenuate the optimal performance of these devices and reduces their efficacy.

All these reasons together served as a compelling demand for this study to design, fabricate, and evaluate a novel smart pressure garment which eliminates the aforesaid problems to the greatest extent possible. Herein, an adaptive compression system (ACS) is proposed that is able to deliver different pressure types and can be used during stasis and ambulation. It is basically a garment with a motorized lacing system, in which rotation of a motor is exploited to tighten and loosen a piece of fabric for delivering pressure in sustained and intermittent modes. The ACS is equipped with flexible force-sensing resistors (FSRs®), which are used as a means to measure the exerted pressure on the skin. The sub-bandage pressure feedback from the FSRs® is beneficial not only in generating reproducible, controlled compression levels, but also in making the device adaptive to physiological changes.

1.2. Objectives of Study

This study pursues two goals:

1. To develop a new adaptive compression system for ameliorating venous stasis and enhancing venous return; this objective has two aspects:
    - To design and fabricate a prototype of a motorized compression bandage
    - To assess and calibrate FSRs® for the purpose of interface pressure measurement

2. To evaluate the performance of the new device during orthostasis through the implementation of pilot experiments, in which graded lower body negative pressure (LBNP) is used to simulate passive standing

Each of the objectives is elaborately discussed in the following chapters.

1.3. Thesis Layout

The remainder of this thesis is organized as follows:

Chapter 2 reviews the literature on venous insufficiency definition, along with its epidemiology, venous system physiology and pathophysiology, and treatment options; concept and terminology of compression therapy, physiological effect of external pressure the lower extremities, and current compression modalities; and finally, measuring the pressure on the skin beneath compression garments.

Chapter 3 consists of two main parts: the first section explains the design and fabrication process of the proposed compression system, and the second section provides in depth information regarding usability of force-sensing resistors in monitoring sub-bandage pressure and describes the path towards their calibration.

Chapter 4 presents the experiments conducted to assess the performance of the newly designed compression device.

Chapter 5 is devoted to statistical analyses, discussion of the results gained from the experimental evaluation of the designed system, and the limitations.

Chapter 6 summarizes the thesis, draws conclusions by highlighting the main findings, and outlines future work.

Chapter 2. **Literature Review**

2.1. Chronic Venous Disorder in Lower Extremities

2.1.1. Clinical Definition and Epidemiology

Chronic venous disease (CVD) and chronic venous insufficiency (CVI) are general terms used to describe a number of conditions that occur in the leg tissue due to poor blood circulation in the veins of lower extremities. In these disorders, blood pools in the legs and if left untreated, it leads to venous hypertension, or elevated blood pressure[1] in the veins. Progressive pathologies, the severity of which varies from slight asymptomatic venous valve incompetence to chronic leg ulcerations, may arise as a consequence of this longstanding high pressure [28]. Some of these abnormalities are depicted in Figure 2-1.

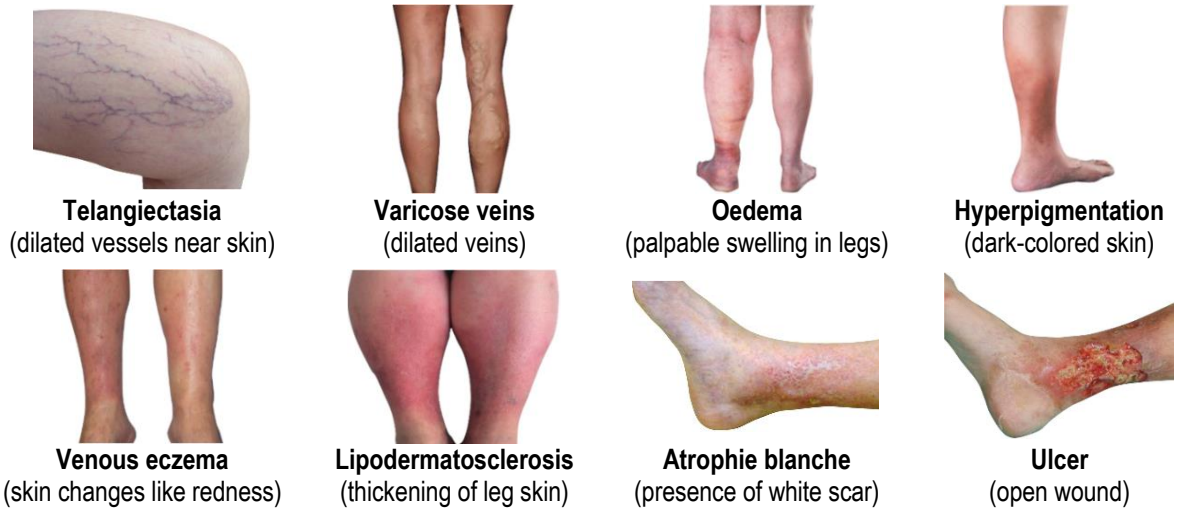

Figure 2-1 Clinical manifestations of chronic venous disorder[2]

[1] Blood pressure is the force per unit area applied by blood against the vessels walls, and is usually expressed in millimeters of mercury (mmHg).

[2] adapted from [98]

While CVD includes functional (e.g. venous reflux) or morphological (e.g. venous dilation) abnormalities of the venous system, CVI refers to only functional defects with more advanced pathologies such as the ones with skin changes, oedema, or ulcers. Accordingly, varicose veins in the absence of skin changes, or uncomplicated varicose veins, are usually excluded from CVI definition [17, 29]. Some of the established risk factors of CVD and CVI are deep vein thrombosis[1] (DVT), heredity, obesity, pregnancy, smoking, aging, female gender, inactivity, and extended periods of standing or sitting. Individuals who have these risk factors are more likely than other people to develop the disease [28, 29].

CVD and CVI result in significant discomfort and reduce the quality of life of individuals who suffer from them [30, 31]. Dyscosmesis (loss of positive body image), feeling of heaviness in the legs, persistent pain, leg cramps, pruritus or itching, hemorrhage, and progressive skin changes are examples of the complications with which sufferers grapple [18]. In a study by Phillips et al., 73 patients with moderate to severe chronic leg ulcer were interviewed and the psychological, social, and financial consequences of the disease were investigated [32]. Leg ulcers were found to have a substantial socioeconomic impact on the lives of patients, and proven to be correlated with time lost from work, job loss, and adverse financial effects. Among the participants, 81% reported mobility impairment, with leg swelling as its main cause, 58% thought that ulcer care was onerous, and 68% believed that the disorder had a negative emotional influence on their lives, such as anger, depression, social isolation, and loss of positive self-image to name a few [32].

In developed countries, approximately 5% and 1% of the adult population suffer from CVI and venous ulcers, respectively [33]. According to the Medical Advisory Secretariat (MAS) of Canada, 0.12-0.32% of the general population, which translates to approximately 50,000 to 500,000 Canadians, have lower limb ulcers [19]. Roughly 2.5 million individuals are affected by leg ulcers in the United States, and as the population ages, the possibility of the spread of the disease increases [32]. In a cross-sectional study of a random sample of 1566 subjects, aged 18 to 64 years old, from the general population in Edinburgh, Scotland, Evans et al. found that varicose veins were present in 40% of men and 32% of women. Telangiectasia was present in more than 80% of all subjects, and the prevalence of CVI was 9% in men and 7% in women [28].

[1] Thrombosis is the formation of blood clots in the blood vessels, and deep vein thrombosis refers to blood clot formation in the deep veins of the legs.

In addition to reducing life quality and causing social impairment, chronic venous disorders can be very costly to the health care system due to prevalence, morbidity, and chronicity [31, 33, 34]. In European countries, 1-2% of the health care budget is dedicated to venous disease [33]. A four-week costing study by Friedberg et al. on individuals with lower leg ulcers in a large urban centre in Ontario, Canada, estimated that 192 people receiving care would annually consume $1 million in nursing-care services and $260,000 in wound-care supplies [35]. In the United Kingdom, between £294 to £650 million a year is allocated to venous disease; in the United States, treatment costs are estimated to be $2.5 to $3 billion and a loss of 2 million work days per year [36].

The statistics that have been presented thus far, portray venous disorder as a debilitating and costly socioeconomic concern to the health care system and necessitate taking action towards disease management. To successfully cope with this situation, first it is vital to study the physiology of leg vascular system and understand the mechanisms that underlie its pathologies.

2.1.2. Venous System Physiology in Lower Limbs

Circulatory System

The circulatory system is a closed network designed to circulate blood throughout the body for the purpose of exchanging substances such as gas, nutrients, hormones, and waste products; and is comprised of the cardiovascular and lymphatic systems. The heart and three types of blood vessels, i.e. arteries, veins, and capillaries, make up the cardiovascular network. The heart, which is basically a hollow muscular organ with four chambers, is the core of this network and is responsible for delivering blood to the entire body. In the cardiovascular network, the arterial system transports high-pressure blood from the heart to the organs and tissues through the thick-walled arteries and arterioles; and the venous system carries low-pressure blood back to the heart via the thin-walled veins and venules. The connection between the arterioles and venules happens at an interweaving network of microscopic capillaries called capillary beds. The cardiovascular system is composed of two distinct circulatory paths: pulmonary circulation, the circuit through the lungs where oxygen-depleted blood releases carbon dioxide and absorbs oxygen; and systemic circulation, the circuit through the rest of the body for delivering oxygen-rich blood to the organs and tissues, and draining oxygen-poor blood and wastes [37]. A simplified illustration of the cardiovascular network is presented in Figure 2-2.

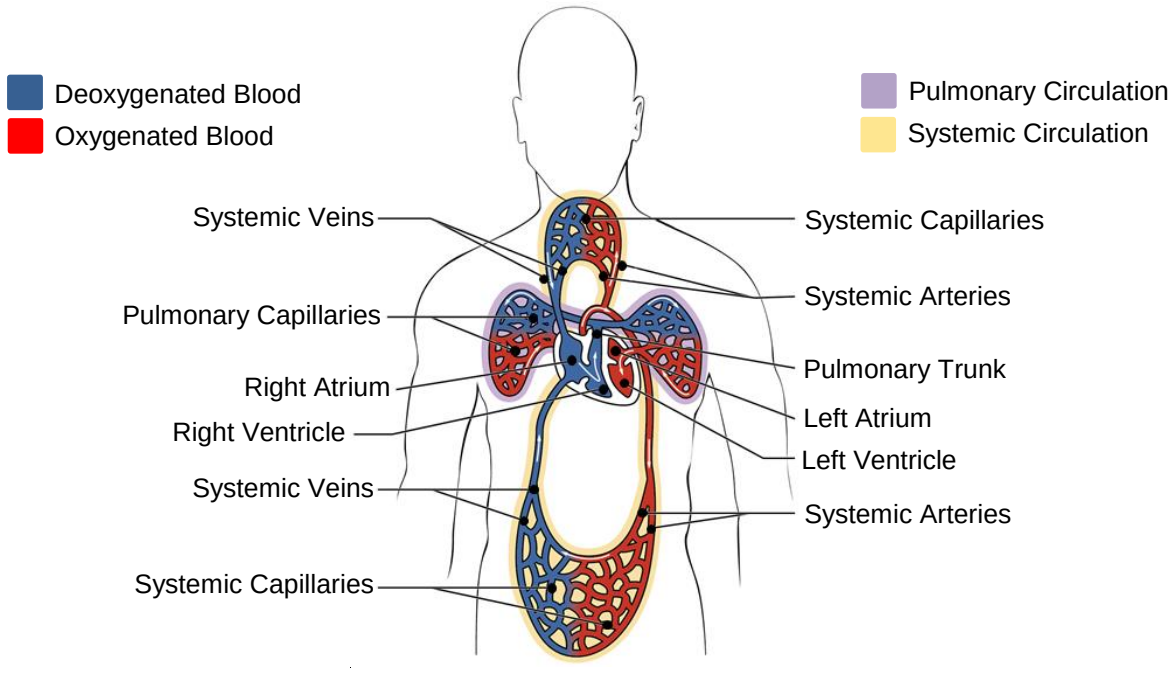

Figure 2-2 Schematic illustration of human cardiovascular system[1]

Transcapillary Exchange

Gas and metabolite movement between the blood and tissue interstitial fluid[2] occurs at capillary beds and is known as transcapillary exchange. The net transcapillary fluid exchange is dependent on physical factors including the hydrostatic[3] and osmotic[4] pressure gradients across the vessel wall, and the wall's nature in terms of permeability; and is described by the Starling relationship:

$$J_v = K_{f,c}[(P_c - P_i) - \sigma(\pi_c - \pi_i)] \qquad \text{Equation 2.1}$$

In Equation 2.1, J_v is the rate of net transcapillary fluid movement, $K_{f,c}$ is the capillary filtration coefficient (hydraulic conductance), P_c and P_i are the opposing capillary and interstitial fluid hydrostatic pressures, σ is the osmotic reflection coefficient (a measure of the permeability of the

[1] adapted from [99]

[2] Tissue interstitial fluid is one of the three components of the extracellular fluid that fills the spaces between body cells and blood vessels (also known as the tissue spaces).

[3] Hydrostatic pressure is defined as the force applied by a fluid pressing against a wall due to the weight of the fluid column.

[4] The difference in solvent concentration between the two sides of a semi-permeable membrane creates osmotic pressure.

capillary barrier to the proteins responsible for generating the osmotic pressure), and π_c and π_i are the opposing capillary and interstitial fluid osmotic pressures. If J_v is positive, fluids move from capillaries into interstitial spaces and filtration happens, and if negative, fluids enter vessels from interstitial spaces and reabsorption takes place [37].

The balance of the pressures inside and outside the capillaries determines whether filtration or reabsorption occurs [38]. The capillary hydrostatic pressure (CHP), which is generated by the pumping action of the heart, is usually at its highest level at the arteriolar end of the capillary bed (around 35 mmHg). Along the length of the vessel, CHP drops and reaches its lowest value at the capillary's venous end (around 16 mmHg). The interstitial fluid hydrostatic pressure (IFHP) is difficult to measure and its reported values vary from small positive to small negative numbers. Accordingly, it is assumed that IFHP is equal to 0 mmHg all along the capillaries. Caused by the presence of large proteins in the blood, the capillary osmotic pressure (COP) is around 26 mmHg and pulls fluid from interstitial spaces into the vessels. Opposing COP is the interstitial fluid osmotic pressure (IFOP) that normally has very small values between 0.1 and 5 mmHg [39]. It is assumed that IFOP equals 1 mmHg during the rest of the current report. The interaction of hydrostatic and osmotic pressures in the capillaries results in a positive pressure gradient across the vessel wall at the arteriolar end of the capillary beds that drives fluid out, i.e. outward flow or filtration; and a negative pressure gradient at the venular end that leads to an inwards fluid movement, i.e. reabsorption. In general, there exists a net filtration across the capillary walls. In other words, capillary filtration exceeds reabsorption. The resulting excess fluid gets returned to the venous bloodstream through the permeable vessels of the lymphatic system [39]. Figure 2-3 schematically depicts fluid exchange at the capillary beds.

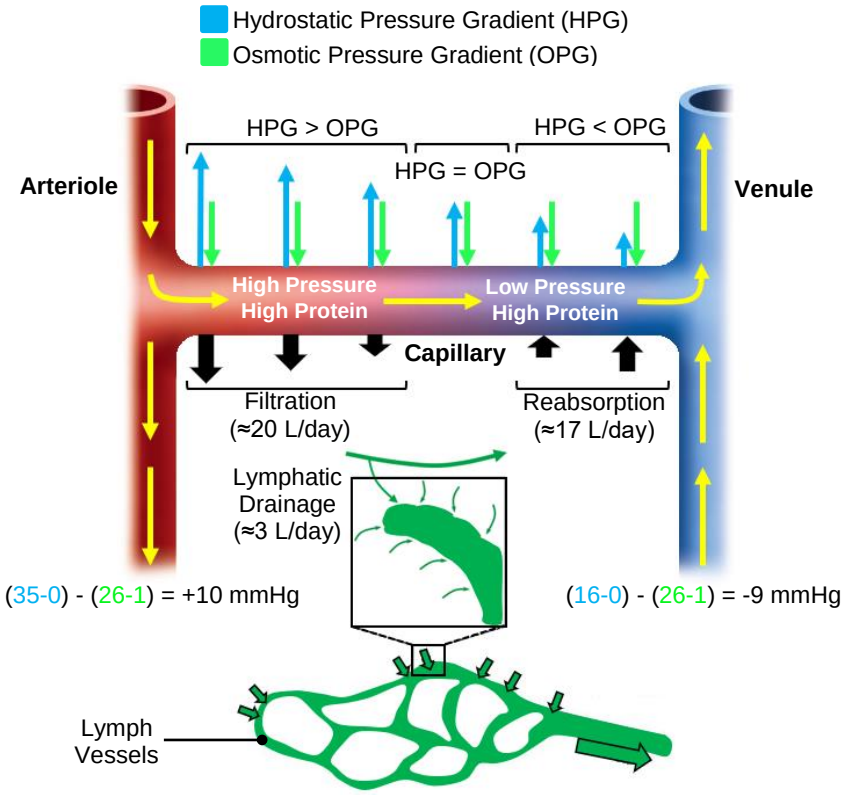

Figure 2-3 Dynamics of transcapillary fluid exchange
Yellow arrows indicate the direction of blood flow.

Venous Return Terminology and Mechanism

With every heart beat, oxygenated blood gets pumped from the left side of the heart to the organs and tissues of the body, which need oxygen to function. After exchanging gas and nutrients at the capillary beds, deoxygenated blood returns to the right side of the heart through the veins. These veins can be classified into the following three main categories in the lower limbs [37]:

- **Deep Veins:** Surrounded by muscles, the deep venous system is located at the central axis of the leg next to the arteries and include the iliac, femoral, popliteal, peroneal, and tibial veins. These veins account for the major part of venous blood return to the heart (approximately 90% to 95%).
- **Superficial Veins:** These vessels, including small and great saphenous veins, can be found in the subcutaneous tissue near the surface of the skin and serve to return around 5-10% of oxygen-poor blood to the heart. Superficial veins eventually drain into the deep veins.
- **Perforator Veins:** The perforating veins connect deep and superficial venous networks.

The venous system of the legs is schematically shown in Figure 2-4.

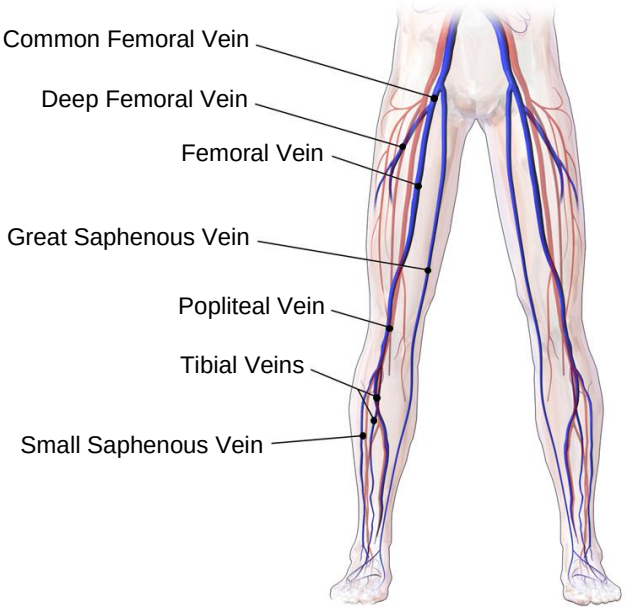

Figure 2-4 Anatomy of leg veins[1]

Blood flow is generated by the contraction of the left ventricle[2] of the heart and is determined by pressure gradient and resistance. Poiseuille's law can be employed to describe the flow of blood through the vessels [40]:

$$Q = \frac{\Delta P}{R} \qquad \text{Equation 2.2}$$

In Equation 2.2, Q is blood flow, ΔP is the pressure difference between any two points, and R is the resistance or impediment to flow encountered by blood as it moves through the body. Resistance is directly proportional to the vessel length and blood viscosity, and inversely proportional to the fourth power of vessel radius [40].

Upon heart contraction, blood is forced into the systemic circulation with the highest pressure in the arteries. When blood flows through the vasculature pathway, its pressure declines, especially in the arterioles with small radii and high resistance [37]. The variation of different components of blood pressure in the vessels of the body is depicted in Figure 2-5.

[1] reproduced from [100]

[2] A ventricle is one of the two lower chambers of the heart. The right ventricle receives deoxygenated blood from the right atrium and pumps it to the lungs or pulmonary circulation. The left ventricle receives oxygenated blood from the left atrium and pumps it to the systemic circulation.

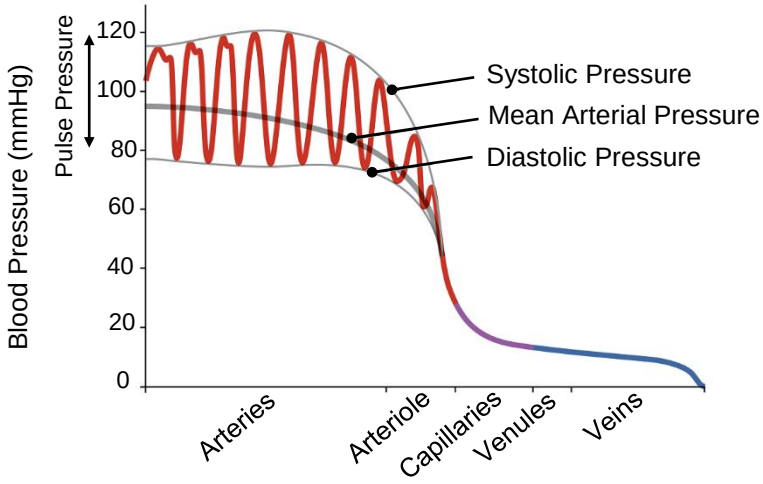

Figure 2-5 Blood pressure throughout different vessels[1]

In Figure 2-5, systolic blood pressure (SBP) is the maximal pressure as blood gets ejected from the left ventricle, diastolic blood pressure (DBP) is the lowest pressure just before ventricular ejection when the left ventricle is relaxing and refilling, pulse pressure (PP) is defined as the difference between SBP and DBP, and mean arterial pressure (MAP) represents the average blood pressure in the arteries or the driving force for blood flow in the arterial system. The following relationships are used to calculate PP and MAP [37]:

$$PP = SBP - DBP \qquad \text{Equation 2.3}$$

$$MAP \cong DBP + \frac{1}{3}PP \qquad \text{Equation 2.4}$$

The blood volume traveling back to the right atrium[2] of the heart from the systemic veins is referred to as *venous return*. Poiseuille's law (Equation 2.2) can be used to determine the rate of blood flow everywhere in the body. When applying this equation to venous return, the pressure gradient is the difference between mean systemic pressure (≈7 mmHg) and right atrial pressure (≈0 mmHg), and the resistance equals systemic vascular resistance (SVR), or total peripheral resistance (TPR), through the entire systemic circulation excluding the pulmonary vasculature. As shown in Figure 2-5, by the time oxygen-depleted blood reaches the venous system, it is so low in pressure, and consequently, the pressure gradient between the veins and heart is insignificant (<10 mmHg). However, according to Poiseuille's law, pressure difference is one of

[1] adapted from [99]

[2] An atrium is one of the two upper chambers of the heart for blood collection. The right atrium collects deoxygenated blood from the systemic circulation and pumps it to the right ventricle. The left atrium receives pulmonary oxygenated blood from the lungs and forces it to the left ventricle.

the main determinants of continuous flow, therefore veins require further assistance to push blood back to the heart; particularly in the standing position while counteracting the force of gravity. There are a number of factors that function concomitantly towards promoting venous return, among which vein valves and skeletal muscle pump are two of the key parameters [41]:

- **Vein Valves:** Unlike arteries, veins contain one-way valves with two thin flaps of tissue that prevent backflow by allowing venous blood to move only in one direction from the superficial venous network to the deep veins, and from the feet towards the heart.
- **Skeletal Muscle Pump:** The calf muscle pump is responsible for approximately 90% of venous return from the legs to the heart, in addition to the negative pressure produced in the thorax because of inhalation [23]. As indicated previously, some of the veins are located within muscle groups. During locomotion, such as walking and running, the veins undergo alternative compression and decompression upon calf muscle contraction and relaxation. When muscles contract, they exert pressure on the veins by squeezing them. As a result of pressure increase, blood flows upwards, opening the one-way valves superior to the contracting muscles. Concurrently, the valves inferior to the muscles get closed and stop blood from flowing backwards [37]. The simultaneous action of the skeletal muscle pump and vein valves enhances venous return, which is schematically presented in Figure 2-6.

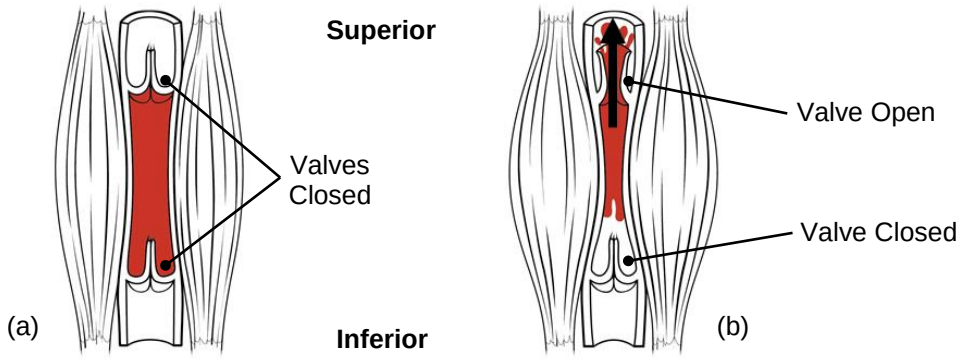

Figure 2-6 Mechanism of action of calf muscle pump and vein valves in venous return[1]
(a) muscle relaxed, (b) muscle contracted
The black arrow indicates blood flow direction.

[1] reproduced from [99]

Role of Venous Return in Regulating Blood Pressure

As highlighted in the previous section, Equation 2.4 presents the mean arterial pressure as a function of diastolic and pulse pressures. The MAP can also be determined by cardiac output (CO), total peripheral resistance, and central venous pressure (CVP) [37]:

$$MAP = (CO \times TPR) + CVP \qquad \text{Equation 2.5}$$

The term cardiac output describes the volume of blood ejected into the systemic circulation per minute by the left ventricle (mL/min), and central venous pressure is defined as blood pressure in the veins near the right atrium, therefore CVP and right atrial pressure are the same. Since CVP is usually close to 0 mmHg, Equation 2.5 can be simplified to [37]:

$$MAP = CO \times TPR \qquad \text{Equation 2.6}$$

It can be seen that MAP is affected by the changes in CO or TPR. Figure 2-7 summarizes a number of the parameters that control cardiac output and total peripheral resistance.

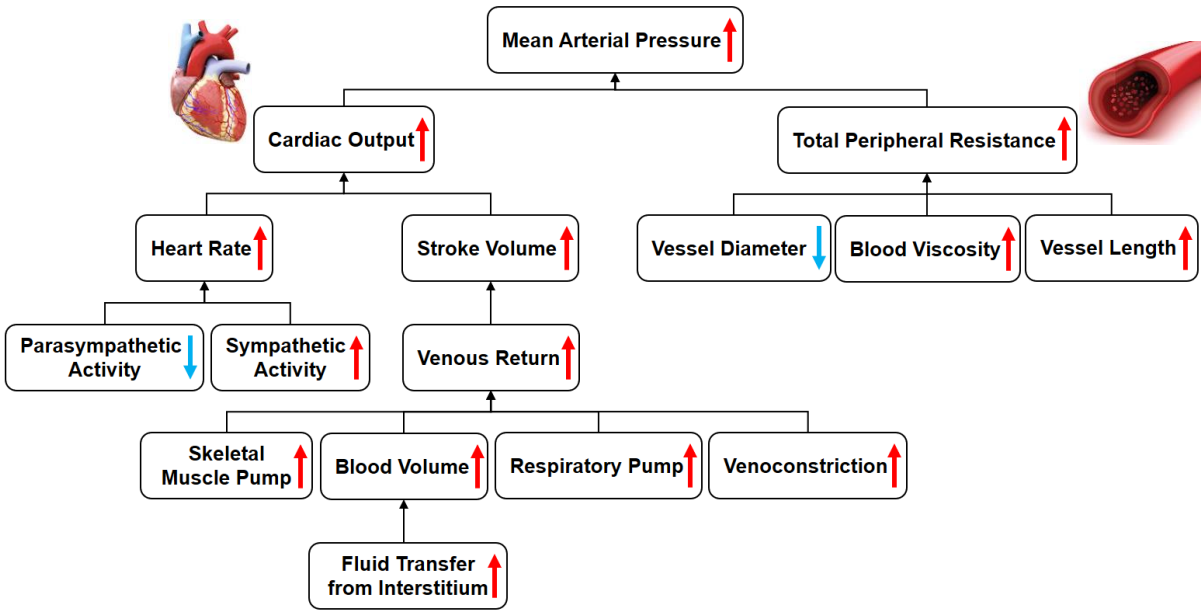

Figure 2-7 Factors affecting blood pressure regulation
Red and blue arrows indicate increase and decrease, respectively.

Increase/decrease in cardiac output results in increased/decreased blood pressure. Cardiac output equals the product of stroke volume and heart rate. Stroke volume (SV) is the blood volume pumped out of the left ventricle per heartbeat (mL/beat), and heart rate (HR) is simply the number of beats per minute (beat/min) [37]:

$$CO = SV \times HR$$ Equation 2.7

Equation 2.7 shows that the changes in heart rate or stroke volume lead to increase or decrease in cardiac output. According to the Frank-Starling mechanism, stroke volume itself alters in response to the changes of venous return. When the amount of venous return increases, the central venous pressure and consequently the ventricular filling volume (or end-diastolic volume) increase, hence preload, which is the initial stretching of the heart prior to contraction, rises. As a consequence, the heart contracts with a stronger force, ejecting more blood, thus increasing the stroke volume. Conversely, decreased venous return leads to a decline in stroke volume [37].

2.1.3. Venous Disease Pathophysiology and Sequelae

Despite the various manifestations of CVD and CVI, it seems likely that all of the symptoms share the same trigger, which is prolonged higher than normal venous pressure, or sustained venous hypertension. Lower leg venous pressure is determined by two components; a hydrostatic component due to the weight of the blood column from the right atrium to the point of interest, and a hydrodynamic component generated by the action of calf muscle pump and the capillary network pressure [17]. Upon a postural change from lying to standing, a large volume of blood redistributes to the lower extremities because of gravitational forces [23, 42, 43]. Since the veins are more compliant[1] than the arteries, most of the shift in blood volume happens in the lower limbs' venous system [37]. Hence, a significant increase occurs in the volume of the veins and hydrostatic pressure reaches around 80-90 mmHg in static standing without any skeletal muscle activity [17]. In addition to increased venous pooling, thoracic venous blood volume and consequently central venous pressure decrease, leading to a decline in ventricular filling pressure (preload). This results in stroke volume fall by the Frank-Starling mechanism, and ultimately decreases cardiac output and arterial blood pressure [37].

[1] The ability of a vessel to increase volume and expand when the transmural pressure (inside minus outside pressure) increases is defined as vascular compliance (C). Compliance can be quantified by dividing volume change by the change in pressure: $C = \frac{\Delta V}{\Delta P}$ [37].

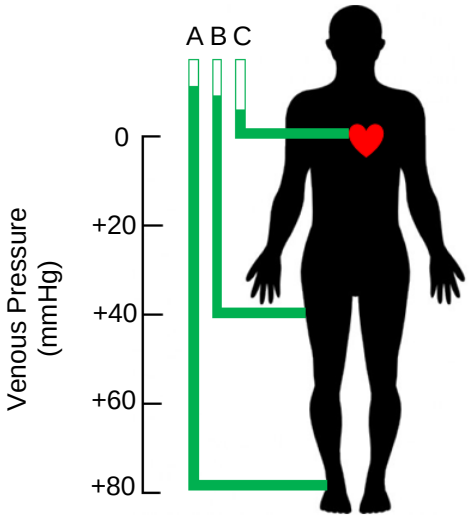

Figure 2-8 Effect of gravity on venous pressure during motionless standing in a healthy individual
The manometers on the left of the figure indicate the height to which a column of blood in a tube would rise if connected to (A) an ankle vein, (B) the femoral vein, and (C) the right atrium, with the subject in the standing position. The approximate pressure in these locations in the recumbent position, i.e. when the ankle, thigh, and right atrium are at the same level, are (A) 10 mmHg, (B) 7.5 mm, and (C) 4.6 mmHg [44].

When a healthy individual stands up, mean arterial pressure is restored through the rapid activation of autonomic reflexes, including vasoconstriction (or narrowing of blood vessels by small muscles in their walls), increased total peripheral resistance, decreased venous compliance, and increased heart rate [38]. Moreover, during ambulation in a normal person, venous pooling and reduced venous return are speedily compensated due to the proper function of venous valves and calf muscles [37]. Therefore, the accumulated blood in the legs gets propelled towards the heart and venous pressure is restored to about 30 mmHg in 20-30 seconds; this is referred to as the ambulatory venous pressure (Figure 2-9) [23, 45].

In the absence of compensatory mechanisms, standing upright can result in various venous complications in the lower extremities in addition to orthostatic hypotension (OH) and syncope [37]. OH is defined as a sustained reduction in systolic blood pressure ≥20 mmHg or diastolic blood pressure ≥10 mmHg within three minutes of standing [43]. Syncope, or fainting, refers to a short transient loss of consciousness and postural tone followed by a spontaneous recuperation [46]. When venous return is impaired for any reason, retrograde flow, or reflux, may arise in the superficial or deep venous systems, the perforating veins or any combination of these, therefore venous pressure decline associated with ambulation gets attenuated and pressure rise during standing occurs more rapidly, resulting in venous hypertension [17, 23, 29, 47]. One out of 4 pathophysiological mechanisms can cause venous hypertension: (1) valves dysfunction in the superficial and/or perforating veins because of congenital or acquired incompetence, (2) valves

dysfunction in the deep venous system because of congenital absence, inherent weakness, or thrombotic damage, (3) obstruction of deep venous outflow, and (4) muscle dysfunction and calf muscle pump failure [29, 30].

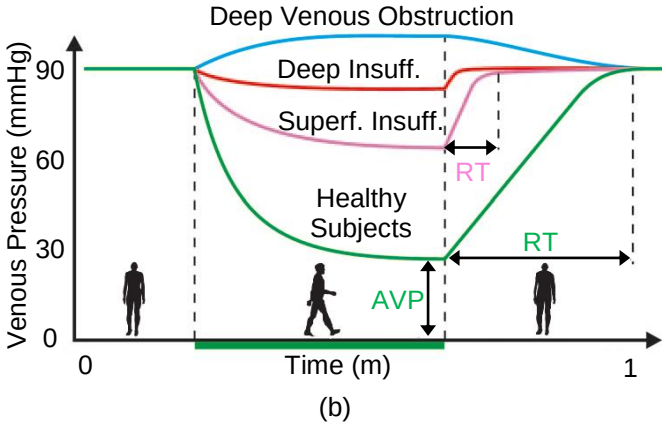

Figure 2-9 Fluctuations in distal calf venous pressure during static standing and walking[1]

The lowest mean pressure during walking at the site of measurement is referred to as the ambulatory venous pressure (AVP). The time interval between the termination of walking until the vein pressure reaches the pressure level at motionless standing is called the recovery time (RT), or venous refill time. The AVP at the distal calf and RT are about 30 mmHg and 20-30 s in healthy subjects, respectively [45].

Unabated venous hypertension interrupts the balance of the pressures inside and outside the capillaries, makes them more permeable, and enhances filtration [20, 23]. In other words, the net transcapillary filtration rate surpasses the lymphatic drainage rate [45]. If not adequately compensated, the exacerbation of venous pooling and capillary filtration results in dilated veins, accumulation of fluid in the tissue (oedema), inflammation, leg pain, changes in skin and subcutaneous tissues, and ultimately ulceration [17, 23, 29]. Furthermore, decreased venous return upon upright posture may lead to sudden reductions in blood pressure (orthostatic hypotension) and blood flow to the brain. Due to cerebral hypoperfusion[2], syncope (or fainting) occurs [46].

[1] adapted from [45]

[2] Cerebral hypoperfusion is defined as a drop in oxygen-rich blood supply to the brain.

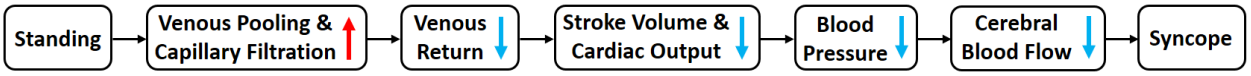

Figure 2-10 Hemodynamics of hypotension-induced syncope[1]
Red and blue arrows indicate increase and decrease, respectively.

2.1.4. Treatment of Chronic Venous Disorders

The principal treatment goals of venous disorders are to improve the symptoms, delay or prevent recurrence, and correct the long-term complications, to the greatest extent possible [20, 29, 30, 48]. There are various treatment methods that can be categorized as follows [29, 49]:

- **Conservative Treatment**

  - Leg Elevation: Elevating the legs is helpful in minimizing oedema.
  - Pharmacological Therapy: Medications that improve blood flow through the vessels may be used.
  - Compression Therapy: The mainstay of conservative treatment is compression therapy [22], which is the central focus of the current study and is described in more details in section 2.2.

- **Interventional Treatment**

  - Sclerotherapy: This procedure involves injecting a solution directly into the veins, forcing blood to reroute through healthier vessels.
  - Ablative Therapy: The use of thermal energy in the form of radiofrequency or laser to obliterate the veins is referred to as ablative therapy.

- **Surgical Treatment:** A number of surgical procedures may be used to treat CVD and CVI, such as removing affected veins, repairing damaged veins and valves, and replacing diseased veins with healthy ones from other parts of the body.

The health care practitioners prescribe a suitable therapeutic strategy by taking into account the conditions of the patient, including age, overall health, extent of the disease, and tolerance to specific therapies [49].

[1] adapted from [38, 42]

2.2. Compression Therapy in Leg Venous Disorders

The concept of applying an external pressure to the body to control, treat, and prevent certain conditions has grown in various areas; including medical and non-medical fields. The following examples show a number of situations with widespread application of compression:

- **Orthostatic Intolerance:** OI refers to the development of signs and symptoms, such as hypotension and light-headedness, during upright posture that are relieved by recumbence [50]. Considering the potential of compression hosiery in improving blood circulation, individuals with recurrent episodes of orthostatic intolerance are usually encouraged to use pressure garments over the lower extremities and abdomen [1, 2].
- **Postpartum Hemorrhage:** Obstetric hemorrhage, which is the leading cause of maternal mortality, especially in low-resource settings, can be decreased using the non-pneumatic anti-shock garment (NASG) before the patient receives definitive treatment. The NASG is a first-aid device made of articulated segments of neoprene and hook-and-loop fasteners (also known as Velcro™) that squeezes blood to the vital core organs when tightly wrapped around the legs, pelvis, and abdomen [3, 4].
- **Burn Scars:** Compression therapy is the most common non-surgical way of preventing and treating hypertrophic burn scars[1] [5, 6]. Pressure garments restrict blood flow to the damaged area and prevent hypertrophic scar tissue growth by applying constant compression [6].
- **Spinal Cord Injury:** In individuals with SCI, the impaired function of the muscle pump and sympathetic nervous system hinders blood redistribution, which in turn causes complications during daily life activities, such as orthostatic hypotension [51]. Compression garments that exert pressure on the lower extremities and abdomen have been proven to be efficacious in improving blood circulation problems [52, 53]. Moreover, it has been shown that inflatable external leg compression can prevent OH in SCI patients [51].
- **Post-Surgical Operation:** Deep vein thrombosis is a serious problem in recumbent patients during surgery and postoperative period. It has been shown that compression devices are capable of reducing DVT by inhibiting venous stasis in the lower limbs [7, 8, 9].

[1] A hypertrophic scar is a cutaneous condition where excess amounts of collagen form a raised scar on the skin.

- **Sports:** The use of compression products in athletics is on the rise due to their capability of improving both performance and recovery in sportspeople [10, 11, 12]. The increased blood flow rate, which is a result of external pressure, leads to a faster uptake of oxygen and nutrients into the muscle cells, and a more rapid removal of metabolic by-products, such as CO_2 and lactate [54].
- **Aviation:** During rapid ascent, acceleration forces in the head-to-foot direction cause blood pooling in the abdomen and legs of aircraft pilots and astronauts, and G-induced loss of consciousness. In order to improve the G-tolerance, pilots use anti-gravity suits, or G-suits, which are designed to exert external pressure on the body to counteract the gravitational forces [13, 14].
- **Spaceflight:** Post-spaceflight orthostatic intolerance is a common problem in astronauts upon returning to Earth and is defined as an inability to remain in upright posture while maintaining adequate blood circulation to the brain [55]. Recent studies have shown that commercially available compression garments are capable of mitigating the symptoms of OT after spaceflight, including tachycardia, dizziness, hypotension, and pre-syncope [15].

What has been mentioned so far, represents a part of the applications of compression therapy. In addition to the examples listed above, another indication for immense use of compression therapy is leg venous insufficiency [16].

2.2.1. Concept and Effect of Compression Therapy in Venous Insufficiency

Leg compression therapy, which refers to the benefits gained from externally compressing the lower limbs, has been used for decades as the gold standard in the management of venous disorders [19, 20, 21, 22]. Circumferential compression aims to reverse the detrimental effects of venous hypertension via increasing the pressure on the skin and underlying structures, thereby improving blood circulation [23]. This goal is achieved by affecting the venous, arterial and lymphatic systems, along with the leg tissue through a series of mechanisms [22]. In the venous system, an adequate level of compression improves venous pump; causes venoconstriction by narrowing the venous diameter and increasing peripheral resistance; restores efficient closure of valves by bringing the walls of the veins closure together; prevents or decreases deep and superficial venous reflux; reduces venous pressure; increases blood flow and velocity in the deep veins; decreases venous stasis; and alleviates venous pooling by counteracting the force of gravity. Moreover, the applied compression enhances lymphatic drainage by elevating tissue

pressure and reducing the pressure gradient between the capillaries and surrounding tissues, thus facilitating the reintegration of interstitial fluids into the intravascular space and reducing oedema. The aforementioned impacts provide the conditions necessary for wound and ulcer healing [20, 21]. In addition to these effects, blood gets squeezed from the lower body towards the central circulation and venous return is promoted, resulting in augmented preload and cardiac output [22].

2.2.2. Compression Therapy Terminology

External pressure can be applied to the lower extremities by means of different compression modalities, including bandages, stockings, Velcro™ devices, and mechanical pumps [56]. To fully understand these modalities and their mechanism of action, first it is necessary to have a sound knowledge of the related terminology:

- **Elasticity and Extensibility:** The elasticity of a bandage refers to its ability to be restored to the original length after tension[1] release. In lieu of elasticity, extensibility, which is the ability of the bandage to stretch upon applying force, is frequently adopted internationally in classifications. Expressed as a percentage of the initial length, extensibility is defined as bandage elongation under a load of 10 N/cm [49].
- **Sub-bandage/Interface Pressure:** Mathematically governed by Laplace's law, this term refers to the pressure between the compression garment and the skin, and is directly proportional to the number of layers and bandage tension during application, but inversely proportional to the leg's radius of curvature and bandage width [23, 25, 57]. Complex interactions between four factors determine the amount of sub-bandage pressure; including properties of the garment, geometry of the limb, skill of the operator, and physical activities and posture of the user [20, 25]. The interface pressure partly declines from the surface of the limb towards deep veins [22].
- **Graduated Compression:** When sub-bandage pressure gradually decreases over the length of the garment from the lower to upper leg, a graduated pattern is produced with the highest amount at the ankle and smaller values at proximal parts. Graduated compression prevents retrograde flow of blood downwards to the feet and ensures that blood moves in the direction of upper body [58]. Considering the law of Laplace, if a bandage is applied

[1] The bandage tension is the force exerted to the fabric during application [25].

with a constant tension all the way up the leg, a descending compression gradient will automatically be achieved as the circumference of the leg increases progressively [25].

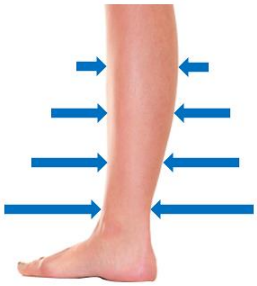

Figure 2-11 Graduated compression on lower leg

- **Stiffness:** The capacity of a bandage to resist to muscle expansion during contraction is referred to as stiffness. In other words, stiffness is the interface pressure increase (in mmHg) per centimeter of circumference increase of the limb [49]. Stiffness of a compression device reflects its elasticity [59].
- **Long-stretch, Short-stretch, and No-stretch Systems:** Long-stretch materials are made of elastic fibers that make them highly extensible, whereas short-stretch materials are comprised of few or no elastic fibers with a considerably low extensibility [20, 23, 25].

Table 2-1 Definition of inelastic and elastic bandages based on in vitro tests[1]

Bandage Type	**Inelastic** ⟷ **Elastic**		
	No-stretch (Rigid)	*Short-stretch*	*Long-stretch*
Extensibility (%)	0 - 10	10 - 100	>100

Capable of adapting to the circumferential changes in the legs, long-stretch bandages minimally influence the interface pressure when small alterations occur in their extension. This is particularly helpful when the limb size changes as a result of oedema reduction. Whereas with short- and no-stretch materials, sub-bandage pressure undergoes large fluctuations upon slight changes in leg geometry [25, 60]. The incapability of these bandages to accommodate to the decrease in limb circumference leads to pressure drop over the course of the treatment, which consequently increases the risk of slippage and necessitates the need for frequent re-applications to maintain adequate compression [20]. However, inelastic bandages have been proven to affect the deep venous system significantly. On the contrary, elastic bandages primarily influence the superficial venous

[1] adapted from [64]

hemodynamics [60, 61]. Mosti et al. investigated the effect of elastic and inelastic compression bandages in 30 patients with venous insufficiency and major venous reflux. They concluded that inelastic compression is much more efficacious in normalizing venous pumping function [62].

- **Passive/Dynamic and Active/Static Compression:** Passive and active compressions are delivered by inelastic and elastic bandages, respectively. Inelastic systems produce little or no pressure in rest, making them tolerable for several days. Moreover, the bandage serves as a rigid container and counteracts the increasing muscle volume during contraction, creating a pressure force that is called working pressure. Elastic systems create high resting and working pressures. Therefore, they might be intolerable for immobile or bedridden individuals [21], which requires the bandage be removed in a supine position.
- **Single- and Multi-Component Bandages:** Compression systems may consist of elastic or inelastic fibers, i.e. single-component, or both fiber types, i.e. multi-component [63]. Combining different bandage materials influences not only sub-bandage pressure but also stiffness [64]. It has been shown that single-component systems are less effective than multi-component compression [63]. The supremacy of the latter system is that sustained pressure is provided by the elastic fibers, and high working and low resting pressures are secured by inelastic fibers, in other words, multi-component systems are a combination of active and passive compressions [25].
- **Single- and Multi-Layer Bandages:** Multi-layer compression is achieved by applying the bandage in an overlapping manner [16]. These systems consist of more than two layers of either a single material or different components [64]. In practice, there is always some degree of overlap during bandage application, therefore single-layer bandaging does not exist [64]. Multi-layer and multi-component systems have different mechanical properties compared to the individual constituents which form them, making in vitro elasticity assessment complicated. As a result, another parameter, namely static stiffness index, is used for in vivo characterization of different bandages [64].
- **Static and Dynamic Stiffness Indices:** The static stiffness index (SSI) of a bandage refers to the difference in sub-bandage pressure from the lying to standing position measured at the transition point of the Achilles tendon to muscle, i.e. the site that exhibits the highest circumferential increase by standing [56]. SSI values of higher and lower than 10 mmHg correspond to inelastic and elastic materials, respectively [59]. The dynamic stiffness index (DSI) is the stiffness of a bandage during walking [49]. In a study by van der Wegen-Franke

et al., a positive correlation was found between the static and dynamic indices of 18 different brands of compression stockings tested in different conditions, and it was concluded that the DSI does not have any additional value over the SSI in classifying medical stockings [65].

Unlike low-SSI systems, bandages with a high SSI, such as inelastic systems and multi-layer compressors, produce intermittent high pressure peaks during ambulation, called the massaging effect [23]. This pressure is beneficial in reducing retrograde blood flow, as it creates venous occlusion by mimicking the closing action of the venous valves [20, 41].

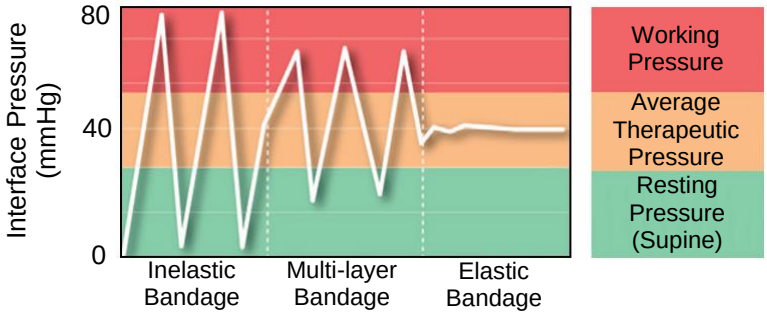

Figure 2-12 Interface pressure values and fluctuations in bandages with different stiffness values[1]

- **Bandage Classification:** According to what has been said so far, compression systems can be categorized based on their pressure level, elasticity, number of layers, and components. In this classification, pressure level refers to the amount of the generated pressure at the ankle of a model limb during laboratory testing and varies from one country to another. The World Union of Wound Healing Societies (WUWHS) has proposed the classification represented in Figure 2-13 for compression level [66].

[1] adapted from [95]

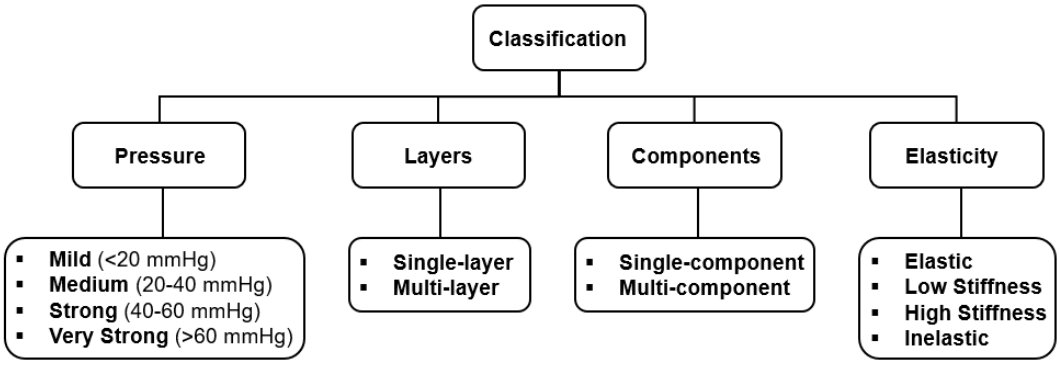

Figure 2-13 Classification of medical compression systems[1]

2.2.3. Review of Compression Therapy Modalities

Currently, there are various types of compression therapy systems for the management of leg venous insufficiency and the associated complications. In the sections ahead, these modalities are explained, along with their mechanism of action, advantages and disadvantages.

Compression Bandages/Wraps

Compression bandages are long strips of fabric that can be wrapped around the leg in a single- or multi-layer fashion [23]. Some of the pros and cons of medical bandages are mentioned in the previous sections.

Figure 2-14 Compression bandage[2]

Graduated Compression Stockings/Hosiery

Available in different sizes, lengths, and strengths, medical compression stockings are single-layer elastic knitted garments with the same shape as human leg [23], and are the most

[1] reproduced from [66]

[2] reproduced from [101]

common form of compression modalities for leg oedema [31]. Despite of self-applicability, stockings can be hard to put on, which makes it necessary to use assistive donning aids [16]. Compression stockings have restricted pressure and stiffness, which diminishes their efficacy in enhancing venous hemodynamics [56]. In a study by Mayberry et al. on 16 patients with venous insufficiency, below- and above-knee 30-40 and 40-50 mmHg gradient elastic compression stockings were shown not to improve deep venous hemodynamic parameters, including ambulatory venous pressure, venous refill time, maximum venous pressure with exercise, and amplitude of venous pressure excursion. Finally, the beneficial effect of elastic stockings was attributed to their impact on the superficial venous system [67].

Figure 2-15 Compression stocking along with donning tool[1]

Adjustable Velcro™ Compression Garments (AVCGs)

AVCGs are inelastic compression modalities that consist of multiple straps, equipped with hook-and-loop fasteners. The straps make the device self-applicable and enable the user to control and adjust the applied pressure to a comfortable level when the AVCG becomes loose [16, 56]. Mosti et al. compared the effectiveness and comfort of Velcro™ garments to inelastic bandages, which are routinely used in lessening chronic venous oedema. The AVGCs were found to be more effective in oedema reduction, with comparable patient comfort [68].

[1] reproduced from [102]

Figure 2-16 Adjustable Velcro™ compression garment[1]

Mechanical Pumps

Another category of compression devices are mechanical pumps, which can be split into the following subgroups:

- **Intermittent Pneumatic Compression (IPC):** IPC systems have been well-proven in various studies to be effective in venous flow augmentation [69, 70], DVT prevention [70, 71, 69] and lymphoedema[2] reduction [72]. Unlike medical bandages and compression hosiery that passively enhance venous return, IPCs actively pressurize the limbs. In these devices, the inflation and deflation of single- or multi-chambered pneumatic cuffs, which are connected to an air pump, resembles the natural rhythmic muscle contraction and relaxation during movement [72, 73]. The working characteristics of IPCs, including the implementation site; pressure cycle, amplitude, rise and fall times; and chamber inflation sequence differs between the manufacturers and depends on the application [7, 72]. As represented in Figure 2-17, most of IPC devices have electrically driven air compressors, and a few function with battery-operated pumps.

[1] reproduced from [106]

[2] Lymphoedema refers to a type of swelling that occurs in the limbs due to an impaired lymphatic system.

(a) (b) (c)

Figure 2-17 Three different pneumatic compression devices[1]
(a) *circumferential calf-length IPC with electrical pump, (b) non-circumferential calf-length IPC with electrical pump, and (c) non-circumferential calf-length IPC with battery-operated pump*
The circumferential cuffs pressurize the whole limb upon inflation, usually need large powerful pumps and have slow inflation rates. Whereas the non-circumferential pumps require smaller input of air.

As the name implies, IPC systems generate intermittent pressure, which makes them suitable to be used during periods of patient rest (when there is no calf muscle pump) rather than ambulation [16, 72]. Depending on the device's brand, the compression takes different forms, which are schematically depicted in Figure 2-18.

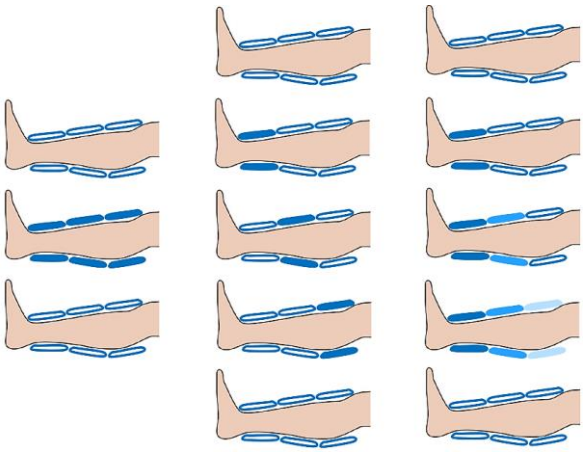

(a) (b) (c)

Figure 2-18 Different compression modes in intermittent pneumatic devices
(a) uniform compression, (b) sequential compression, and (c) graded sequential compression

- **Hybrid Pumps:** Unlike IPCs that only deliver intermittent pressure, hybrid devices generate both intermittent pneumatic compression (beneficial during rest) and sustained gradient pressure (useful in ambulation) in order to achieve a better treatment [16]. As far as the author is aware, the ACTitouch® system (Tactile Medical, Minnesota, USA) is the only hybrid pump available in the market, which uses pneumatic technology to exert controlled gradient compression to the lower extremities. In a study by Harding et al.,

[1] reproduced from [107, 108, 109]

ACTitouch® was shown to be as effective as a conventional four-layer bandage in healing leg venous ulcers but with better acceptance in terms of tolerability and quality-of-life improvement [74]. Although possessing great characteristics, this device is limited to two pressure paradigms with fixed values as follows: sequential intermittent compression of 50 mmHg at the foot and ankle, 45 mmHg at the mid-calf and 40 mmHg at upper calf; and sustained gradient compression of 40 mmHg at the foot and ankle, 30 mmHg mid-calf and 20 mmHg at upper calf [74].

Figure 2-19 ACTitouch® hybrid compression device[1]

- **Non-pneumatic Pumps:** To the best of the author's knowledge, the only constituent of the last group of mechanical pumps is Venowave (Saringer Life Science Technologies Inc, Stouffville, Canada). The Venowave system, as shown in Figure 2-20, is a portable peristaltic pump, consisting of a rotating gear-motor attached to a flexible sheet. Upon motor rotation, a repetitive waveform motion is generated, which produces upward volumetric displacement, increasing blood flow. According to the manufacturer's claims, this device is useful in oedema, DVT preventions, venous insufficiency, and athletic enhancement to name a few.

Figure 2-20 Venowave peristaltic pump[2]

[1] reproduced from [103]

[2] reproduced from [104]

Different types of the existing compression therapy modalities, along with their advantages and disadvantage are summarized in Table 2-2.

Table 2-2 Comparison of current compression therapy modalities[1]

	Type	Stiffness	Advantage	Disadvantage	Example
(1) Bandage / Wrap	Inelastic	Very High	High working pressure, Well-tolerated in rest	Trained bandager, Non-adaptive to changes, Slippage, Frequent re-application, Pressure loss over time	Zinc paste (Unna's boot)
	Short-stretch single-layer	High	High working pressure, Well-tolerated in rest	Trained bandager, Non-adaptive to changes, Slippage, Frequent re-application, Pressure loss over time [75]	Lastolan®, Acrylastic®, Comprilan™
	Long-stretch single-layer	Low	Self-applicable [56], High working pressure, Adaptive to changes, Little pressure loss over time	High resting pressure, Intolerable during rest	Tensopress®, Setopress®, Surepress™
	Multi-component	High	High working pressure, Well-tolerated in rest, Adaptive to changes	Trained bandager	Actico®, Profore©, Urgo KTwo©
(2) Stocking		Low	Self-applicable, Possibility of daily skin care	Difficult to don, Non-adaptive to changes, Low efficacy in improving venous hemodynamics [56], Fitting problems [31]	Various brands: Jobst, Mediven, Sigvaris
(3) Adjustable Velcro™ device		Moderate to High	Self-applicable, Self-adjustable, Possibility of daily skin care	Not appealing	CircAid©
(4) Mechanical Pump	Pneumatic	Variable	Self-applicable, Self-adjustable, Possibility of daily skin care	Bulky, Not appealing, Non-ambulatory use, Need for air pump, Difficulty of portability	VenaPro™, Medshoola™
	Hybrid	Variable	Self-applicable, Self-adjustable, Adaptive to changes, Possibility of daily skin care	Limited pressure range, Bulky, Not appealing	ACTitouch®
	Non-pneumatic	Variable	Self-applicable, Self-adjustable, Possibility of daily skin care	Limited to peristaltic mode, Bulky, Not appealing	Venowave

[1] adapted from [16, 96]

2.2.4. Ideal Compression Therapy System

The benchmarks for a perfect compression system include clinical efficacy; capability of delivering and sustaining targeted compression levels to empty the veins and prevent refilling [22]; calf muscle pump enhancement; comfortability; conformability to various limb sizes and shapes; ease of application and training; and durability to name a few [60]. Moreover, an ideal device generates tolerable resting pressure, and high working pressure, in excess of 50 mmHg, to markedly reduce ambulatory venous hypertension [22, 56].

2.3. Interface Pressure Measurement

The efficacy of compression therapy as an intervention in treatment and prevention of leg venous and lymphatic disorders relies on the amount of exerted pressure to the limbs [26, 56], and the right way of bandage application [20, 23]. Sub-bandage pressure needs to be in specific ranges, which is governed by the severity of the disease and patient's conditions. If the applied pressure is insufficient or non-sustained, it leads to a less effective treatment, and if the pressure is excess, in addition to intolerability, tissue damage occurs [41, 64]. In order to resolve such problems and ensure that the patients receive the full treatment benefits, the interface pressure between the leg and the compression system should be monitored in vivo during static and dynamic conditions, i.e. during rest and movement. Knowing the quantity of sub-bandage pressure can be used not only to characterize the effectiveness of different compression devices and compare them, but also to help physicians in providing their patients with an optimal medical care and expediting the treatment process [76].

Various types of measurement systems can be used for the purpose of monitoring the interface pressure, including resistive, capacitive, pneumatic, piezoelectric, and piezoresistive. An ideal measurement system is biocompatible (not causing skin irritation when left in contact with the skin for extended periods of time), thin (less than 0.5 mm in thickness), flexible yet insensitive to bending, conformable to leg's curvature, durable, accurate, linear, resistant to physical changes (insensitive to temperature and humidity changes), and has simple electronics, low hysteresis, low cost, suitable resolution (time<0.1 sec, amplitude<0.1 mmHg), continuous output, and little creep [26].

2.4. Summary

The main purpose of this chapter was to address the pathophysiology of chronic venous disorder and its most common non-pharmacological treatment approach, i.e. compression therapy. To summarize, the one-way valves in the leg veins, along with the calf muscle pump action during contraction and relaxation, play a vital role in expelling blood from the lower extremities towards the heart and promoting venous return. In the presence of venous insufficiency, this function, for any reason, is disturbed. Hence blood accumulates in the vessels, causing elevated venous pressure. Failure to redress this condition leads to successive, enervating complications, including varicose veins, pain, limb swelling, skin changes, and ulceration. Another consequence of reduced venous return is less cerebral blood perfusion, which eventually can result in fainting.

Compression therapy is one of the most promising treatments for venous insufficiency. In this method, application of adequate external pressure over the limbs squeezes blood out of the vessels, abolishing venous hypertension and augmenting blood flow. Medical wraps, compression stockings, and mechanical pumps are well-known modalities for compression therapy. Nonetheless, these products have disadvantages that influence their optimal performance. In order to provide patients with better treatment, improved compression systems should be developed.

Chapter 3. **Design and Fabrication of ACS Prototype**

The concepts explored in Chapter 2 were adequate to reach the conclusion that the existing compression modalities have downsides, eclipsing their efficacy. Thus there is a need for developing improved systems. This chapter is aimed at providing detailed information on the efforts that were made towards the development of a novel compression therapy device with the potential to elevate the problems of the current systems and improve the treatment procedure.

3.1. Design Objectives

A number of objectives were set to smooth the design process. The goal was to have a device which was:

1. easy to apply, hence eliminating the need for a trained bandager;
2. capable of producing gradient pressure modes, including constant and intermittent compression, that decrease from ankle to upper calf (distal to proximal);
3. able to sustain constant tension in the garment, thereby creating a pressure gradient up the leg;
4. adaptive to the changing physiological conditions of the user;
5. usable during stasis (including recumbence and passive orthostasis) and ambulation; and
6. safe.

3.2. Conceptual Design

In the next step, a conceptual design was developed to satisfy the foregoing objectives. One plan that seemed to fulfil the desired expectations was a garment with a motorized lacing system. In this design, which is schematically shown in Figure 3-1, an electrical motor is used for tightening and loosening a piece of fabric through guided laces to pressurize and depressurize the lower leg. In the back, the garment is equipped with pieces of hook-and-loop fastener, or Velcro^{TM}, which makes it easy to don the device and gratifies the first objective.

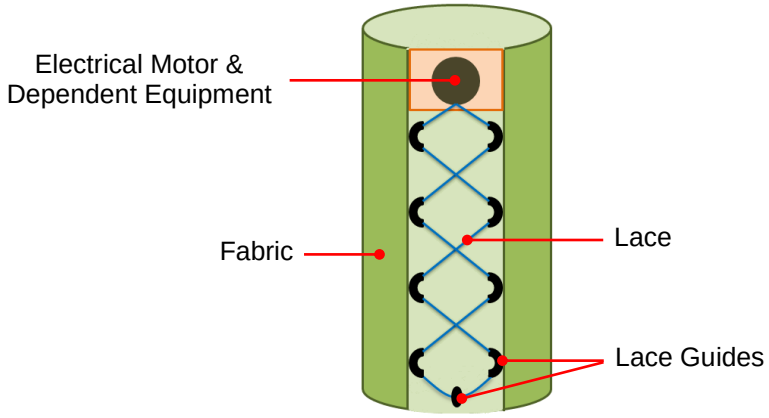

Figure 3-1 Conceptual design of compression garment

The lacing system, including the electrical motor, lace, and lace guides, are attached to the front of the instrument that will be placed on the leg shin. Employing such a system not only empowers the device to exert various compression types on the calf by controlling the motor operation, but also makes it feasible to maintain a constant tension in the lace, therefore producing a gradient pressure up the leg. This feature meets the second and third objectives. In order to prevent the lace from getting entangled while the motor is switched either on or off, a housing was designed in SolidWorks2014 (Dassault Systèmes SolidWorks Corporation, Massachusetts, USA) along with a spool to be placed inside it. The corresponding mechanical drawings can be found in Appendences A and B. The lace passes through two embedded holes on the sides of the housing and winds around the freely rotating spool, therefore the housing restrains entanglement.

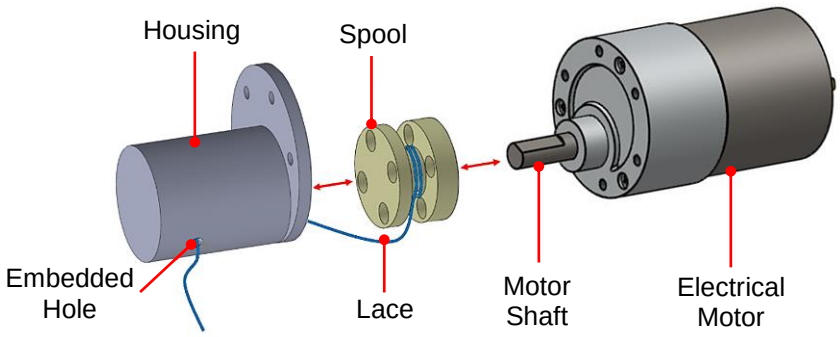

Figure 3-2 Lacing system of compression garment

As previously mentioned, the incapability of the current compression therapy products in adapting to the physiological changes of the user stems from the fact that they are not equipped with any technology to sense these changes. This issue can be tackled by utilizing interface pressure sensors between the leg and compression garment. The sensors measure the applied pressure and its alterations due to physiological changes, and provide a feedback, which in turn

can be employed to adjust and control the motor's operation towards re-setting the desired compression. This feature makes the garment adaptive to changes, satisfying the fourth goal.

Although the electrical motor and its dependent equipment are slightly bulky, the compression system is still appropriate to be used in stasis and ambulation. Moreover, the device is totally battery-operated, guaranteeing its safety. These two properties fulfil the fifth and sixth objectives, respectively. Considering that such a design meets all of the expected needs, it was time to manufacture the ACS.

3.3. Prototype Requirements

Prior to manufacturing the proposed conceptual design in section 3.2, the required parts were prepared, most of which were off-the-shelf components:

- **Fabric:** A non-stretchable yet flexible piece of fabric was used in the ACS. It was flexible enough to allow for normal movements, and sufficiently non-stretchable to provide the needed pressure.
- **Velcro™:** Because of its ease of use, hook-and-loop fastener has been used extensively where a temporary bonding is needed. For the same reason, adhesive Velcro™ was utilized for the purpose of compression garment fastening.
- **Electrical Motor:** The *thin-walled pressure vessel theory* was used to calculate the needed amount of motor torque which met the requirements of the study. The designed garment was assumed to form a thin-walled cylinder of radius R and thickness t ($R/t > 10$) loaded by internal pressure of p. The garment is subjected to two types of stresses; including longitudinal and circumferential (or hoop) as shown in Figure 3-4. It has to be mentioned that considering the thin-walled assumption, the magnitude of the radial stress is very small and can be neglected.

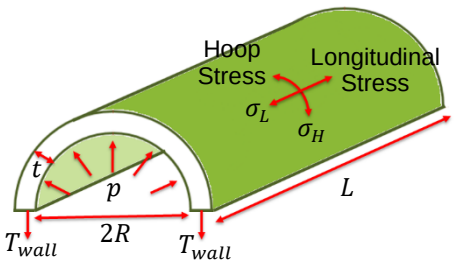

Figure 3-3 Half of thin-walled cylinder subjected to internal pressure

The hoop stress or σ_H can be expressed by Equation 3.1:

$$\sigma_H = \frac{p \times R}{t} \qquad \text{Equation 3.1}$$

Where, σ_H is hoop stress in newton per square meter (N/m^2), p is internal pressure in pascal (Pa) which is equal to the interface pressure applied by the garment, R is the garment or limb radius in meter (m) assuming that the lower leg has a cylindrical shape, and t is the garment thickness in meter (m).

The hoop stress can be written in terms of the tension in the wall of the ACS:

$$\sigma_H = \frac{T_{wall}}{A_{wall}} = \frac{T_{wall}}{t \times L} \qquad \text{Equation 3.2}$$

L is the length of the garment (m).

As depicted in Figure 3-4, each lace guide applies force on the garment. The following equality holds between the wall tension and these forces, wherein n corresponds to the number of the guides at each side of the fabric:

$$T_{wall} = n \times F_{guide} \qquad \text{Equation 3.3}$$

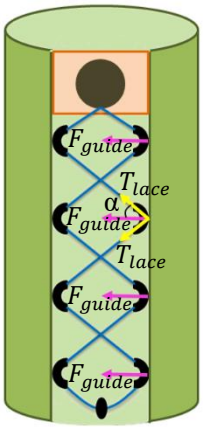

Figure 3-4 Forces on compression garment

The extracted F_{guide} from Equation 3.3 can be used to find the lace tension, which in turn is useful in calculating the motor torque.

$$T_{lace} = \frac{F_{guide}}{2 \times \cos\alpha} \qquad \text{Equation 3.4}$$

$$\tau = r \times T_{lace} \qquad \text{Equation 3.5}$$

In Equation 3.5, τ is torque in newton meter (Nm) and r is the moment arm or spool radius in meter (m).

Equations 3.1 to 3.5 were utilized to calculate the required motor torque suitable for the purpose of the current study. Based on the calculations, a DC motor (Pololu Corporation, Nevada, USA)[1] with a gear ration of 131:1 intended for operation at 12 V was selected. The specifications are available in Table 3-1.

Table 3-1 Electrical motor specifications

Gear ratio	Weight (g)	Shaft diameter (mm)	Free-run speed (rpm)	Free-run current (mA)	Stall current (mA)	Stall torque (N.m)
131:1	205	6	80	300	5000	1.77

- **Motor Driver:** An L298 dual H bridge module (OSEPP, British Columbia, Canada)[2] was used to drive the motor. The driver was capable of controlling the motor direction and speed when used with a controller. It should be pointed out that two driver modules were used in total; one for each motor.
- **Mounting Hub:** A universal hub (Lynxmotion, Vermont, USA)[3] was used to mount the custom spool to the motor shaft.
- **L-bracket:** In order to fix the motor to the garment, a lightweight aluminium L-bracket (Pololu Corporation, Nevada, USA)[4] was utilized, which weighed 11 g.
- **Lace and Guide:** In the preliminary prototypes of the compression device, a steel lace, along with nylon guides (Boa Technology Inc., Colorado, USA)[5] were used. The lace had a high tensile strength and was coated with a plastic layer, which was effective in reducing friction. Although the lace seemed to have the desired properties, in terms of strength and smoothness, to be used in the compression gadget, it was replaced with a 4-ply fishing line in the final prototype. The reason for this substitution was that upon motor rotation, the steel lace hardly got unwound without manual intervention. A similar but much less severe problem existed with the fishing thread, with the exception that there was no need to manually loosen the garment.

[1] www.pololu.com/product/1107

[2] osepp.com/products/breakout-board/motor-driver-module

[3] www.robotshop.com/ca/en/lynxmotion-hub-02-universal-hub.html

[4] www.pololu.com/product/1084/specs

[5] www.boatechnology.com

- **Spool and Housing:** In section 3.2, the conceptual design of a spool and housing was presented. The two parts were 3D-printed in ABS plastic, as shown in Figure 3-5, and used in the compression system.

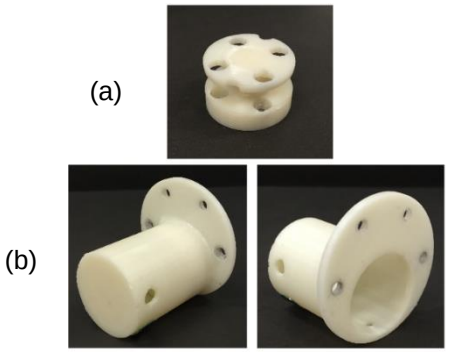

Figure 3-5 3D-printed parts
(a) spool, (b) housing in two different views

The spool and housing were fixed to the mounting hub and L-bracket, respectively, using screws through the embedded holes. The final configuration is depicted in Figure 3-6.

Figure 3-6 Configuration of mounted spool and housing to electrical motor

- **Mounting Base:** In order to fix the motor and dependent equipment to the fabric, a rigid structure was needed on which these compartments could be mounted. The structure had to be strong enough not to bend due to the weight of the parts attached to it. Two different mounting bases, including an acrylic sheet (known as Plexiglas) and a plastic shin guard, were used for this purpose which is discussed in details in section 3.4.

3.4. Prototype Manufacturing

After procuring the required parts described in section 3.3, the next step took place which was manufacturing. Two prototypes were fabricated before reaching the final design. Each of them had some sort of deficiency that was fixed in the subsequent attempts. The following sections will describe the detailed manufacturing processes of the two preliminary prototypes, along with the final one.

3.4.1. Preliminary Prototypes

1st Preliminary Prototype

Presented in Figure 3-7, the first prototype (ACS_v1) was fabricated in order to be used in the sensor calibration process for pressurizing and de-pressurizing the FSRs® over a rigid cylinder, which is thoroughly discussed in section 3.5.2. Since ACS_v1 was not intended for human use, the electrical motor and dependent equipment were not mounted on the garment. Instead, they were fixed to the experiment table using a C-clamp during the tests. In this cylindrically-shaped prototype, the steel lace and a total of eight lace guides were used. Firstly, every group of four guides was sewn to a thin polycarbonate sheet (known by the trademarked name Lexan) 5 cm apart and the sheets in turn were sewn to the fabric, one at each side. The Lexan sheet, which was 0.6 mm in thickness, was helpful in distributing the forces applied by the guides and preventing possible damages to the fabric due to point loads.

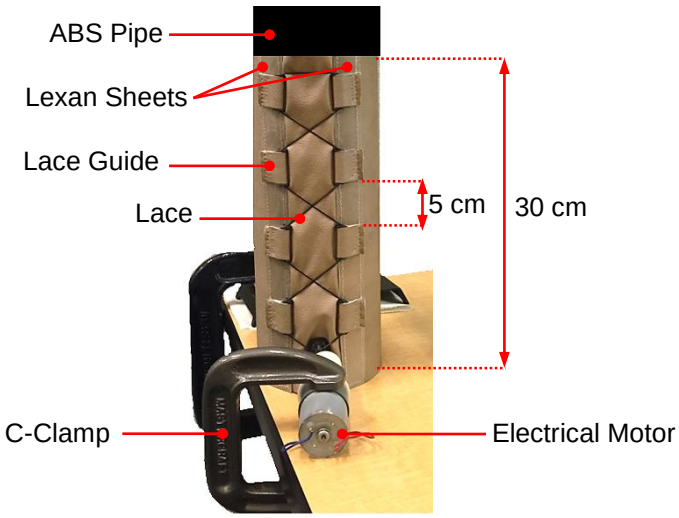

Figure 3-7 Front view of first prototype or ACS_v1 wrapped around ABS pipe

2nd Preliminary Prototype

Unlike ACS_v1, the second prototype (ACS_v2) was shaped as a truncated cone to fit well on cone-shaped surfaces such as human leg. Similar previously-mentioned Lexan sheets with mounted lace guides were used in this prototype, along with the steel lace. For the purpose of easy fastening, pieces of Velcro™ were adhered to the back of the garment. A Plexiglas sheet, 0.3 cm in thickness, was cut into an 18 cm by 5 cm rectangle with multiple holes, as depicted in Figure 3-8d. The sheet was sewn to the front of the fabric as a mounting base for the electrical motor and dependent equipment including the spool, housing, and aluminium L-bracket. The

peripherally spread holes on the sheet were designed to provide various mounting options. Since the Plexiglas sheet was in direct contact with the shin while the garment was donned on the leg, a layer of adhesive padding foam was attached to it to provide protection and comfort. The final configuration of ACS_v2 is represented in Figure 3-8.

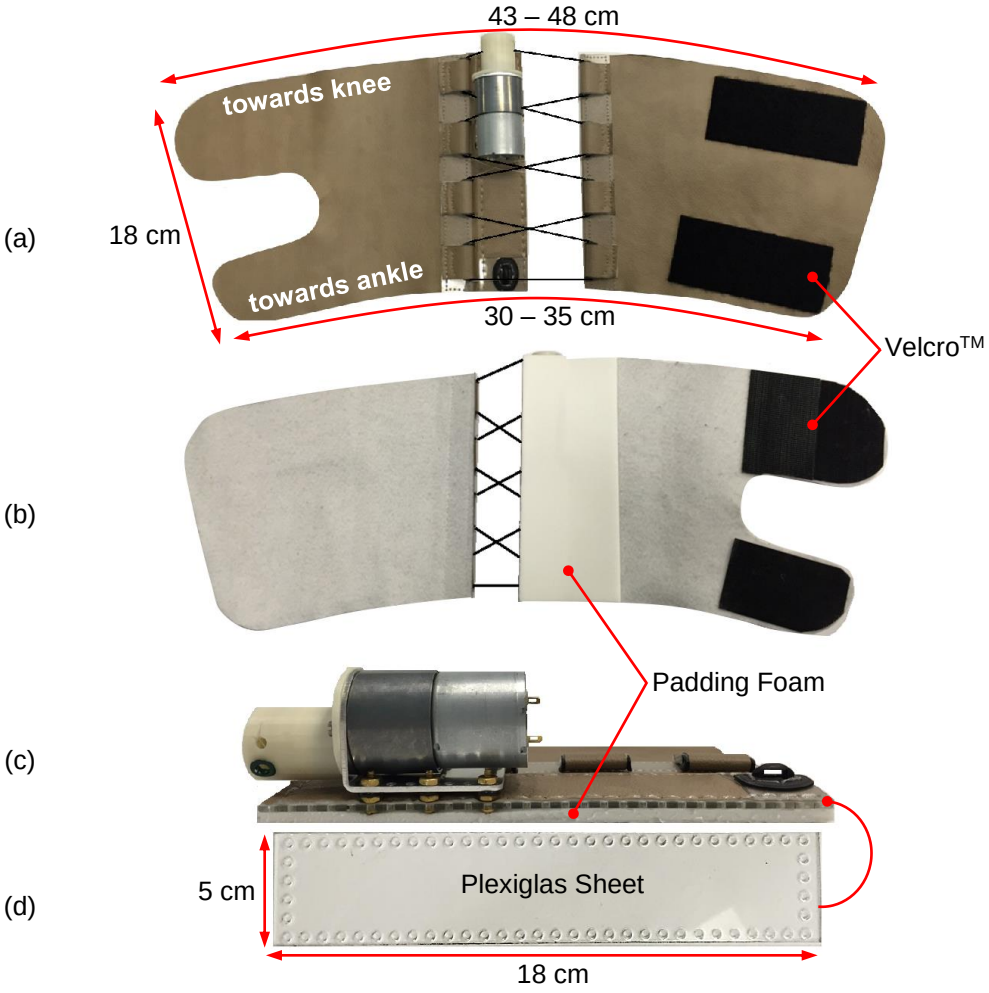

Figure 3-8 Second prototype, or ACS_v2
(a) front view, (b) back view, (c) side view, and (d) Plexiglas sheet with multiple holes as mounting base

When tested on the human leg, although ACS_v2 could successfully compress/de-compress the calf to the desired values, several problems remained that needed to be fixed for the sake of a better performance. The first drawback was that ACS_v2 pinched the anterior leg flesh, causing an unpleasant feeling in the user. As can be seen in Figure 3-8, the garment comprised of two pieces of fabric; a stationary piece and a moving one. Since the Lexan sheet and mounted compartments were fixed to just one fabric piece, making it stationary, the other piece slid on the shin, pinching it when the bandage was getting tightened. The second problem was due to the mounting location of the electrical motor. The motor was placed at the top of the

garment, with the spool and housing facing upwards. As a result, the bandage first got tightened at the top and then at the bottom upon switching the motor on. This delayed action of pressurizing was not desirable. The third and last problem which was mentioned previously, was the need of manual intervention in loosening the steel lace completely. These shortcomings necessiated the fabrication of an improved prototype that is described in the next section.

3.4.2. Final Prototype

The final prototype (ACS_v3) was very similar to ACS_v2, with minor changes (Figure 3-9). The pinching problem was elevated by replacing the Lexan sheet with a soccer shin guard. The guard was shaped to fit the leg. Moreover, it had a padding foam which eliminated the need for extra protection. Unlike the Lexan sheet, the shin guard was not sewn to the fabric. As a result, both fabric pieces could easily slide on the guard without pinching the leg. In ACS_v3, the mounting location of the motor was changed to the middle of the shin guard, with the spool and housing facing downwards. This configuration resolved the problem of delayed pressurizing which existed in ACS_v2. Lastly, the steel lace was replaced by a 4-ply fishing line. This substitution cancelled the need for manually loosening the garment. The final design conforms to various limb sizes and shapes and is capable of generating graduated pressure with rising time of ≤2 seconds and approximate maximal values of 160 and 180 mmHg over the mid- and lower calf, respectively. ACS_v3 is referred to as ACS throughout the rest of the thesis.

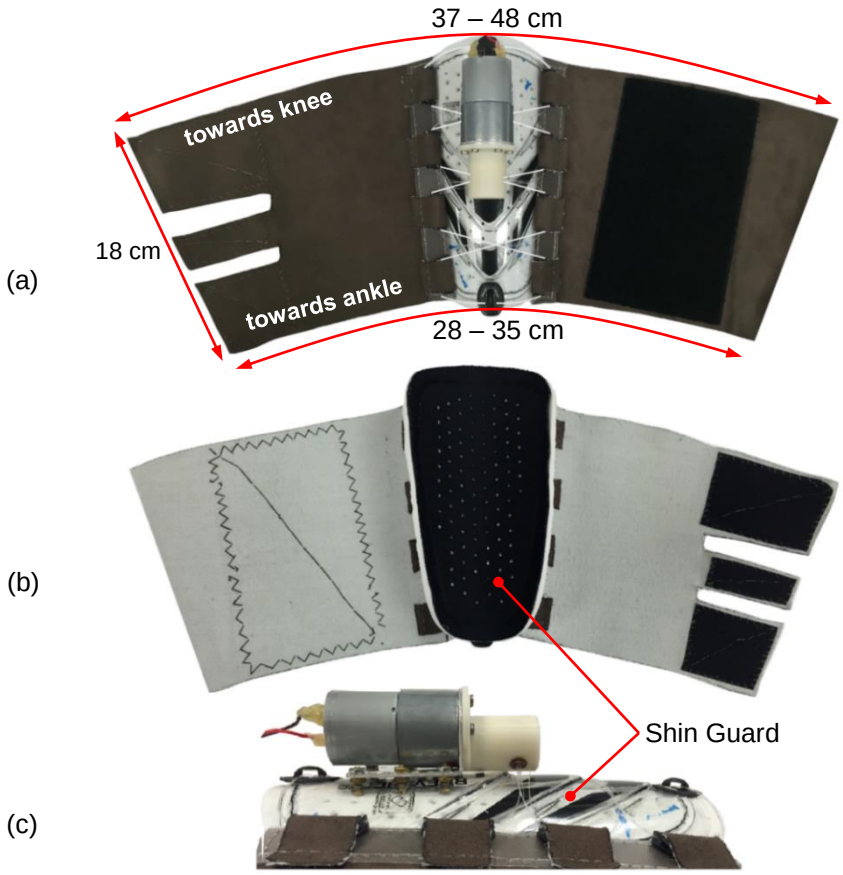

Figure 3-9 Third and final prototype, or ACS_v3
(a) front view, (b) back view, and (c) side view

3.5. Interface Pressure Measurement System

3.5.1. Measurement System Specification Terms

Researchers employ a variety of terminologies to describe measurement systems and their performance. A number of them that were used in the current study are described below.

- **Calibration:** Calibration is defined as comparing the output of a measurement system against standards of known accuracy [77].
- **Full Scale (FS):** FS refers to the difference of maximum and minimum values of the input or the span of the output measured for the input span. In this study, the value of FS is stated before being used in the calculations [77].
- **Hysteresis Error:** This term refers to the difference in the output of a measurement system given for the same input value when this value is approached from opposite directions, i.e.

ascending order or loading, and then descending order or unloading. This error is usually quantified in terms of maximum hysteresis as a percentage of FS [77]:

$$max\, E_{hysteresis} = max(\frac{\left|output_{loading} - output_{unloading}\right|}{FS_{output}}) \times 100 \quad \text{Equation 3.6}$$

The maximum hysteresis error is referred to as hysteresis error throughout the rest of the thesis.

- **Repeatability Error:** This term shows the capability of a sensor to produce the same results for repeated measurements with the same input value. It is often quantified as the percentage of FS [77].

$$max\, E_{repeatability} = max(\frac{output_{run\,1} - output_{run\,2}}{FS_{output}}) \times 100 \quad \text{Equation 3.7}$$

Henceforth, the maximum repeatability error is referred to as repeatability error.

- **Accuracy:** The accuracy of a measurement system is the extent to which its reading might be wrong and far from the true value due to all the possible errors. In this thesis, accuracy represents the combined errors of hysteresis and repeatability and is calculated using Equation 3.8 [77]:

$$Accuracy = \sqrt{{E_{hysteresis}}^2 + {E_{repeatability}}^2} \quad \text{Equation 3.8}$$

- **Relative Error:** The absolute difference between the true output and the measured output divided by the true output is referred to as the relative error. In the current study, the true output is the input pressure applied to the sensor and the measured output equals the pressure calculated from the output signal of the sensing device using data fitting [77].

$$E_{relative} = average(\frac{|true\ output - measured\ output|}{true\ output} \times 100) \quad \text{Equation 3.9}$$

3.5.2. Preparations for Calibrating and Evaluating Interface Pressure Measurement System

For continuous monitoring of the exerted pressure by the compression garment, there was a need to integrate a valid and reliable measurement system into the device with the desired characteristics, including appropriate geometry, flexibility, accuracy, capability of being used in a closed-loop controller, compatibility with human skin, cost-effectiveness, and ease of application. Most of the commercially available sub-bandage pressure measurement systems are expensive,

complex to use, difficult to calibrate, and not portable [78]. Thus in the current study, force-sensing resistors (FSRs®), which are portable, thin, flexible, low-cost, and easy-to-use sensors, were investigated.

The Interlink Electronics FSR® 400 Series, which is part of the single zone force-sensing resistor family, met the requirements of the study [79]. Among six different models of the FSR® 400 Series sensors, two were picked for interface pressure measurement ─models 402 and 408.

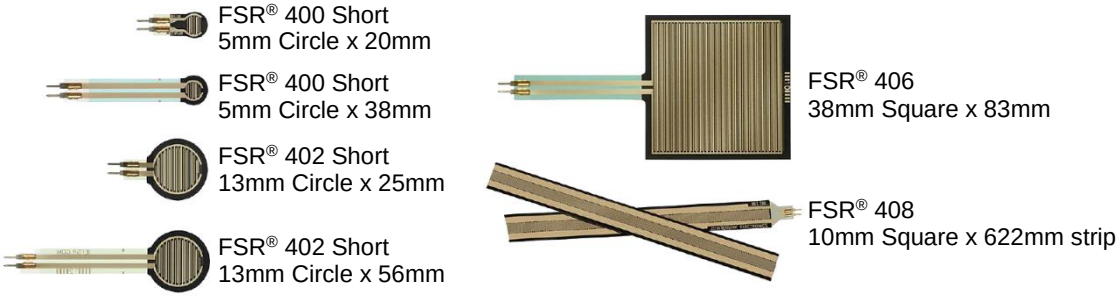

Figure 3-10 Interlink Electronics FSR® 400 Series[1]

A force-sensing resistor, or FSR®, is a sensor that allows for detecting physical pressure, squeezing and weight. It is basically a resistor that exhibits a decrease in resistance with increase in the force applied to the surface of the sensor. The FSR® consists of two polymer layers separated by a spacer; one layer is covered with a semi-conductive material, and the other layer is made up of two sets of interdigitated electrodes that are electrically distinct and each set is connected to one trace on a tail. When there is no force, the resistance between the electrodes is so high and the sensor acts like an infinite resistor (open circuit). The more the FSR® is pressed, the more interdigitated elements get in contact with the semiconductor, causing a short circuit. As a result, the resistance goes down. FSRs® are fairly simple to use and low cost. The exploded view of an FSR® is represented in Figure 3-11 .

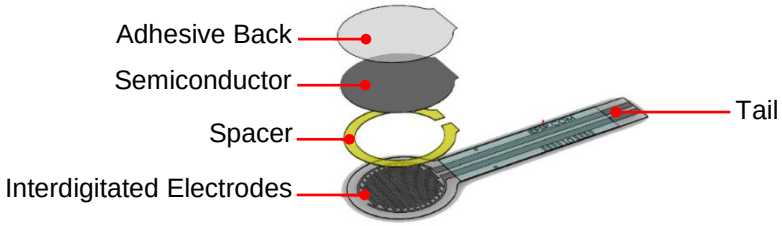

Figure 3-11 Different layers of an FSRs®[2]

[1] reproduced from [79]

[2] adapted from [79]

Like many other flexible resistive sensors, a force-sensing resistor is known for its qualitative rather than quantitative measurements. Therefore, FSR® needs to be validated for clinical use. In other words, a mathematical relationship should be found between its output signal and the exerted pressure on its surface, called the calibration function. Herein, the FSR® was calibrated and evaluated in six subsequent attempts. In all cases, the same approach was adopted:

1. The FSR® was incorporated into an excitation circuit.
2. The sensor was pressurized and depressurized using either the ACS_v1 or a regular blood pressure arm cuff with an inflation pump (Figure 3-12).
3. The applied pressure and FSR's® output voltage were recorded. Pressure was monitored utilizing a reference measurement system, which was either the pressure gauge connected to the arm cuff (sphygmomanometer) or a commercially available device called PicoPress® (MediGroup, Melbourne, Australia). The PicoPress® is a portable pneumatic transducer for pressure measurement beneath medical bandages in both static and dynamic conditions.
4. A calibration function was extracted.
5. The FSR® was evaluated on human leg to assess its performance in measuring known pressures applied to the calf and investigate the efficacy of the extracted calibration function in converting output voltages to equivalent pressure values.
6. After reviewing the results of the 5th step, necessary measures were taken to improve the next attempt and steps 1 through 5 were repeated. These measures were either replacing the sensor (FSR® 402 vs. FSR® 408), or changing the surface on which the FSR® was calibrated (including a rigid ABS pipe with a diameter of 0.075 meters, the ABS pipe covered with adhesive foam, and human calf). The pipe is referred to as the *test rig* henceforth.

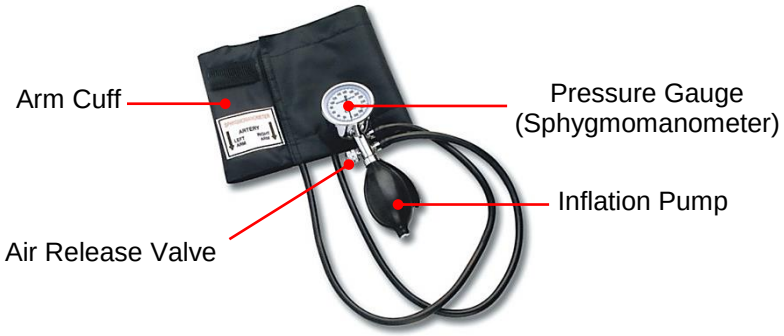

Figure 3-12 Blood pressure arm cuff and accessories[1]

As suggested by the manufacturer, in all five attempts towards FSR® pressure-to-voltage conversion (or calibration), a voltage divider was used as the excitation circuit [79].

[1] reproduced from [110]

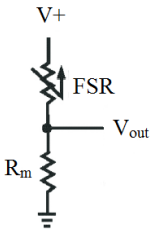

Figure 3-13 Voltage divider used for FSR® calibration[1]

R_m is the measuring resistor with a known resistance. The circuit was powered by V_+ of 5 V and Equation 3.10 was used to calculate the output:

$$V_{out} = \frac{R_m V_+}{R_m + R_{FSR}} \qquad \text{Equation 3.10}$$

In the depicted configuration, the output voltage increases with increasing pressure. After placing different values of R_m in the excitation circuit, a family of pressure versus V_{out} curves were plotted and fitted, and a calibration function was extracted based on each graph. The tested measuring resistors were 3.3, 10, 30, 47, and 100 kΩ. Finally, an R_m which maximized the desired pressure sensitivity range and limited the current was chosen for further experiments.

Before starting the calibration process, two experiments were conducted in order to investigate whether or not the reference measurement devices, i.e. the PicoPress® transducer and the sphygmomanometer, produce reliable and consistent results. In the first experiment, the sphygmomanometer values were compared to a high performance pressure transducer. A test set-up was used which was designed and developed by Pourazadi et al. to measure the exerted pressure by medical bandages [80]. The set-up consisted of a customized calf prototype and a pressure transducer (Omegadyne PX309-001G5V) connected to it. The prototype had three separate chambers mimicking different regions of human calf. Sealed individually, each chamber could be filled with a fluid (liquid or gas) and its pressure was monitored with the pressure transducer connected to the chamber via tubes.

[1] adapted from [79]

Figure 3-14 Calf prototype[1]

After filling the middle chamber of the calf prototype with water, the arm cuff was wrapped around it. The manual pump was used to inflate and deflate the cuff from 0 to 50 mmHg and 50 to 0 mmHg, respectively, with 30 seconds of 10 mmHg increments. Greater pressures were not exerted to prevent any possible damages to the test set-up. The tests were repeated three times and the output signal of the pressure transducer was recorded using a data acquisition board and a customized program written in NI LabVIEW 2013 (National Instruments, Texas, USA). Column charts of the averaged data of the tests are illustrated in Figure 3-15. The results showed that there is consistency between sphygmomanometer and the high performance pressure transducer. The hysteresis and repeatability errors of the high performance pressure transducer were 1% and 2%, respectively. The overall accuracy of the sensor was ±2%FS with an FS of 50 mmHg, i.e. ±1mmHg.

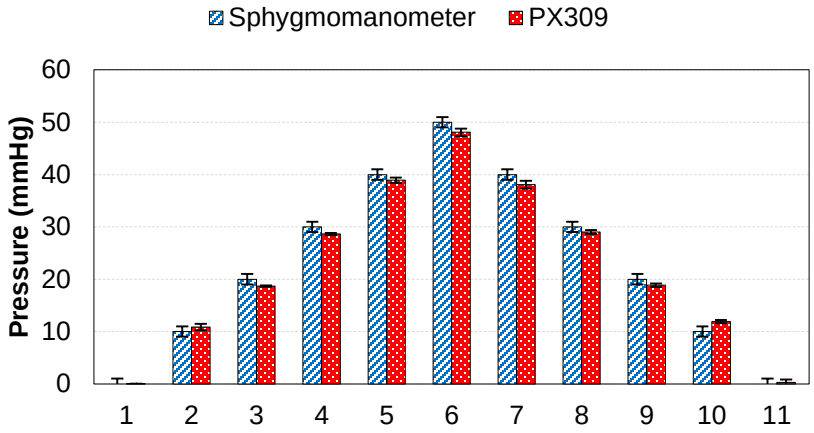

Figure 3-15 Pressure comparison between sphygmomanometer and PX309
The bars are standard deviations.

In the second experiment, the PicoPress® transducer was compared to the sphygmomanometer. The PicoPress® probe was placed on the test rig and covered with the arm

[1] adapted from [80]

cuff. It was assumed that the intra-cuff pressure was almost equal to the interface pressure. Repeated for three times, the cuff was manually inflated in 10 mmHg increments from 0 to 120 mmHg followed by 10 mmHg decrements from 120 to 0 mmHg, with each pressure level lasting for 30 seconds. PicoPress® data were recorded using the furnished operating software by the manufacturer. The results were averaged and plotted as shown in Figure 3-16. The hysteresis, repeatability, relative errors of the PicoPress® were 4%, 7%, and 23% respectively.

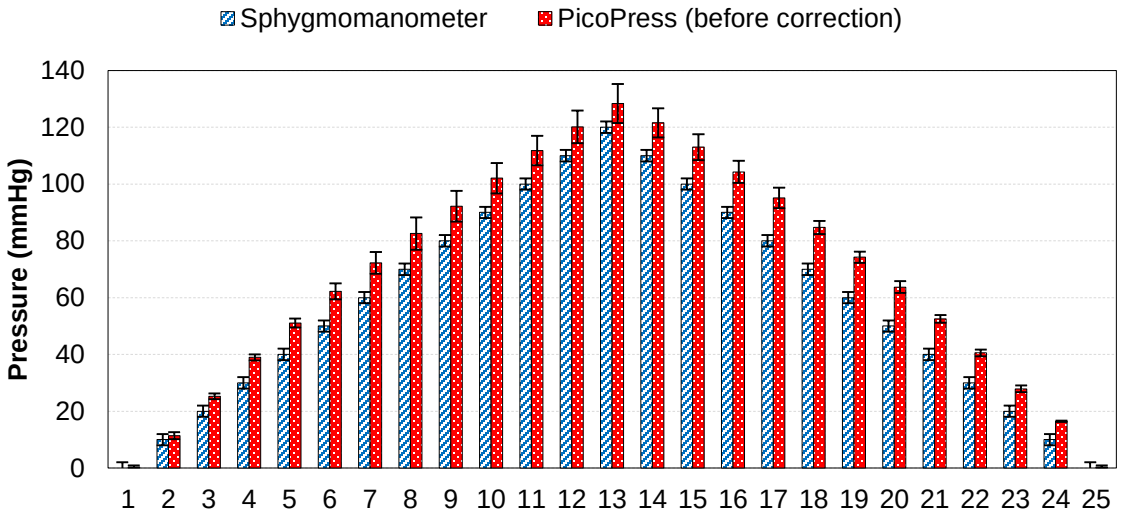

Figure 3-16 Pressure comparison between sphygmomanometer and PicoPress® (before correction)
The bars are standard deviations.

Substantial differences were found between the two devices; the PicoPress® overestimated pressure values. According to Vinckx et al., this could have happened due to the effect of physical dimensions of the probe on interface pressure [81].

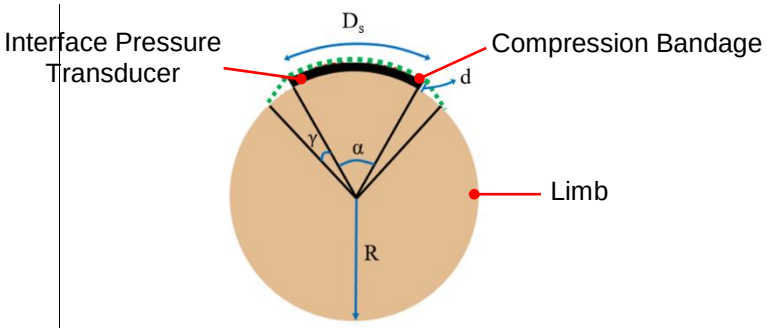

Figure 3-17 Schematic representation of perturbation effect of interface pressure transducer's physical dimensions[1]

[1] adapted from [81]

Therefore, PicoPress® output was multiplied by a correction factor (C_f) which was derived using Equation 3.11:

$$C_f = \frac{1}{C_{pp}} \quad \text{Equation 3.11}$$

C_{pp} is coefficient of pressure perturbation:

$$C_{pp} = \frac{sin(\alpha/2 + \gamma)}{sin(\alpha/2)} \quad \text{Equation 3.12}$$

$$\alpha = \frac{D_s}{R} \quad \text{Equation 3.13}$$

$$\gamma = arccos(\frac{R}{R + d}) \quad \text{Equation 3.14}$$

In Equation 3.13 and Equation 3.14, d is sensor thickness when inflated, D_s is sensor diameter, and R is limb (test rig in this case) radius, all measured in meters [81].

PicoPress® pressures were plotted again after applying the correction factor. As can be seen in Figure 3-18, better results were achieved with more closeness to the sphygmomanometer response. As a result of using the correction factor, the relative error of the PicoPress® considerably improved to 11%, which is less than half of the previous value.

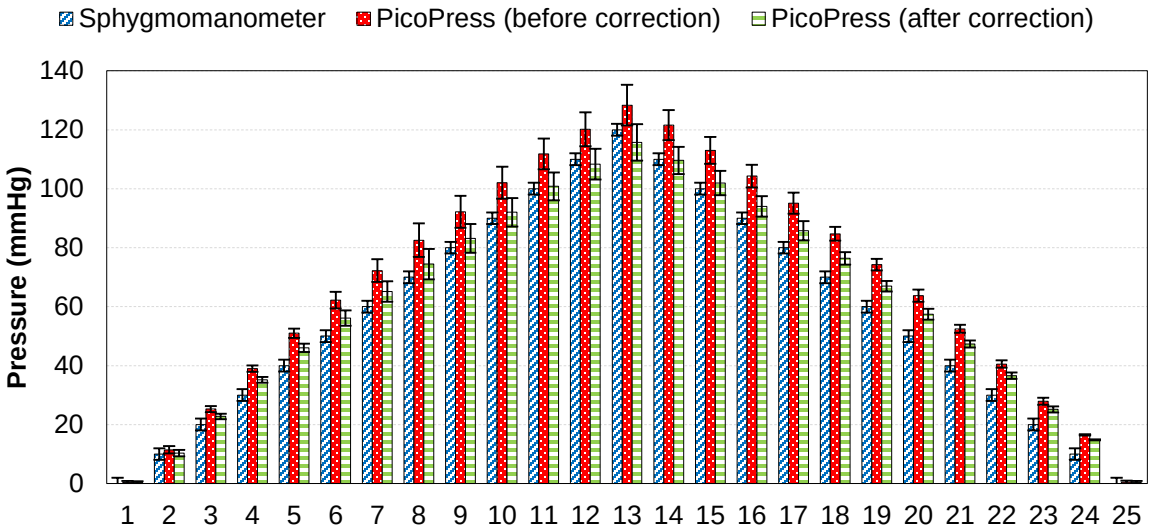

Figure 3-18 Pressure comparison between sphygmomanometer and PicoPress® (before & after correction)
The bars are standard deviations.

Table 3-2 PicoPress® characteristics before and after applying correction factor (FS=120 mmHg)

Corrected?	PicoPress®				
	$E_{hysteresis}$ (%)	$E_{repeatability}$ (%)	Accuracy (%)	Accuracy (mmHg)	$E_{relative}$ (%)
Before correction	4	7	8	±10	23
After correction	4	6	7	±9	11

Although finer outcomes were attained by applying the correction factor to the PicoPress® output when it was used on the rigid surface of the test rig, further investigations showed that while placed on soft surfaces, there were negligible differences between the PicoPress® and sphygmomanometer. As a result, throughout the later experiments, application of the correction factor was limited to when the probe was placed on the rigid test rig rather than soft surfaces.

3.5.3. Calibration and Evaluation of Force-Sensing Resistors

Before addressing the calibration and evaluation processes of the FSRs®, a number of points should be highlighted in order to avoid repetition:

- Two sensors were chosen for interface pressure measurement among six different models of the FSR® 400 Series sensors: (a) FSR® 402 which has a circular active area with diameter of 14.68 mm and nominal thickness of 0.46 mm. This sensor is referred to as *circular FSR®* in the rest of the thesis, and (b) FSR® 408 which is a long sensor with an active area of 609.6 × 10.2 mm^2 and nominal thickness of 0.41 mm. Since a sensor shorter in length was needed for the current study, this FSR® was cut into a smaller piece with an active area of 50 × 10.2 mm^2. The truncated sensor is referred to as *rectangular FSR®* henceforward.

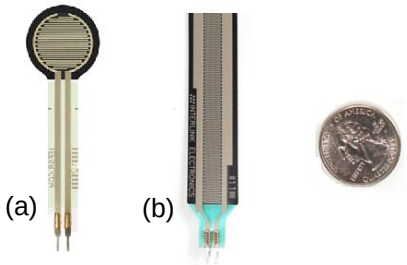

Figure 3-19 Selected sensors for the experiments
(a) circular FSR®, (b) rectangular FSR®

- Output of the excitation circuit was acquired with a sampling frequency of 1000 Hz using an analog-to-digital converter (National Instruments USB-6002, Texas, USA), and

subsequently routed to NI LabVIEW 2013 (National Instruments, Texas, USA). A program was written in LabVIEW to collect the signal, calculate the DC and root mean square (RMS) values of it using the built-in Averaged DC-RMS VI, and store it for further offline analysis.

- PicoPress® data acquisition was done using the provided operating software by its manufacturer.
- In the experiments with the developed compression device as the pressurizing device, the motor was controlled manually to tighten or loosen the garment and reach the desired pressure value.
- Microsoft Excel 2013 and MATLAB R2012b (The MathWorks Inc, Massachusetts, USA) were employed for the sake of data analysis and fitting.

As highlighted previously, five attempts were made to validate the FSRs®. Prior to succeeding to the detailed explanation of each procedure, the conditions of all calibration attempts and the corresponding evaluation trials are summarized in Table 3-3.

Table 3-3 Summary of FSRs® calibration and evaluation conditions

Condition	**Calibration Attempt**				
	1st	*2nd*	*3rd*	*4th*	*5th*
FSR® Type	Circular, Rectangular	Circular, Rectangular	Rectangular	Rectangular	Circular
Calibration Surface	ABS Pipe	ABS Pipe	Foam-covered ABS Pipe	Human Leg (subject A)	Human Leg (subject A)
Pressure (mmHg)	0 – 110 – 10	0 – 110 – 10	0 – 110 – 10	0 – 90 – 10	0 – 90 – 10
Increment (mmHg)	10	10	10	10	10
Pressure Level Duration (s)	30	30	30	15	15
R_m *(kΩ)*	3.3, 10, 30, 47	3.3, 10, 30, 47, 100	3.3, 10, 30, 47, 100	10	10
Test Repeats per R_m	2	2	2	3	3
Condition	**Evaluation Attempt**				
	1st	*2nd*	*3rd*	*4th*	*5th*
FSR® Type	N/A	Rectangular	Rectangular	Rectangular	Circular
Number of FSRs®	N/A	1	1	1	3
Subject	N/A	A	A	A	A, B, C
Pressure Level Duration (s)	N/A	15	15	15	15
R_m *(kΩ)*	N/A	10	10	10	10
Test Repeats per Subject	N/A	1	1	1	3

Each attempt is thoroughly discussed as follows.

1st Attempt

In the first attempt towards sensor calibration, the rectangular and circular FSRs®, and the PicoPress® transducer were placed on the rigid test rig, 0.5 cm apart from each other.

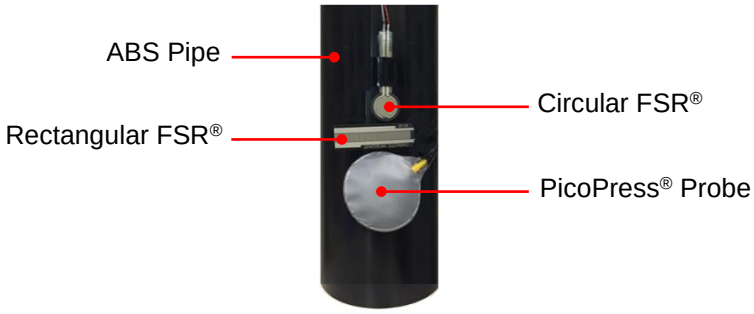

Figure 3-20 FSRs® placement on test rig in 1st calibration trial

Once the ACS_v1 was wrapped around the test rig covering the sensors, the garment was activated to apply pressure in 10 mmHg increments from 0 to 110 mmHg followed by 10 mmHg decrements from 110 to 10 mmHg, with each pressure level lasting for 30 seconds.

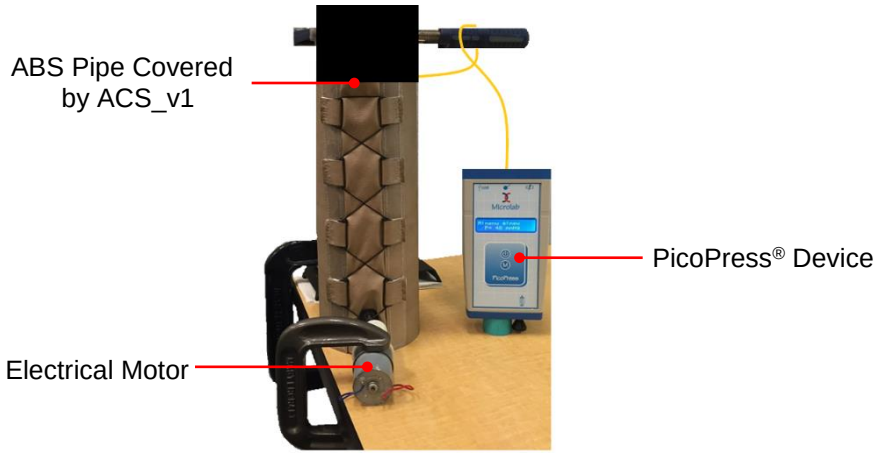

Figure 3-21 Experimental setup for FSR® calibration in 1st trial

Reaching a complete untightened and loose stage in the garment was impossible without manual intervention; hence the descending step was not continued further than 10 mmHg. The tests were repeated twice for four different R_m values, including 3.3, 10, 30, and 47 kΩ. Data, including the output voltage and corrected PicoPress® pressure, were averaged through the last 10 seconds of each test level, 5 seconds prior to switching to the next level. Plotted curves of the corrected interface pressure versus output voltage for both sensors showed that neither the rectangular nor the circular FSR® could detect pressure values less than 45 mmHg. The PicoPress® probe thickness is 0.2 mm when it is not inflated and 3 mm when it is inflated. This could have prevented

the FSRs® from getting exposed to pressures smaller than 45 mmHg. Moreover, there was a significant difference between loading and unloading graphs. Insensitivity of the sensors to a big range of applied pressures along with the noticeable amount of hysteresis made the results unreliable, and necessitated the need for repeating the tests with another approach. Table 3-4 summarizes the hysteresis and repeatability errors of the rectangular and circular FSRs®, along with their overall accuracy.

Table 3-4 Characteristics of FSRs® in 1st calibration trial (FS=65 mmHg)

R_m (kΩ)	Rectangular FSR®				Circular FSR®			
	$E_{hysteresis}$ (%)	$E_{repeatability}$ (%)	Accuracy (%)	Accuracy (mmHg)	$E_{hysteresis}$ (%)	$E_{repeatability}$ (%)	Accuracy (%)	Accuracy (mmHg)
3.3	18	10	21	±13	37	11	38	±25
10	18	19	27	±17	34	10	36	±23
30	16	4	17	±11	46	6	46	±30
47	21	8	23	±15	40	14	42	±27
Average	19	10	22	±14	39	10	41	±26

2nd Attempt

Every step of the first effort described above was repeated in the second attempt, i.e. pressurizing and de-pressurizing phases, number of test repeats for different R_m values, multiplying interface pressure by the correction factor, and data averaging. The only major difference was that the FSRs® were placed beneath the PicoPress® probe once at a time in order to overcome the sensors reading problem. Moreover, an R_m of 100 kΩ was also tested.

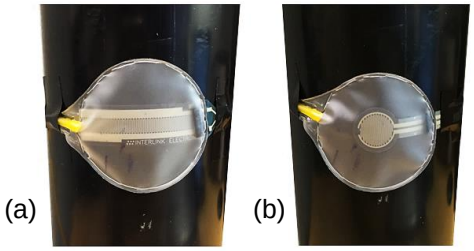

Figure 3-22 Placement of FSRs® beneath PicoPress® probe in 2nd calibration trial
(a) rectangular FSR®, (b) circular FSR®

Table 3-5 summarizes the hysteresis and repeatability errors, and the overall accuracy of the sensors. During the experiments, it was noticed that the FSRs® were not sensitive to pressure values smaller than 10 mmHg. Therefore, the corresponding numbers were excluded from the error calculations.

Table 3-5 Characteristics of FSRs® in 2nd calibration trial (FS=100 mmHg)

R_m (kΩ)	Rectangular FSR®				Circular FSR®			
	$E_{hysteresis}$ (%)	$E_{repeatability}$ (%)	Accuracy (%)	Accuracy (mmHg)	$E_{hysteresis}$ (%)	$E_{repeatability}$ (%)	Accuracy (%)	Accuracy (mmHg)
3.3	4	2	5	±5	3	2	4	±4
10	4	2	5	±5	4	5	6	±6
30	5	2	6	±6	6	5	8	±8
47	5	8	9	±9	10	21	23	±23
100	8	4	9	±9	8	12	14	±14
Average	5	4	7	±7	6	9	11	±11

The curve fitting toolbox in MATLAB was employed to fit the data with either one or two-term exponential models and extract the calibration functions for both the rectangular and circular FSRs®. The fitted plots are displayed in Figure 3-23.

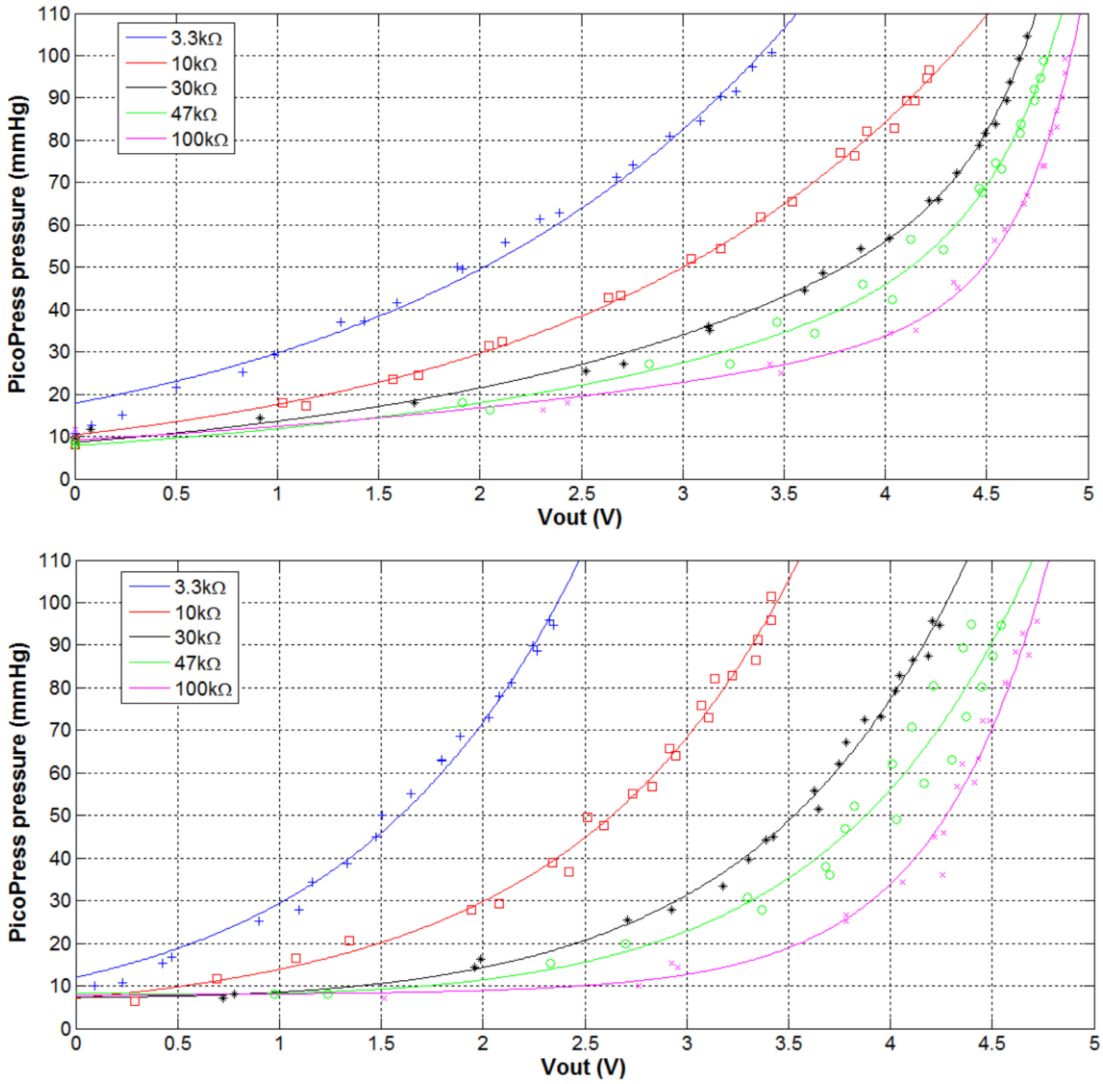

Figure 3-23 A family of PicoPress® pressure vs. V_{out} curves for different R_m values in 2nd calibration trial *(top) rectangular FSR®, (bottom) circular FSR®*

In the graphs with same R_m, the rectangular FSR® had higher output voltages than the circular FSR® given for the same pressure values. Moreover, R_m = 10 kΩ met the needs of the study in terms of pressure sensitivity. As a result, the rectangular sensor with R_m = 10 kΩ was selected for the next experiment.

In order to assess the rectangular FSR's® performance in measuring pressure accurately on soft tissue, it was tested on human leg. The sensor was vertically placed on the bare mid-calf of an individual while seated on a stool with the knees flexed at 90°, and the PicoPress® probe was put on top of it. ACS_v2 was wrapped around the subject's calf, covering both sensors, and activated to exert 10 pressure levels, each for 15 seconds. The calibration function, which was

derived beforehand, was employed to convert the output voltage to the equivalent pressure values. Comparing the calculated pressures with the corresponding values measured by the PicoPress® revealed big differences, showing that the rectangular FSR® overestimated the applied pressure, in some cases double the true value. The average relative error of the FSR® was 151%.

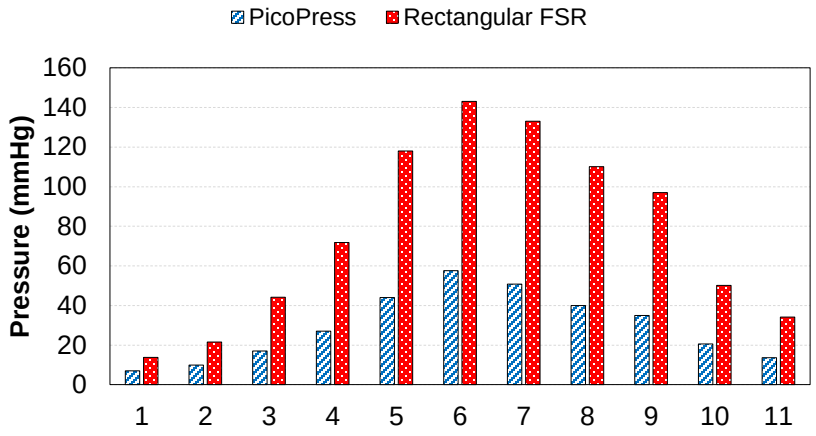

Figure 3-24 Pressure comparison between PicoPress® and calibrated rectangular FSR® on leg

The inconsistency between the sensors was thought to be a consequence of calibrating the FSR® on the rigid surface of the test rig while evaluating it on soft tissue. Therefore, the sensor was calibrated over a soft surface in the next attempt.

3rd Attempt

Following the poor performance of the rectangular FSR® on human leg, it was decided to calibrate the sensor on a surface more similar to human leg in terms of softness. To do so, the test rig was covered by two layers of a relatively soft adhesive foam. After placing the FSR® and PicoPress® probe on the foam-covered rig, the blood pressure arm cuff was used for pressurizing and de-pressurizing the sensors.

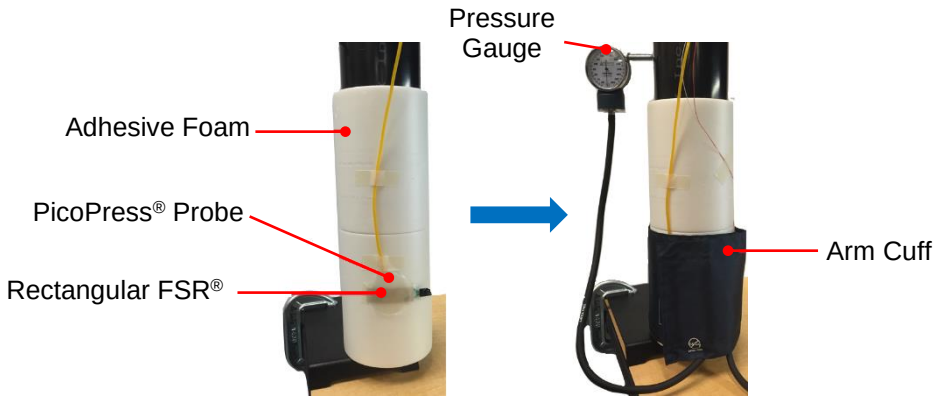

Figure 3-25 Experimental setup in 3rd calibration trial

The calibration process and evaluation on human leg were done in a similar manner as the previous attempt. The hysteresis and repeatability errors, and the overall accuracy of the rectangular FSR® are summarized in Table 3-6.

Table 3-6 Characteristics of rectangular FSR® in 3rd calibration trial (FS=110 mmHg)

R_m (kΩ)	Rectangular FSR®			
	$E_{hysteresis}$ (%)	$E_{repeatability}$ (%)	Accuracy (%)	Accuracy (mmHg)
3.3	10	2	10	±11
10	12	4	13	±14
30	12	9	15	±16
47	12	3	12	±13
100	9	2	9	±10
Average	11	4	12	±13

The data were fitted by exponential models and calibration functions were extracted.

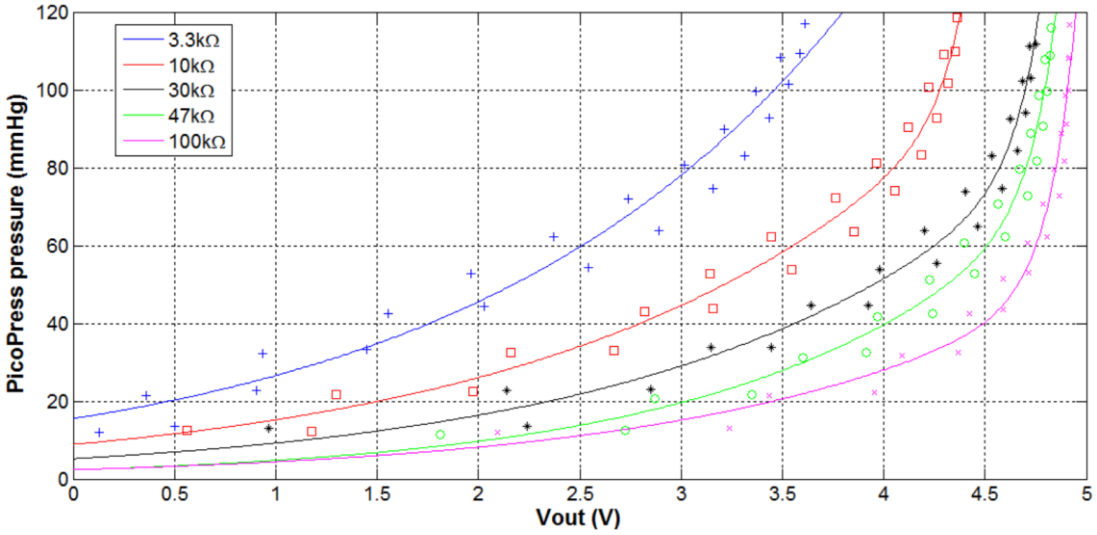

Figure 3-26 A family of PicoPress® pressure vs. V_{out} curves for different R_m values in 3rd calibration trial of rectangular FSR®

The R_m = 10 kΩ was chosen for the evaluation process on human leg. Disappointingly, inconsistent results between the FSR® and PicoPress® were achieved once again. The average relative error of the FSR® was 49%.

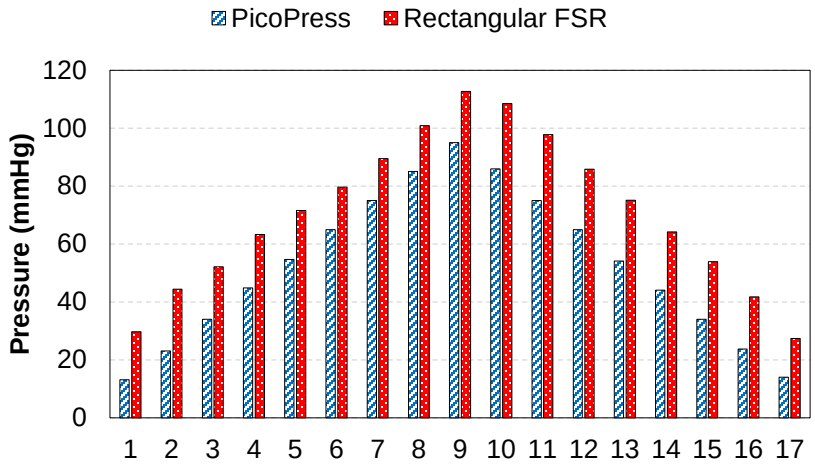

Figure 3-27 Pressure comparison between PicoPress® and calibrated rectangular FSR® on leg

4th Attempt

Although the rectangular FSR's® performance in measuring applied pressures on human leg was not satisfactory, the decline in relative error from 151% in the 2nd trial to 49% in the 3rd trial revealed that the calibration surface played an important role in the outcomes. This begot the idea of calibrating the FSR® on human leg rather than the test rig. In this test, the rectangular FSR® was placed beneath the PicoPress® probe on an individual's calf while covered with the arm cuff. The individual who participated in the test is referred to as subject_A henceforth. The R_m = 10 kΩ was used in the excitation circuit. Using the cuff, the calf was sequentially pressurized from 0 to 90 mmHg with 10 mmHg increments, and de-pressurized from 90 to 0 mmHg with 10 mmHg decrements, with each level lasting for 15 seconds. The experiment was repeated three times and the averaged data of the tests were fitted by an exponential model to find the calibration function. The hysteresis and repeatability errors of the rectangular FSR® are represented in Table 3-7.

Table 3-7 Characteristics of rectangular FSR® in 4th calibration trial (FS=80 mmHg)

	Rectangular FSR®			
R_m (kΩ)	*$E_{hysteresis}$ (%)*	*$E_{repeatability}$ (%)*	*Accuracy (%)*	*Accuracy (mmHg)*
10	12	3	12	±10

Figure 3-28 depicts the averaged data points along with the fitted curve.

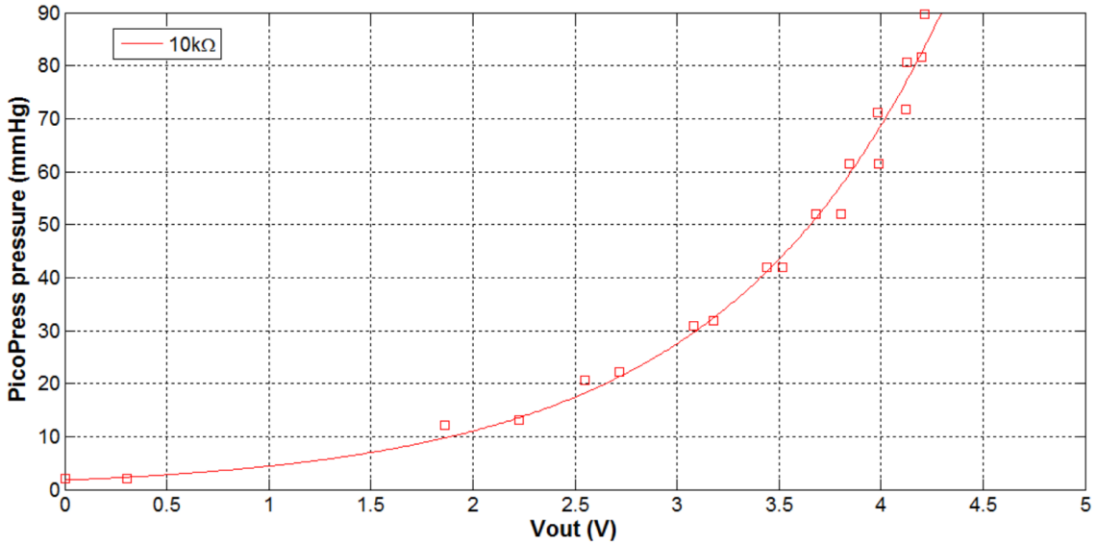

Figure 3-28 PicoPress® pressure vs. V_{out} curve for R_m = 10 kΩ in 4th calibration trial of rectangular FSR®

Once the calibration function was extracted, the rectangular FSR® was evaluated on subject_A's bare leg. The sensor's relative error was 33%.

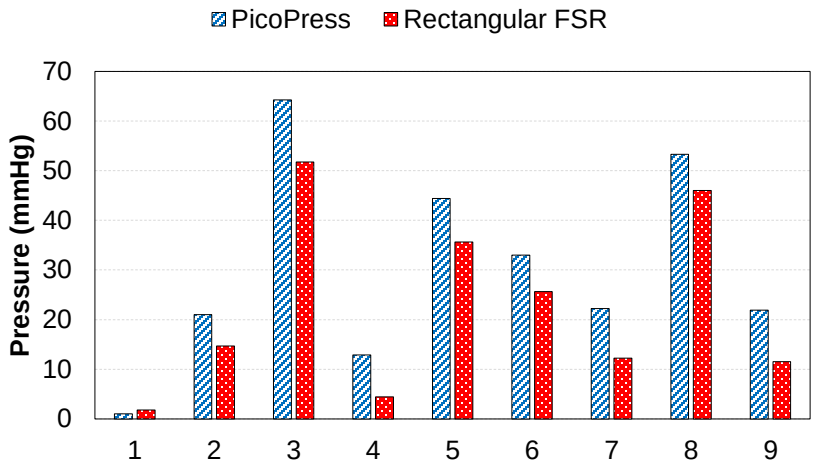

Figure 3-29 Pressure comparison between PicoPress® and calibrated rectangular FSR® on subject_A

5th Attempt

The results of the 4th evaluation trial revealed that the relative error of the rectangular FSR®, which was calibrated on human calf, had decreased to 33% in comparison with the 3rd attempt with an error value of 49%. Despite the improvement, the results were not satisfactory

enough for the sensor to be used in the next experiments. Thus an alternative strategy was devised. The rectangular FSR® was replaced by six circular FSRs® and each sensor was calibrated individually on subject_A following the same steps as the 4th trial. The results are summarized in Table 3-8.

Table 3-8 Characteristics of circular FSRs® in 5th calibration trial (R_m=10 kΩ, FS=80 mmHg)

FSR_x	Circular FSR®			
	$E_{hysteresis}$ (%)	$E_{repeatability}$ (%)	Accuracy (%)	Accuracy (mmHg)
FSR_a®	6	3	7	±5
FSR_b®	9	2	9	±7
FSR_c®	13	2	13	±10
FSR_d®	7	5	9	±7
FSR_e®	7	5	8	±7
FSR_f®	6	3	7	±5
Average	8	3	9	±7

The acquired data were used to find a calibration function for each circular FSR® (Figure 3-30).

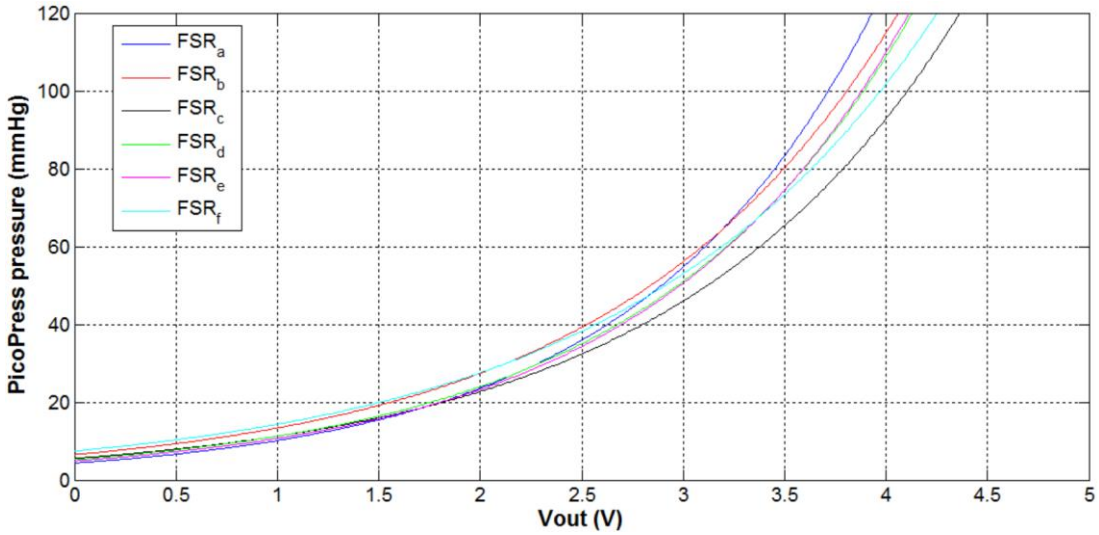

Figure 3-30 A family of PicoPress® pressure vs. V_{out} curves for R_m = 10 kΩ in 5th calibration trial of six circular FSRs®

Once the circular FSRs® were calibrated, their performance was investigated on human calf and compared to the reference pressure measurement system, i.e. the PicoPress®. Unlike the previous four attempts with only one FSR®, an array of three circular FSRs®, arranged in the form of a 3×1 matrix, was used to increase the sensing area and decrease measurement errors by averaging the sensors' outputs (Figure 3-31).

Figure 3-31 Array of three circular FSRs® placed on human calves

The FSRs® array was evaluated not only on subject_A, but also on two other individuals: subject_B and subject_C. Every subject underwent three evaluation experiments, with each test consisting of seven pressure levels. The PicoPress® pressure was then compared to that of the FSRs® array and relative errors were calculated. The results are presented in Figure 3-32 and Table 3-9.

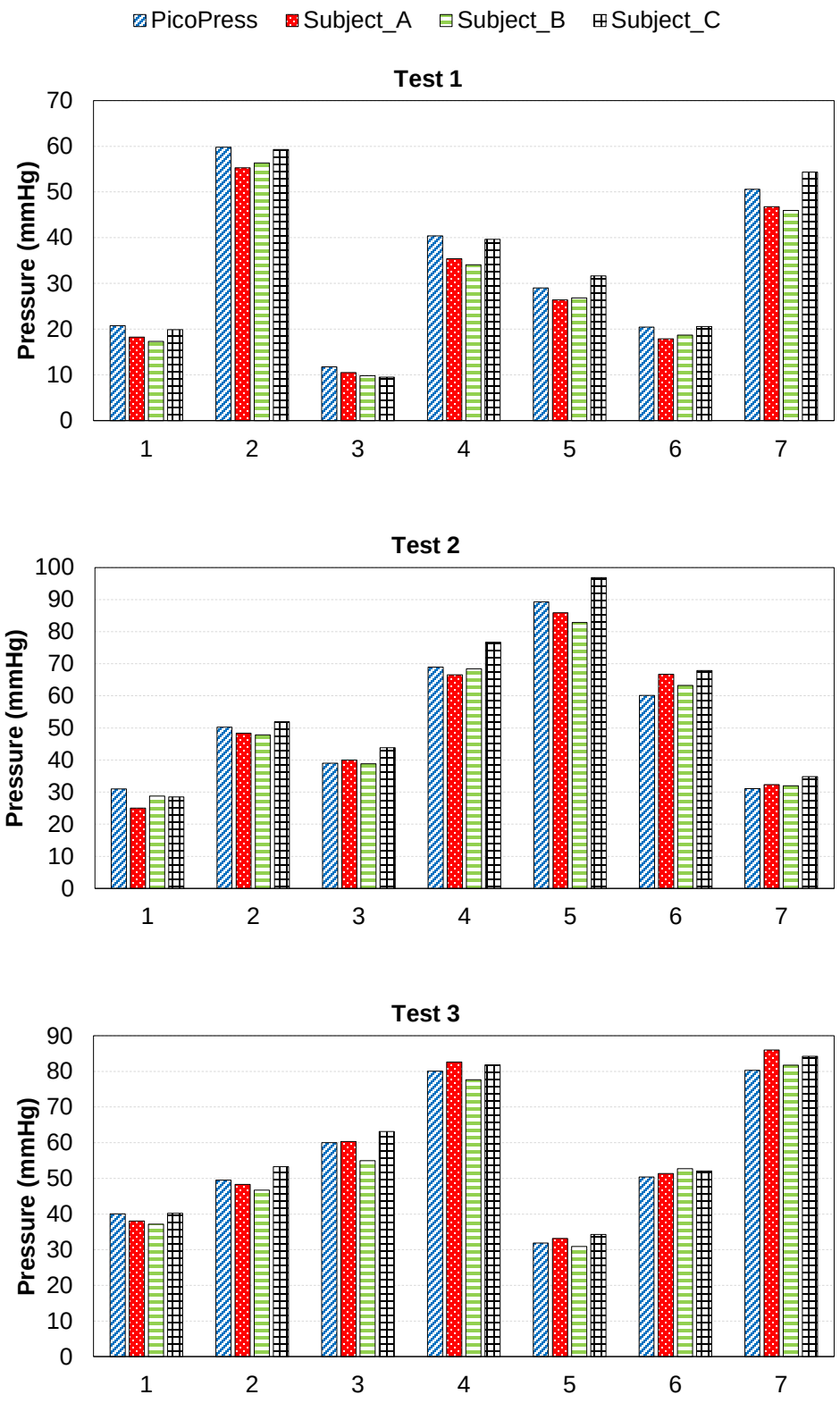

Figure 3-32 Pressure comparison between PicoPress® and array of circular FSRs® in three tests on subject_A, subject_B, and subject_C

Table 3-9 Percentage of relative error in pressure readings of circular FSRs® array

Test	$E_{relative}$ (%)		
	Subject_A	*Subject_B*	*Subject_C*
1	10	11	5
2	6	4	8
3	4	4	4
Average	7	6	6

The circular FSRs® that were calibrated on subject_A, showed promising results when tested as an array on other individuals. Considering significant improvements in the relative error values to 7% and less, the calibration and evaluation processes were discontinued at this point and the functions achieved in the 5th attempt were used in the human tests, which are thoroughly discussed in the Chapter 4.

3.6. Summary

The first objective of the study, which was to develop a new adaptive compression system for ameliorating venous stasis and enhancing venous return, was addressed in this chapter. The objective had two aspects, each of which was discussed in a separate section. In the first part, the design and fabrication of a motorized compression garment was explained. The final prototype of the proposed device consisted of laces, which were attached to a piece of non-stretchable, flexible fabric at one end and connected to a motor at the other end. Upon motor rotation, the sides of the fabric got closer/farther, resulting in tightening/loosening the garment, and consequently compressing/de-compressing the limbs.

In the second part, circular and rectangular force-sensing resistors were calibrated and tested to assess their capability in reporting sub-bandage pressure. Calibration took place on different surfaces. The circular FSRs® exhibited relatively low hysteresis and repeatability errors, i.e. 8% and 3%, respectively. Moreover, the results revealed that the more the calibration surface was close to human tissue in terms of softness, the less the FSR®s' relative error would be. After calibrating on a rigid surface and testing on leg tissue, the relative error was approximately 151% for the rectangular FSR®. The error value decreased to around 48% when the same FSR® was calibrated on a less rigid surface. When both calibration and evaluation processes were done on human leg, the relative error declined to 33%. Finally, circular FSRs® were substituted for their rectangular counterparts, calibrated on a volunteer, and evaluated in form of an array on the same participant as well as other individuals. Taking the average of sensors' output led to significantly

better pressure readings with relative error values of smaller than 7%. Based on the results, it can be claimed that an array of multiple force-sensing resistors has the potential to be used in monitoring the interface pressure during leg compression therapy.

Chapter 4. Experimental Assessment of ACS Prototype

4.1. Ethics Statement

Ethical approval was obtained from the Simon Fraser University Department of Research Ethics. All subjects followed the informed consent procedure and provided written consent.

4.2. Study Design

In section 2.1.3, it was highlighted that a considerable volume of blood redistributes to the lower extremities upon standing due to gravitational forces. Without the operation of counteractive mechanisms, one of which is the calf muscle pump, prolonged motionless standing causes venous hypertension and excessive accumulation of fluid within the leg tissue; reduces venous return, stroke volume (thus cardiac output), and cerebral perfusion; and leads to orthostatic hypotension in addition to syncope. If the reduction of venous return and stroke volume could be compensated prior to the consequent cerebral hypo-perfusion, syncope would be prevented. As mentioned in the previous chapters, lots of the existing compression therapy modalities have been proven to be ineffective in passive orthostasis; this can be attributed to their incapability in generating waveform pressure to compensate for the lack of calf muscle pump action. Employing these concepts, a controlled pilot experiment was designed to assess the performance of the developed adaptive compression system in pumping blood back to the heart from the lower legs by monitoring its capability of preventing stroke volume decline during simulated passive standing. It was hypothesized that the ACS is an effective intervention for improving venous return through the exertion of intermittent compression over the lower leg.

A total of 12 healthy adults took part in the study (Table 4-1). In order to induce autonomous and hemodynamic responses identical to standing erect and create the needed shift in blood volume from the thoracic circulation to the lower extremities circulation, graded lower

body negative pressure (LBNP) was used. The LBNP is a procedure that is used to simulate the cardiovascular responses associated with orthostatic stress and hemorrhage (blood loss from the circulatory system) in humans while facilitating measurements [82, 83, 84]. During LBNP, air is vacuumed from a box that encloses the lower body below the iliac crests. Consequently, pressure decreases in the box and blood gets translocated to the legs, resulting in increased venous pooling; and decreased venous return, preload and cardiac output [82]. These changes are similar to hemodynamic alterations during upright standing and hemorrhage (while maintaining total blood volume).

Table 4-1 Anthropometric values of participants along with standard deviation (SD) values

Sex	Number	Age ± SD (year)	Height ± SD (cm)	Weight ± SD (kg)
Male	9	28 ± 3	178 ± 7	77 ± 10
Female	3	28 ± 5	155 ± 3	57 ± 8
Total	12	28 ± 3	173 ± 12	72 ± 13

Prior to testing, participants completed a brief medical history; all volunteers were non-smokers and had no history of cardiovascular, respiratory, or neurological disease, or major musculoskeletal injuries. The participants were asked to abstain from alcohol, caffeinated beverages, and heavy exercise within 24 hours of the test and eat a light breakfast/lunch on the experiment day. Every subject completed two sets of experiments at the same time of two separate days within a week. The order of the test days was randomized. Female subjects were tested in the same phase of their menstrual cycle, achieved by testing on consecutive days.

The tests were performed in the Aerospace Physiology Laboratory at the Simon Fraser University. Upon arrival in the lab, the volunteers were asked to remove their shoes and socks, and change into a pair of shorts. Their age, gender, height, and weight was recorded and afterwards, the subjects were directed towards the LBNP box for equipment instrumentation while lying in the supine position.

4.3. Test Protocol

Each participant's lower body was placed in the LBNP chamber and sealed at the iliac crests. After 12 minutes of rest at ambient pressure (0 mmHg), vacuum was applied to the box to decrease the pressure at 15 mmHg decrements through -45 mmHg, each for 12 minutes (12-min stages of LBNP at -15, -30, and -45 mmHg). Following the last LBNP phase, a recovery stage

took place where the chamber pressure was brought back to ambient pressure for another 12 minutes of data collection. During the tests, negative pressure was immediately terminated upon the participants' request and/or if a sudden drop in heart rate or blood pressure, or a sustained drop in systolic blood pressure below 90 mmHg were observed. The participants were asked not to contract and move their leg muscles throughout testing in order to avoid noise and muscle pump activity in the course of data collection.

As highlighted in section 4.2, each participant underwent two experiments. On one day, the ACSs were not donned by the subjects (control model). Whereas on the other day, prior to getting into the LBNP box, a pair of ACSs was wrapped around the participants' calves on top of a 3×1 array of circular FSRs® (Figure 3-31) and activated while graded vacuum was applied (treatment model). The exerted pressure by the garments per leg was considered to be the average of the FSRs® in each array. Figure 4-1 shows a participant wearing a pair of ACSs.

(a) (b) (c)

Figure 4-1 A pair of ACSs worn on human calf
(a) front view, (b) back view, and (c) side view

The ACSs were set to apply a compression paradigm, consisting of four intermittent pressure cycles per minute over the mid-calf. Every cycle lasted for 15 seconds and contained low and high levels of 15 and 50 mmHg, respectively. The maximal pressurizing stages were 5 seconds in duration with an approximate rising time of 2 seconds (Figure 4-4). The rationale behind picking this compression pattern is explained in the following paragraphs.

External compression of around 50 mmHg has been shown to positively impact the cardiovascular variables. In a study by Hansen et al., peristaltic pneumatic compression of 55 mmHg over the upper and lower legs, with an inflation time of 12 seconds and deflation time of 48 seconds, significantly reduced the risk of syncope in immobile individuals during standing magnetic resonance imaging [85]. In another study, Vanscheidt et al. assessed dose-dependency

of oedema reduction in patients suffering from leg swelling and chronic venous insufficiency. They used a 4-chambered intermittent pneumatic compression device, including foot, ankle, mid-calf, and upper calf sections, to deliver three pressure profiles to the lower legs: 35, 45, and 55 mmHg over the mid-calf. While all the patterns were beneficial in decreasing leg volume, higher pressures were associated with greater reduction [86]. The key element in advantageous compression treatment is the ability to narrow the veins. According to Partsch et al., initial narrowing and complete occlusion of leg veins during standing occur at external pressure values of 40 and 70 mmHg on the calf, respectively [87]. Considering the aforesaid points, 50 mmHg of maximal pressure, which has been illustrated to be influential both in narrowing the veins and altering hemodynamic parameters, seemed to be a proper choice for the experiments. And as for the minimal pressure, 15 mmHg was selected since the FSRs® were insensitive to values smaller than 10 mmHg.

Previously indicated in Figure 2-9, venous refill time is defined as the time interval between the termination of walking, hence muscle pump discontinuance, until the vein pressure reaches the pressure level at motionless standing; this period is around 20-30 seconds in a healthy individual [45]. In the human tests, pressurizing and de-pressurizing periods were selected in a way to hinder complete venous refill.

A closed-loop controller was designed to regulate the ACSs' exerted pressure on the calves. The built-in PID VI in LabVIEW was used along with the PID Gain Schedule VI (Figure 4-2). The system had different pressure regions of operation and as a result, required different sets of gains. This was achieved by implementing the PID Gain Schedule VI to define the proper values for proportional, integral, and derivative gain parameters, as depicted in Figure 4-3 .Max values are different pressure levels in ascending order. Each set of gains in the array is used for all gain scheduling values less than the corresponding max value. The output of the feedback controller was routed to the duty cycle of the motor to determine its desired output for driving the system.

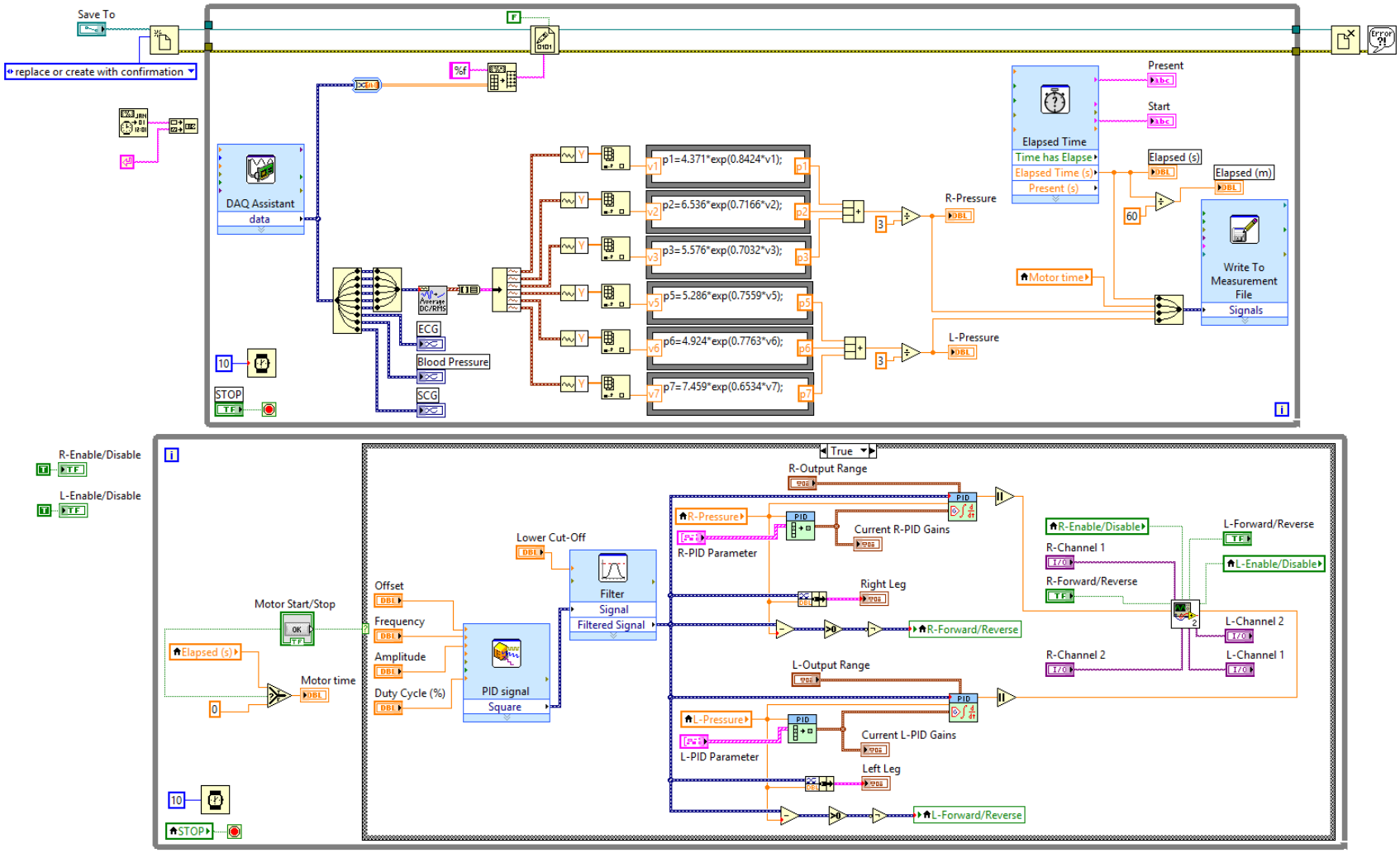

Figure 4-2 Block diagram of the written program in LabVIEW

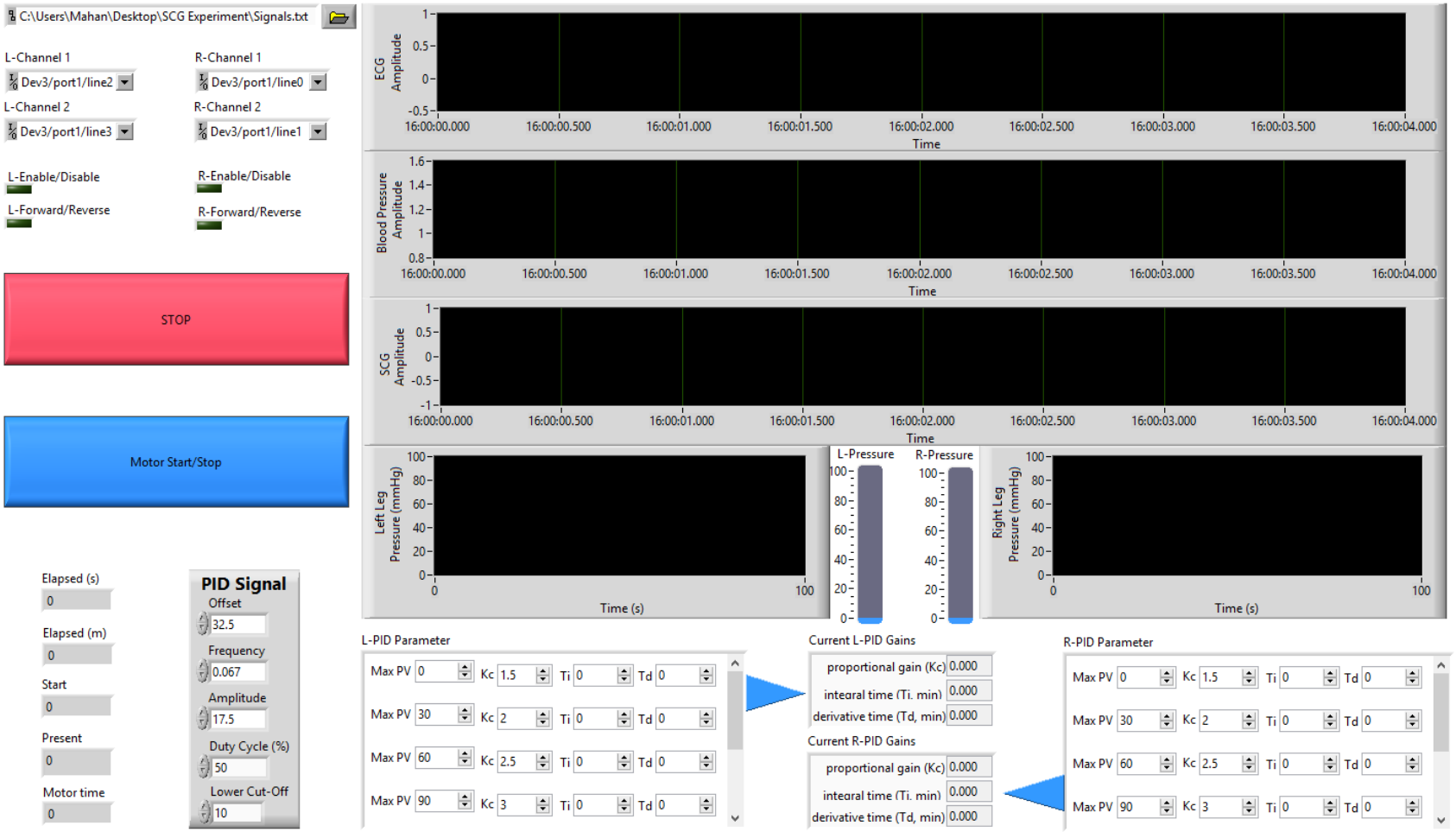

Figure 4-3 Graphical user interface of written program in LabVIEW

Owing to the vital role of calf muscle pump in augmenting venous return, it is crucial to make sure that adequate pressure is exerted on the calf muscle in compression therapy [23]. During the tests, the applied pressure (called the process variable) was measured by the FSRs® arrays at the mid-calf and fed back to the control system. The set point, or the desired value for the process variable, was simulated as a square waveform with the following properties: frequency = 0.067 Hz (corresponds to four cycles per minute), amplitude = 17.5 mmHg, offset = 32.5 mmHg, and duty cycle = 50%. A snapshot of the square signal during one minute, which mimics intermittent pressure cycles with low and high levels of 15 and 50 mmHg, is depicted in Figure 4-4.

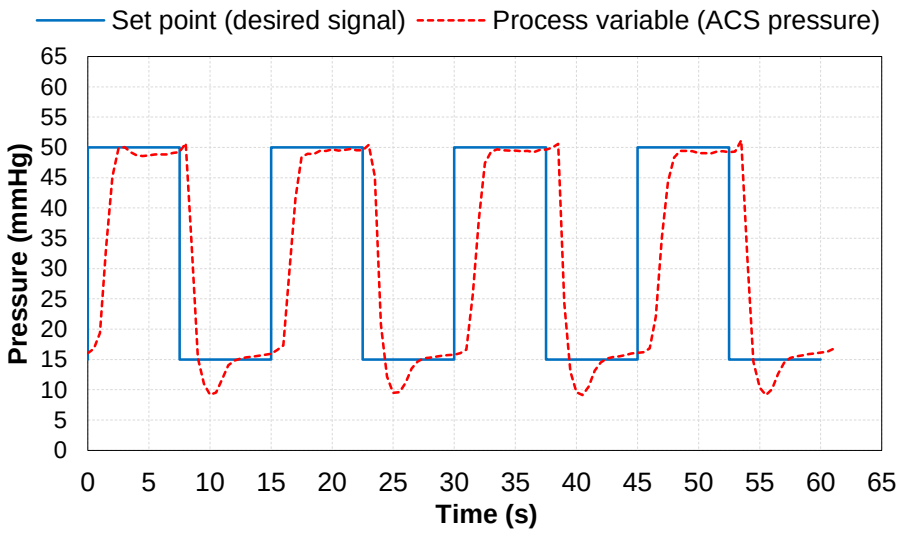

Figure 4-4 Desired interface pressure signal along with controlled pressure of ACS

Throughout the experiments, the participants had continuous measure of beat-to-beat arterial blood pressure through a non-invasive photoplethysmography finger cuff. The cuff was placed on the middle phalanx of the left middle finger (Finopres, Ohmeda, Inglewood, CO, USA). For the sake of rate analysis, electrocardiogram (ECG) signal was acquired using a standard 4-lead placement with non-invasive disposable surface electrodes (LifePak 8, Medtronic Inc, Minnesota, USA). Seismocardiogram (SCG) signal, which represents the low-frequency vibrations and acceleration of the chest wall caused by the beating heart, was measured in back-to-front direction, perpendicular to the body surface, with a high-sensitivity accelerometer (Brüel & Kjær model 4381, Nærum,

Denmark)[1], placed on the sternum. The device was affixed to the skin with double-sided hypoallergenic tape. While ECG shows the electrical activity of the heart, SCG is a manifestation of its mechanical performance.

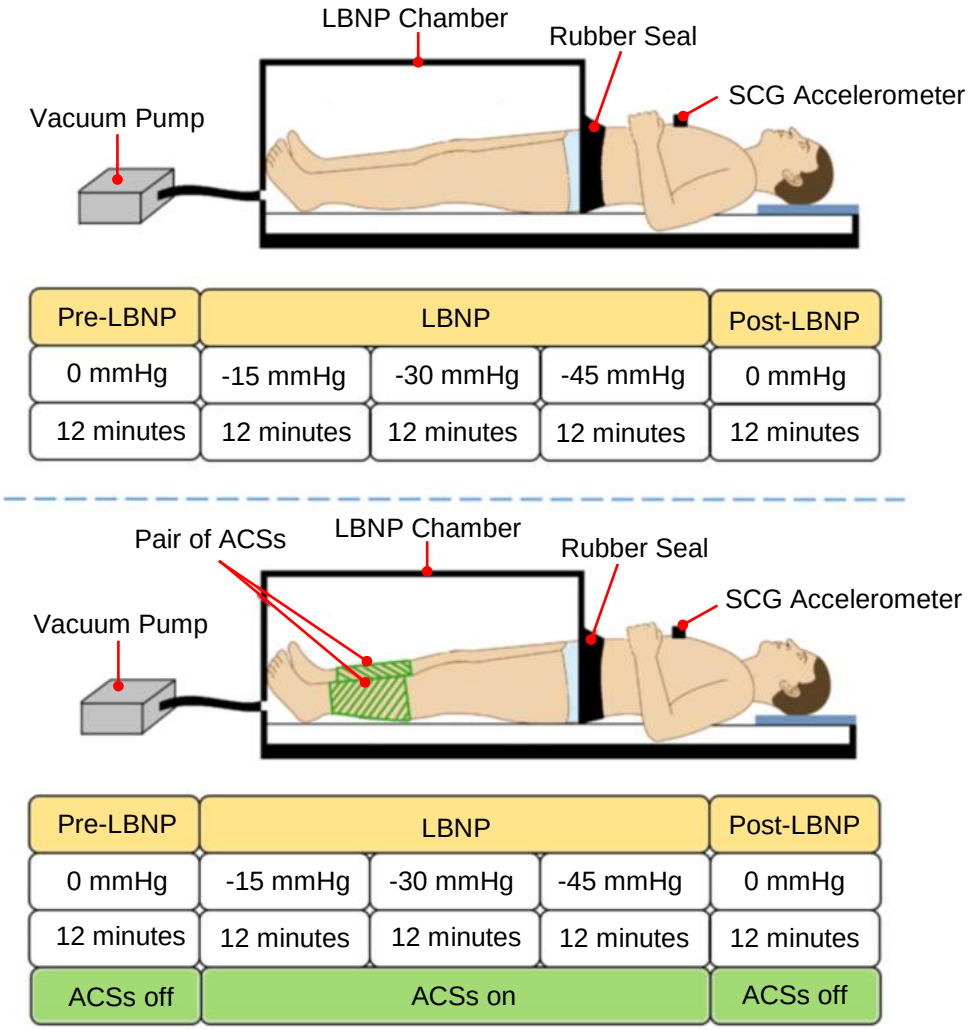

Figure 4-5 Schematic diagram of the LBNP setup along with experiments' protocols *(top) control model without ACSs, (bottom) treatment model with ACSs*

4.4. Data Acquisition

Data were acquired with a sampling frequency of 1000 Hz using an analog-to-digital converter (National Instruments USB-6212 BNC, Texas, USA), and subsequently routed to NI LabVIEW 2013 (National Instruments, Texas, USA). A program was written

[1] www.bksv.com/Products/transducers/vibration/accelerometers/accelerometers/4381

in LabVIEW to collect all signals, convert the output voltage to the equivalent pressure values, and store them for further offline analyses.

4.5. Data Analysis

MATLAB R2012b (The MathWorks Inc, Massachusetts, USA) was employed to average the data as 10-second intervals. A total of six cardiovascular responses were analyzed, including systolic blood pressure (SBP), mean arterial pressure (MAP), diastolic blood pressure (DBP), heart rate (HR), pulse pressure (PP), and left ventricular ejection time (LVET). Systolic and diastolic blood pressures were used to calculate pulse pressure and mean arterial pressure using Equation 2.3 and Equation 2.4, respectively. Heart rate, or the number of heart beats per minute, was calculated by Equation 4.1 after finding the R-R intervals, or a pair of successive R-peaks, in the electrocardiograms:

$$HR = 60 \times \frac{sampling\ rate}{R-R\ interval} = 60 \times \frac{1}{(sampling\ period) \times (R-R\ interval)} \qquad \text{Equation 4.1}$$

The last parameter analyzed was the left ventricular ejection time. The LVET, a commonly used systolic time interval in cardiovascular studies, is defined as the time of ejection of blood from the left ventricle starting with aortic valve opening and ending with aortic valve closure; and can be extracted from an SCG signal. Since systolic time intervals undergo changes in individuals with cardiac disease, they are widely used in cardiology to non-invasively investigate left ventricular performance [88]. It has been demonstrated that SCG-derived systolic time intervals, including LVET, are sensitive to LBNP-induced hemodynamic changes and are correlated with stroke volume [82]. Therefore, in the current study, the changes in LVET were used to track the changes in stroke volume rather than determining its absolute value. Figure 4-6 depicts typical ECG and SCG signals, along with a number of features that correspond to specific cardiac events. It should be mentioned that extraction of the SCG signal features was done by Dr. Farzad Khosrow-Khavar.

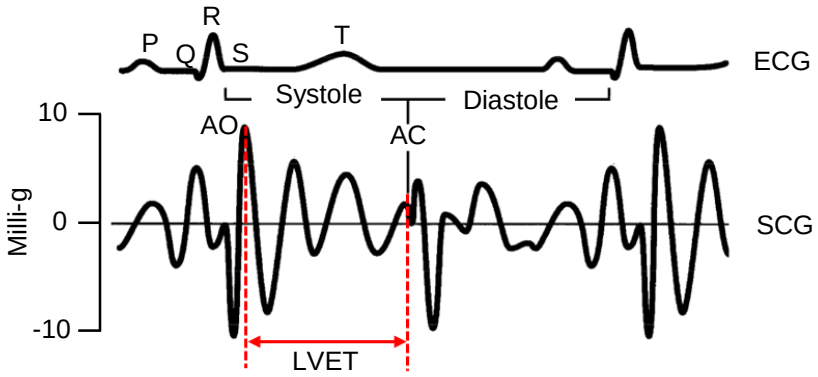

Figure 4-6 Schematic diagrams of ECG and SCG signals and their features[1]
In the SCG signal, AO and AC stand for aortic valve opening and closure, respectively. The LVET equals the difference between AO and AC.

4.6. Summary

The second objective of the study, which was to evaluate the potential of the developed adaptive compression system in assisting with blood circulation and fluid volume control in the human lower leg during orthostasis, was pursued in this chapter. Graded lower body negative pressure served to induce cardiovascular stress similar to passive standing. Twelve subjects completed two sets of experiments with and without ACS application, and throughout testing, cardiovascular variables were continuously recorded for the offline analyses. Systolic blood pressure, mean arterial pressure, diastolic blood pressure, heart rate, pulse pressure, and left ventricular ejection time were the responses of most interest, which were either directly measured during the experiments or extracted from the recorded signals. The results of the statistical analyses are presented in the next chapter.

[1] adapted from [97]

Chapter 5. **Results and Discussion**

As described in Chapter 4, twelve individuals participated in the tests that were conducted to assess the performance of the ACS. One participant's data were excluded from the analyses due to a non-reported cardiac abnormality. Another subject experienced pre-syncope in the experiment without the ACS at the onset of -45 mmHg, warranting early termination of the test. The data for that experiment are partially included.

5.1. Statistical Analyses

Statistical analyses were carried out in JMP12 (Statistical Analysis Systems, Cary, North Carolina) using the averaged data of the last five minutes of each test level, 30 seconds prior to switching to the next level. Data were assessed for normality using the Shapiro-Wilk test. A two-factor repeated-measures analysis of variance (ANOVA) with blocking was performed to evaluate if there were statistically significant changes in mean cardiovascular responses, namely systolic blood pressure (SBP), mean arterial pressure (MAP), diastolic blood pressure (DBP), heart rate (HR), pulse pressure (PP), and left ventricular ejection time (LVET). Test condition, LBNP level, and their interaction were regarded as fixed effects in the model, and subject (block) was considered the random effect factor. Test condition had two levels (no ACS and with ACS) and LBNP stage consisted of five levels (pre-LBNP, -15 mmHg, -30 mmHg, -45 mmHg, and post-LBNP). Post hoc tests using the Tukey-Kramer adjustment were used to compare mean responses between pairs of test condition and/or LBNP level. A level of significance α = 0.05 was used in the post hoc tests, and effects with p-values less then 0.05 were considered to be statistically significant. Data are reported as means ± SEM[1].

[1] SEM stands for the standard error of the mean.

Pulse pressure and left ventricular ejection time violated the assumptions of normality. Hence, the non-parametric Friedman test followed by a series of Wilcoxon matched pairs tests with the Bonferroni correction were carried out. Moreover, the original PP and LVET data were transformed using a Box-Cox transformation to omit the problem of non-normally distributed residuals, and a two-way repeated-measures ANOVA with the Tukey-Kramer post hoc test was conducted. The results of these analyses are not reported in the current document as they were in complete accordance with the factorial ANOVA on the non-normal data.

5.2. Results

The statistical analyses yielded a main effect for test condition that was significant in all cardiovascular responses except for systolic blood pressure. The main effect of LBNP level was significant in all of the responses. The interaction effect was non-significant. Table 5-1 presents the *F* ratios, along with *p*-values for the two-way repeated-measures ANOVA.

Table 5-1 Summary of factorial ANOVA

Response	Fixed effect								
	Test condition			*LBNP level*			*Test condition * LBNP level*		
	F ratio	*p*-value	Significant?	*F* ratio	*p*-value	Significant?	*F* ratio	*p*-value	Interact?
SBP	2.41	0.1241	No ✗	3.16	0.0177	Yes ✓	0.12	0.9799	No ✓
MAP	9.98	0.0022	Yes ✓	5.85	0.0003	Yes ✓	0.07	0.9914	No ✓
DBP	17.17	<0.0001	Yes ✓	8.92	<0.0001	Yes ✓	0.10	0.9820	No ✓
HR	12.64	0.0006	Yes ✓	35.78	<0.0001	Yes ✓	0.65	0.6265	No ✓
PP	8.79	0.0039	Yes ✓	8.81	<0.0001	Yes ✓	0.53	0.7157	No ✓
LVET	9.17	0.0032	Yes ✓	28.16	<0.0001	Yes ✓	0.36	0.8360	No ✓

There was no meaningful change in systolic blood pressure with and without the ACS. Mean arterial pressure, diastolic blood pressure, and left ventricular ejection time were significantly higher with the ACS, while the mean values of heart rate and pulse pressure were higher without the ACS. The values of the mean cardiovascular responses are numerically represented in Table 5-2 and graphically illustrated in Figure 5-1.

Table 5-2 Mean values of cardiovascular responses in two test conditions

Fixed effect	**Cardiovascular response mean ± SEM**					
Test condition	*SBP (mmHg)*	*MAP (mmHg)*	*DBP (mmHg)*	*HR (bpm)*	*PP (mmHg)*	*LVET (ms)*
no ACS	118 ± 4	87 ± 3	72 ± 3	74 ± 3	47 ± 2	272 ± 5
with ACS	121 ± 4	92 ± 3	77 ± 3	70 ± 3	44 ± 2	284 ± 5

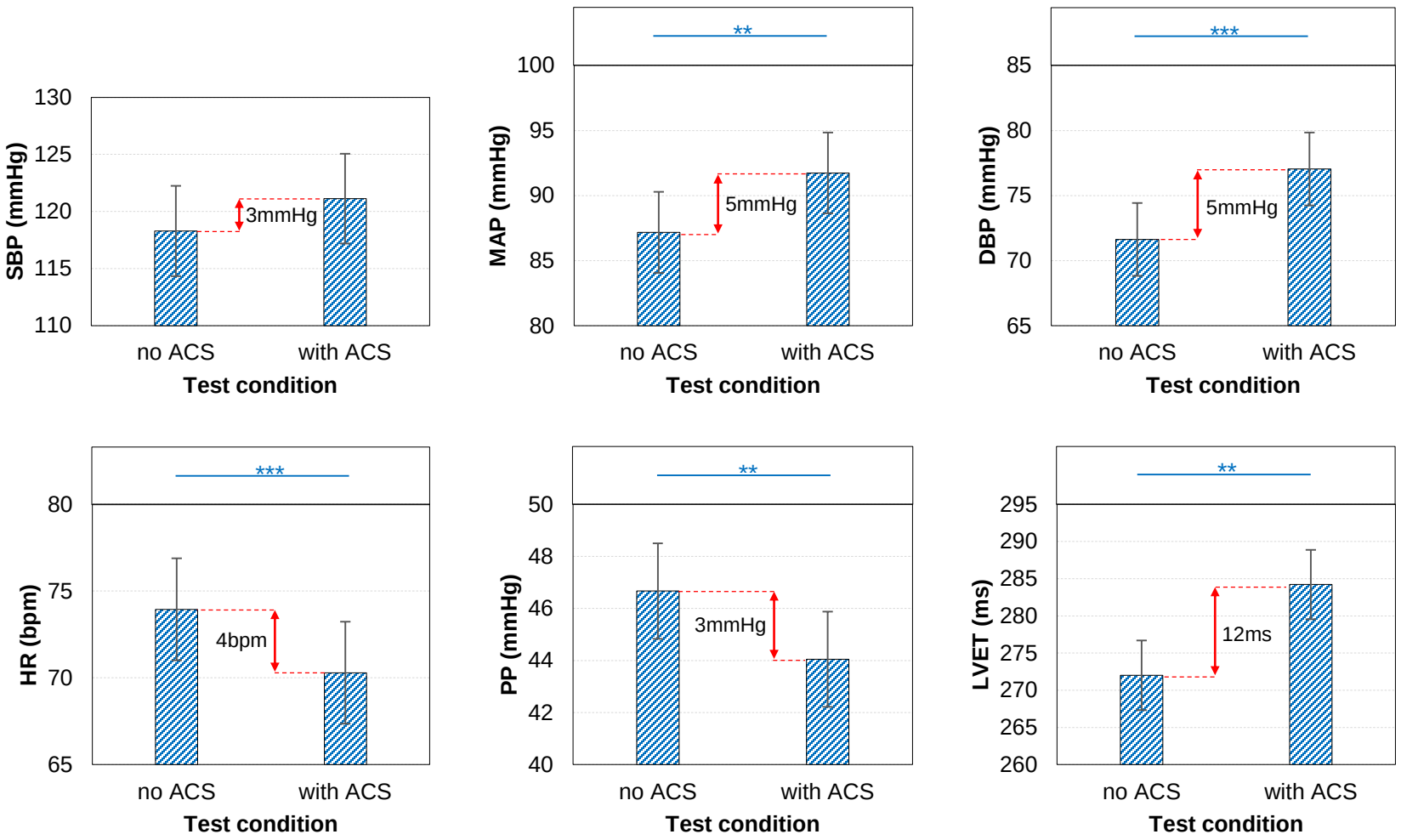

Figure 5-1 Mean values of cardiovascular responses at two test conditions, along with absolute changes
Horizontal bars denote statistical significance between test conditions. Vertical bars correspond to SEM for each condition.
*Symbols: *p-value < 0.05, **p-value < 0.01, ***p-value < 0.001*

As depicted in Table 5-3 and Figure 5-2, through the LBNP levels from resting pre-LBNP stage to the peak negative pressure of -45 mmHg, systolic blood pressure was maintained; mean arterial pressure, diastolic blood pressure, and heart rate increased; and pulse pressure and left ventricular ejection time decreased gradually. These results are congruent with other studies [82, 89, 90, 91]. Among the six cardiovascular responses, LVET and HR were the two variables statistically different in most LBNP levels.

Table 5-3 Mean values of cardiovascular responses in five LBNP levels

Fixed effect	**Cardiovascular response mean ± SEM**					
LBNP level	*SBP (mmHg)*	*MAP (mmHg)*	*DBP (mmHg)*	*HR (bpm)*	*PP (mmHg)*	*LVET (ms)*
Pre-LBNP	118 ± 4	86 ± 3	70 ± 3	67 ± 3	48 ± 2	299 ± 6
-15mmHg	116 ± 4	86 ± 3	70 ± 3	67 ± 3	46 ± 2	287 ± 6
-30mmHg	118 ± 4	89 ± 3	74 ± 3	73 ± 3	44 ± 2	267 ± 6
-45mmHg	120 ± 4	93 ± 3	79 ± 3	84 ± 3	41 ± 2	241 ± 6
Post-LBNP	126 ± 4	94 ±3	78 ± 3	69 ± 3	48 ± 2	296 ± 6

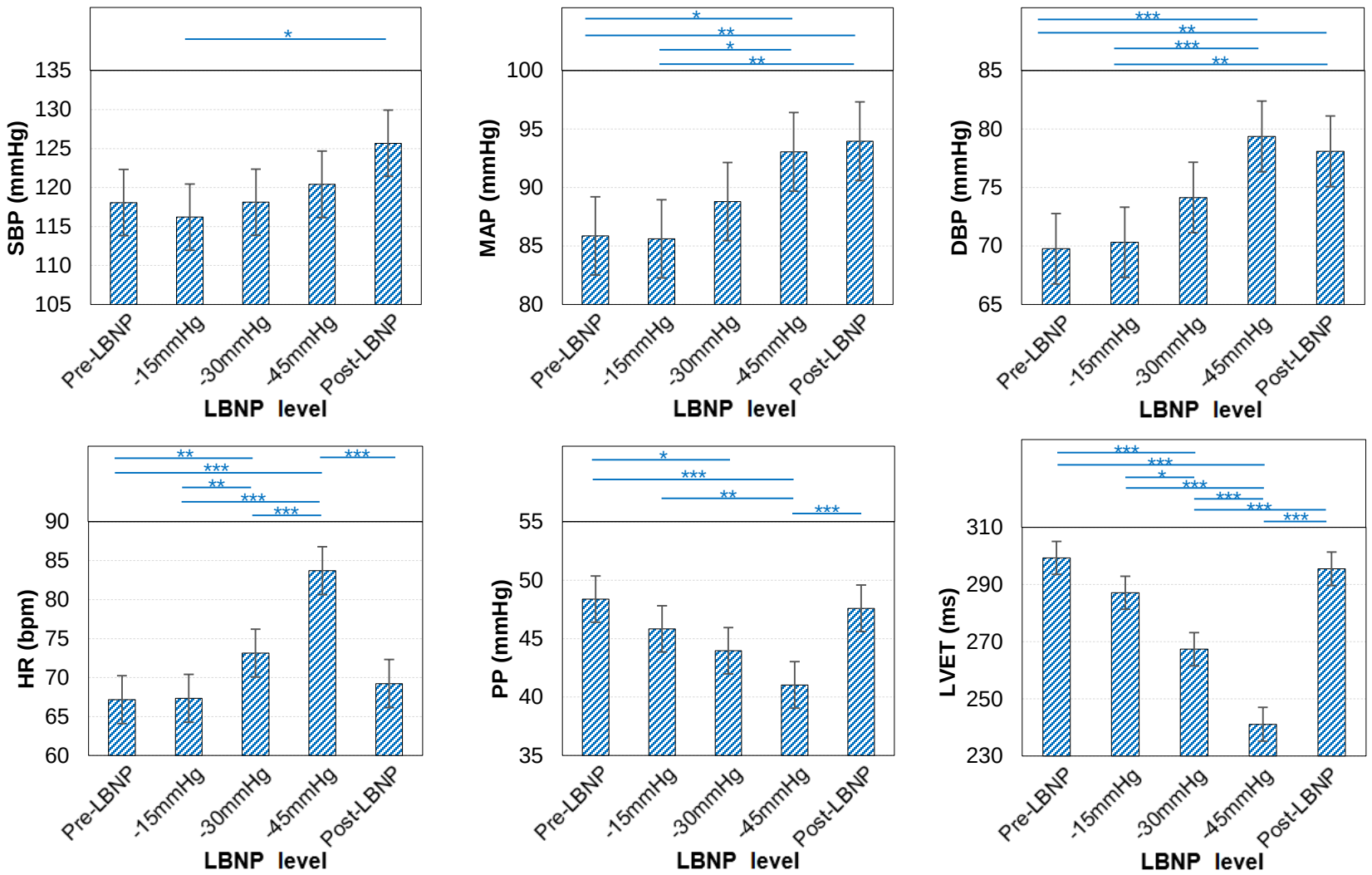

Figure 5-2 Mean values of cardiovascular responses at five LBNP levels

*Horizontal bars denote statistical significance between LBNP levels. Vertical bars correspond to SEM for each level. Symbols: *p-value < 0.05, **p-value < 0.01, ***p-value < 0.001*

Table 5-4 summarizes the mean cardiovascular variables in the course of different LBNP stages and at the two test conditions, i.e. with and without the ACS.

Table 5-4 Mean values of cardiovascular responses at different LBNP levels with and without ACS application

Fixed effects interaction		**Cardiovascular response mean ± SEM**					
*Test condition * LBNP level*		*SBP (mmHg)*	*MAP (mmHg)*	*DBP (mmHg)*	*HR (bpm)*	*PP (mmHg)*	*LVET (ms)*
no ACS	Pre-LBNP	117 ± 5	84 ± 4	67 ± 3	68 ± 3	50 ± 2	297 ± 7
	-15mmHg	114 ± 5	83 ± 4	67 ± 3	69 ± 3	47 ± 2	283 ± 7
	-30mmHg	116 ± 5	86 ± 4	72 ± 3	75 ± 3	45 ± 2	259 ± 7
	-45mmHg	119 ± 5	91 ± 4	77 ± 3	87 ± 3	42 ± 2	232 ± 7
	Post-LBNP	125 ± 5	92 ± 4	75 ± 3	71 ± 3	50 ± 2	289 ± 7
with ACS	Pre-LBNP	119 ± 5	88 ± 4	73 ± 3	66 ± 3	47 ± 2	302 ± 7
	-15mmHg	118 ± 5	89 ± 4	74 ± 3	66 ± 3	45 ± 2	291 ± 7
	-30mmHg	120 ± 5	91 ± 4	77 ± 3	71 ± 3	43 ± 2	276 ± 7
	-45mmHg	122 ± 5	95 ± 4	81 ± 3	80 ± 3	40 ± 2	250 ± 7
	Post-LBNP	126 ± 5	96 ± 4	81 ± 3	68 ± 3	45 ± 2	302 ± 7

The absolute change of the hemodynamic parameters throughout LBNP levels from the baseline, or pre-LBNP stage, are shown in Table 5-5 for the two test conditions.

Table 5-5 Absolute change of cardiovascular responses relative to baseline (pre-LBNP) at different LBNP levels with and without ACS application

Fixed effects interaction		**∆Cardiovascular response mean ± SEM**					
*Test condition * LBNP level*		*SBP (mmHg)*	*MAP (mmHg)*	*DBP (mmHg)*	*HR (bpm)*	*PP (mmHg)*	*LVET (ms)*
no ACS	-15mmHg	-3 ± 4	-1 ± 3	0 ± 3	1 ± 2	-3 ± 2	-14 ± 9
	-30mmHg	-1 ± 4	3 ± 3	5 ± 3	7 ± 2	-5 ± 2	-38 ± 9
	-45mmHg	2 ± 4	8 ± 3	11 ± 3	19 ± 2	-8 ± 2	-64 ± 9
	Post-LBNP	8 ± 4	8 ± 3	8 ± 3	3 ± 2	0 ± 2	-8 ± 9
with ACS	-15mmHg	-1 ± 4	0 ± 3	1 ± 3	0 ± 2	-2 ± 2	-10 ± 9
	-30mmHg	1 ± 4	3 ± 3	4 ± 3	5 ± 2	-3 ± 2	-26 ± 9
	-45mmHg	2 ± 4	7 ± 3	9 ± 3	14 ± 2	-6 ± 2	-52 ± 9
	Post-LBNP	7 ± 4	8 ± 3	8 ± 3	1 ± 2	-1 ± 2	1 ± 9

Table 5-6 delineates the percentage change of the cardiovascular responses during different LBNP levels that were calculated in relation to the baseline. The results of the two test conditions are included.

Table 5-6 Percentage change of cardiovascular responses relative to baseline (pre-LBNP) at different LBNP levels with and without ACS application

Fixed effects interaction		**∆Cardiovascular response mean (%) ± SEM**					
*Test condition * LBNP level*		*SBP*	*MAP*	*DBP*	*HR*	*PP*	*LVET*
no ACS	-15mmHg	-2 ± 4	-1 ± 4	1 ± 4	1 ± 3	-7 ± 3	-5 ± 5
	-30mmHg	-1 ± 4	4 ± 4	7 ± 4	11 ± 3	-11 ± 3	-12 ± 5
	-45mmHg	1 ± 4	8 ± 4	14 ± 4	26 ± 3	-17 ± 3	-20 ± 5
	Post-LBNP	6 ± 4	9 ± 4	11 ± 4	3 ± 3	-1 ± 3	-2 ± 5
with ACS	-15mmHg	-1 ± 4	0 ± 3	1 ± 4	0 ± 3	-4 ± 3	-3 ± 5
	-30mmHg	1 ± 4	3 ± 3	5 ± 4	8 ± 3	-7 ± 3	-8 ± 5
	-45mmHg	2 ± 4	7 ± 3	12 ± 4	22 ± 3	-13 ± 3	-17 ± 5
	Post-LBNP	6 ± 4	9 ± 3	11 ± 4	3 ± 3	-3 ± 3	1 ± 5

The results presented in the previous three tables are graphically portrayed in Figure 5-3 through Figure 5-5.

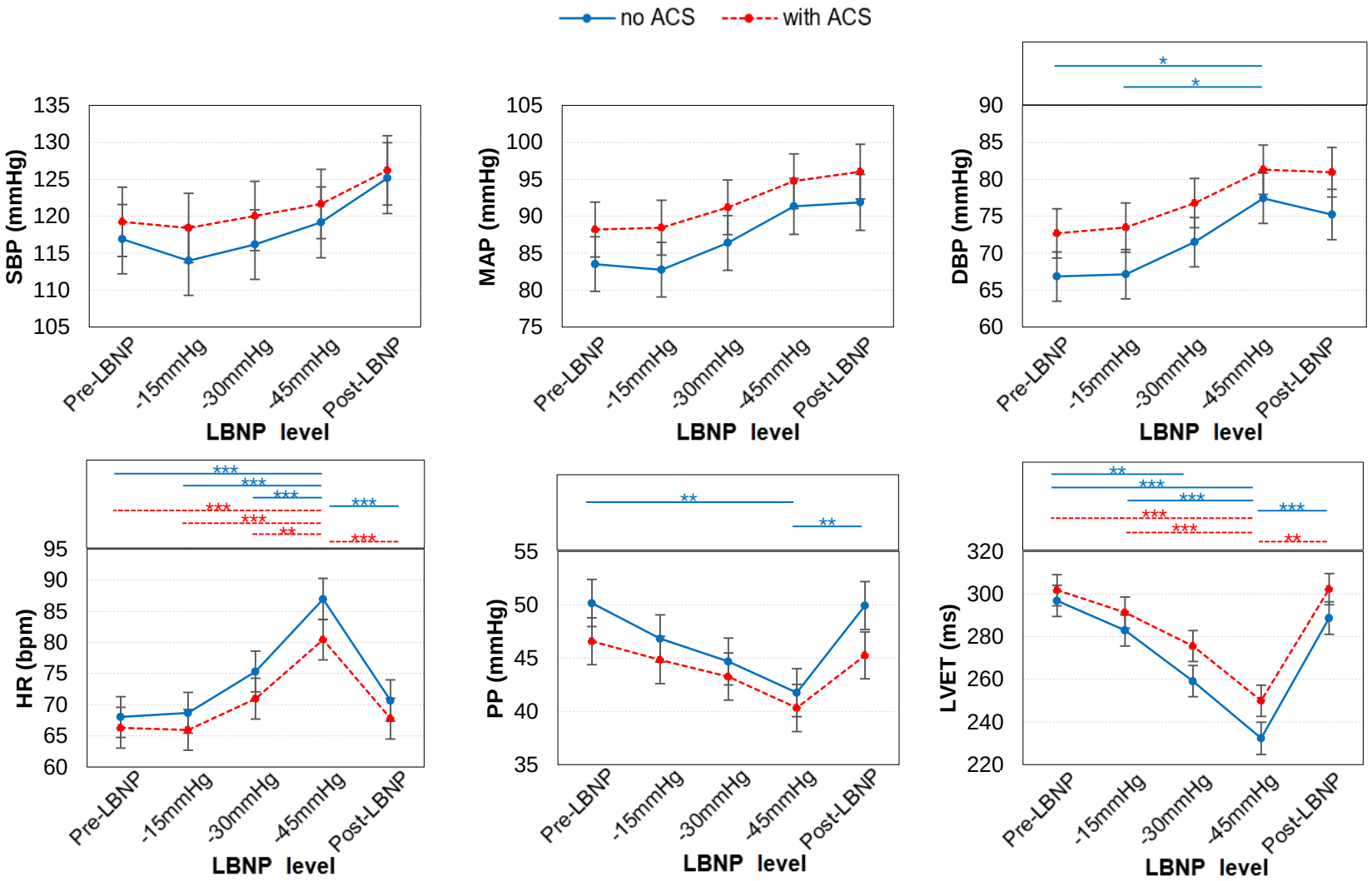

Figure 5-3 Mean values of cardiovascular responses at two test conditions and five LBNP levels

Horizontal bars denote statistical significance between LBNP levels. Vertical bars correspond to SEM for each level.
*Symbols: *p-value < 0.05, **p-value < 0.01, ***p-value < 0.001*

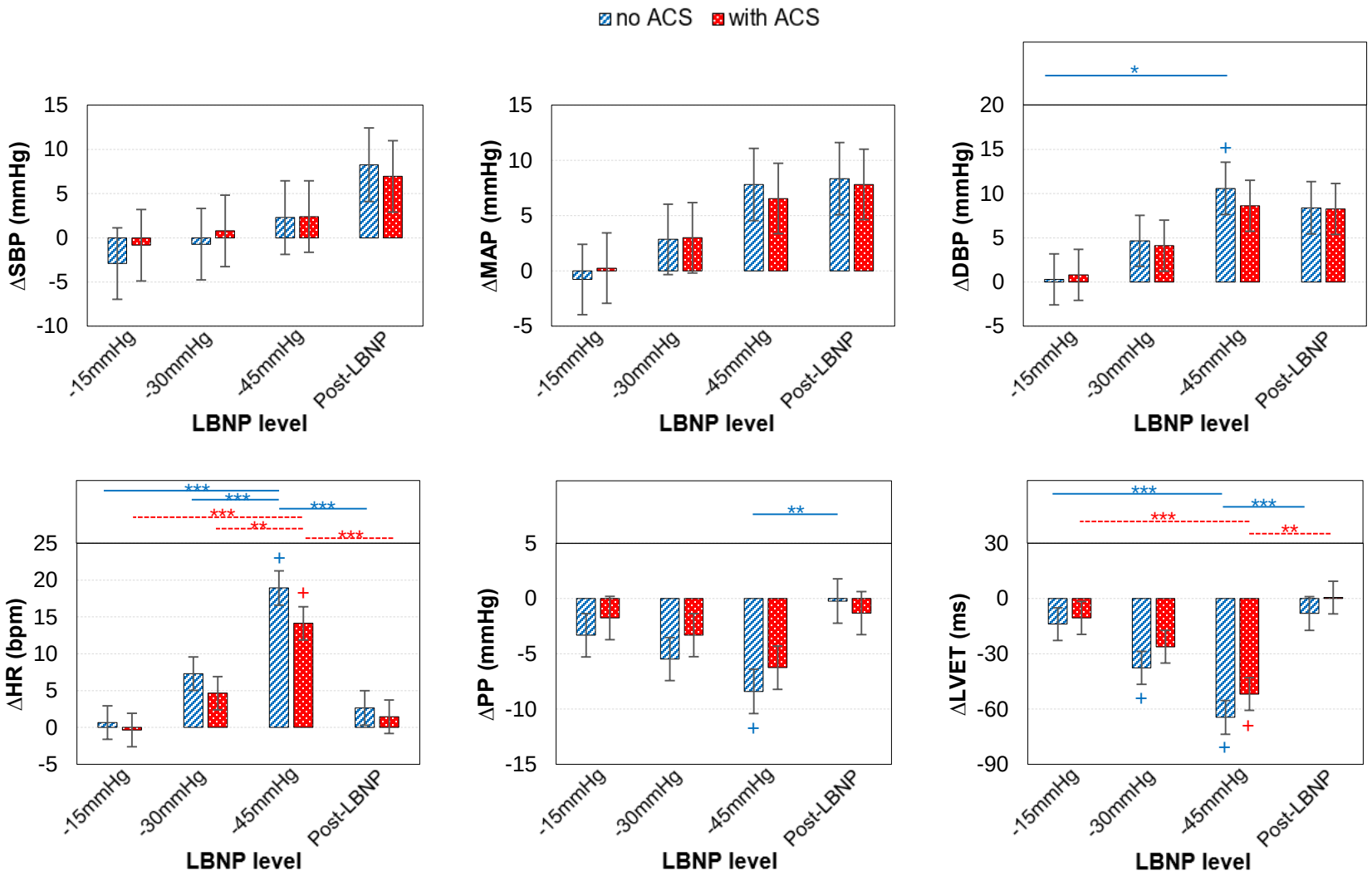

Figure 5-4 Absolute change of cardiovascular responses from baseline during different LBNP levels at two test conditions
Horizontal bars denote statistical significance between LBNP levels. Vertical bars correspond to SEM for each level.
*Symbols: *p-value < 0.05, **p-value < 0.01, ***p-value < 0.001, + = different from baseline*

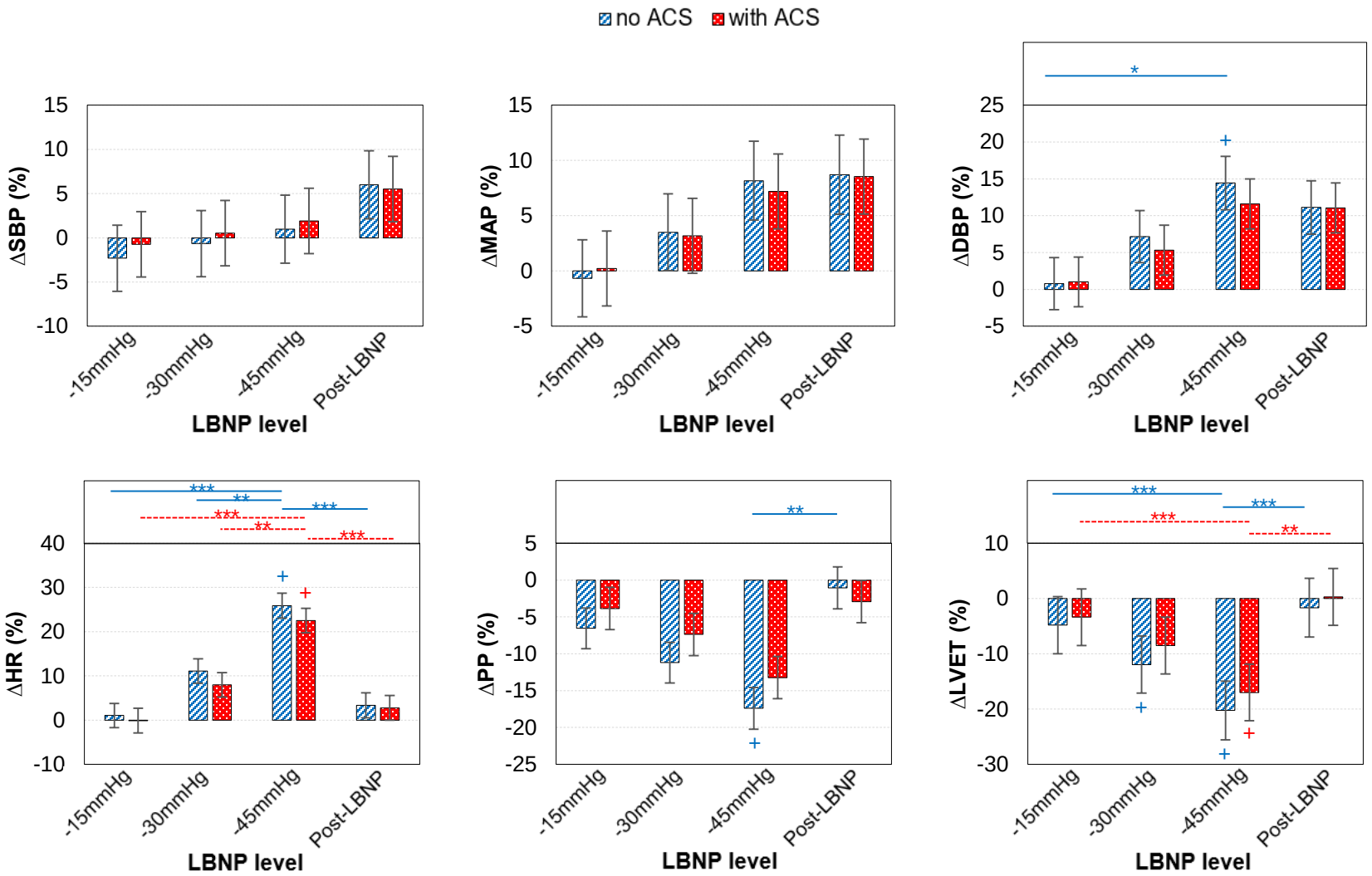

Figure 5-5 Percentage change of cardiovascular responses from baseline during different LBNP levels at two test conditions
Horizontal bars denote statistical significance between LBNP levels. Vertical bars correspond to SEM for each level.
*Symbols: *p-value < 0.05, **p-value < 0.01, ***p-value < 0.001, + = different from baseline*

5.3. Discussion

Systolic blood pressure and mean arterial pressure were maintained throughout different LBNP levels at the two test conditions, which can be attributed to the fact that the participants were young healthy individuals without a history of cardiovascular regulatory dysfunction.

Without the ACS, diastolic blood pressure significantly increased from the resting pre-LBNP level through the peak negative pressure of -45 mmHg by 14%, demonstrating a normal baroreflex[1] response to the fluid shifts imposed. In clarification it should be pointed out that a rise in diastolic pressure occurs as a result of an increase in total peripheral resistance, which is one of the key elements in regulating blood pressure [92]. Although diastolic pressure increased with the ACS application as well, its elevation was attenuated with a percentage change of 12% relative to the baseline.

In a compensatory attempt to increase cardiac output and maintain constant blood pressure, a gradual baroreflex-mediated tachycardia was noticed through the LBNP stages, corresponding to overall rises of 26% and 22% from the baseline to the LBNP peak negative pressure without and with the ACS, respectively. As the numbers indicate, in the treatment mode the heart rate was not elevated as much compared to the control mode.

Pulse pressure exhibited a meaningful drop of 17% from the baseline to the negative pressure of -45 mmHg in the absence of the ACS. This decline was in agreement with the previous observations, which were systolic blood pressure maintenance and diastolic blood pressure increase. By applying the ACS, the percentage change of pulse pressure reduction was lessened to 13%.

[1] The baroreflex is one of the mechanisms in the body that helps to regulate blood pressure by controlling total peripheral resistance and cardiac output via affecting vasoconstriction, heart rate, and heart contractility.

Finally, the left ventricular ejection time progressively diminished from the pre-LBNP level through the peak negative pressure by 20% in the control mode and by 17% in the treatment mode. Considering the positive correlation between left ventricular ejection time and stroke volume, the blunted fall-off in LVET with the ACS could reflect attenuation of stroke volume decline.

The results of this study suggest that the developed adaptive compression system is capable of dampening the LBNP-imposed orthostatic stress on the cardiovascular system of healthy subjects via attenuating the increase in diastolic blood pressure and heart rate, and lessening the decrease in left ventricular ejection time and stroke volume. It is likely that these beneficial changes are due to venous return augmentation, which occurs a result of the intermittent pumping action of the ACS, contributing to the emptying of the lower legs vasculature.

5.4. Study Limitations

In order to save time, the force-sensing resistors were calibrated on one individual's calf and used on twelve other subjects during the human experiments. However, more accurate calibration functions might have been achieved if the FSRs® were exclusively calibrated for each participant.

A second limitation was that all experiments were conducted on healthy volunteers. Although it is not known whether the results would apply similarly to patient populations, it is expected that this would be the case, since other non-pharmacological approaches have been shown to hold across both patients and controls [93, 94].

Finally, no placebo was used during the control mode of the human experiments. The first reason for this choice was that due to the weight of the motor, there was a possibility of ACS rotation if wrapped around the calf without generating compression. Hence, the ACS itself could not be utilized as a placebo. Secondly, no other device could be found which was visually indistinct from the ACS.

Chapter 6. Conclusion and Future Work

6.1. Summary and Conclusion

Chronic venous disease of the lower extremities is an incapacitating health issue with a wide spectrum of manifestations, ranging from varicose veins to ulceration. This disease not only negatively affects quality of life, but also is associated with profound socioeconomic impacts, in addition to exorbitant costs on the health care system. In the presence of any deficiency in the normal function of calf muscle pump and one-way venous valves, which serve to counteract gravitational forces and direct blood flow to the heart, the efforts towards emptying the veins fail, resulting in progressive complications due to elevated hydrostatic pressure in the lower limbs, especially during locomotory activities (i.e. walking and running).

Compression therapy, which has been established as the cornerstone in managing leg venous disorders, exploits the power of external pressure on the limbs to reverse the damaging consequences of venous hypertension by abolishing blood reflux and improving venous return. Notwithstanding the extensive use of conventional compression modalities, such as medical bandages, stockings, and mechanical pumps, these devices have shortages that diminish their treatment efficacy and lessen patient adherence to therapy. Some of the major flaws of the existing systems include difficulty of donning; inability to apply specific pressure ranges, which is a bare essential of effective treatment; failure to sustain recommended pressure levels as a result of anatomical changes of the user; lack of an embedded interface pressure measurement system, hence being dependent on the bandaging skills of clinicians or the manufacturer's listed class of compression (which is not utterly reliable); dependency of performance on user's anthropometric variables; limitation of compression type to either static or dynamic mode, while both paradigms are important in pursuit of beneficial treatment; inefficacy during passive orthostasis; and non-ambulatory use.

The goal of this study was to develop and evaluate a prototype of an adaptive compression system, which combines on-demand sustained and intermittent gradient compression in an easy-to-wear device and can be used during stasis and ambulation. To accomplish this objective, a compression garment, with Velcro™ fasteners at the back and a motorized lacing system at the front, was designed and fabricated out of off-the-shelf components. The device was equipped with force-sensing resistors as a means for monitoring sub-bandage pressure to ensure delivery of reproducible, effective compression regardless of limb size and shape. Moreover, the interface pressure feedback from the FSRs® was employed to control the garment tightness through the adjustment of the motor's function in response to the changing physiological conditions of the user.

The adaptive compression system was evaluated in a controlled study on twelve participants to investigate its performance in venous return enhancement during passive orthostasis by mechanical pulsatile pumping of blood up the leg vasculature. The subjects completed two sets of experiments, without and with the ACS, in which graded lower body negative pressure was used to increase venous pooling and induce blood volume shift in the legs similar to motionless standing. In the course of testing, beat-to-beat blood pressure was continuously monitored, along with electrical and mechanical activities of the heart via electrocardiography and seismocardiography, respectively. The results of the experiments revealed a significant reduction in the mean cardiovascular changes to LBNP, including diastolic blood pressure, pulse pressure, heart rate, and left ventricular ejection time: {absolute change from baseline ± SEM: without ACS: HR = 19bpm ± 2, LVET = -64ms ± 9, DBP = 11mmHg ± 3, PP = -8mmHg ± 2; with ACS: HR = 14bpm ± 2, LVET = -52ms ± 9, DBP = 9mmHg ± 3, PP = -6mmHg ± 2; $p<0.05$}. These outcomes indicate that the baroreflex compensatory mechanism, which involves stimulation of sympathetic nerves to restore arterial blood pressure by increasing heart rate and constricting vascular beds, is less activated while the subjects are wearing the ACS. In conclusion, the cardiovascular system undergoes less stress upon the operation of the developed compression device that can be ascribed to the designed system's role in facilitating blood circulation and enhancing venous return via pressurizing the lower extremities.

6.2. Future Considerations

Although the two objectives of the study were met, a few modifications could improve the performance of the developed compression system. Moreover, complementary studies are necessary to establish its efficacy. A number of the areas for future work are specified as follows:

- Integrating the motor and its dependent components into a single housing to be place around the waist or upper legs
- Adding an improved control unit with feedbacks from the user's bio-signals which could be employed as triggers to start compression, e.g. upon blood pressure drop
- Fabricating the device out of lightweight material
- Substituting the interface pressure measurement system with an improved telemetric sensing unit
- Evaluating the device during ambulation
- Assessing the ACS's performance in clinical trials on patients rather than healthy individuals
- Investigating deep venous hemodynamics in the course of clinical tests on patient populations to determine optimal combinations of applied pressure, frequency, and mode of compression that enable the ACS to induce meaningful changes to the cardiovascular responses for minimizing the complications associated with venous insufficiency

References

[1] C. L. Protheroe, A. Dikareva, C. Menon, Claydon and V. Elizabeth, "Are Compression Stockings an Effective Treatment for Orthostatic Presyncope?," *PLoS ONE,* vol. 6, no. 12, 2011.

[2] S. E. Privett, K. P. George, G. P. Whyte and N. T. Cable, "The effectiveness of compression garments and lower limb exercise on post-exercise blood pressure regulation in orthostatically intolerant athletes," *Clinical Journal of Sport Medicine,* vol. 20, no. 5, pp. 362-367, 2010.

[3] S. Miller, E. F. Bergel, A. M. El Ayadi, L. Gibbons, E. A. Butrick, T. Magwali, G. Mkumba, C. Kaseba, N. Huong, J. D. Geissler and M. Merialdi, "Non-Pneumatic Anti-Shock Garment (NASG), a First-Aid Device to Decrease Maternal Mortality from Obstetric Hemorrhage: A Cluster Randomized Trial," *PLoS One,* vol. 8, no. 10, 2013.

[4] S. Miller, H. B. Martin and J. L. Morris, "Anti-shock garment in postpartum haemorrhage," *Best Practice & Research Clinical Obstetrics and Gynaecology,* vol. 22, no. 6, pp. 1057-1074, 2008.

[5] R. S. Ward, "Pressure Therapy for the Control of Hypertrophic Scar Formation after Burn Injury A History and Review," *Journal of Burn Care & Rehabilitation,* vol. 12, no. 3, pp. 257-262, 1991.

[6] B. S. Atiyeh, A. M. El Khatib and S. A. Dibo, "Pressure garment therapy (PGT) of burn scars: evidence-based efficacy," *Annals of Burns and Fire Disasters,* vol. 26, no. 4, pp. 205-212, 2013.

[7] R. Eisele, L. Kinzl and T. Koelsch, "Rapid-inflation intermittent pneumatic compression for prevention of deep venous thrombosis," *Journal of Bone and Joint Surgery,* vol. 89, no. 5, pp. 1050-1056, 2007.

[8] S. K. Kakkos, M. Griffin, G. Geroulakos and A. N. Nicolaides, "The efficacy of a new portable sequential compression device (SCD Express) in preventing venous stasis," *Journal of Vascular Surgery,* vol. 42, no. 2, pp. 296-303, 2005.

[9] S. K. Kakkos, G. Szendro, M. Griffin, S. S. Daskalopoulou and A. N. Nicolaides, "The efficacy of the new SCD response compression system in the prevention of venous stasis," *Journal of Vascular Surgery,* vol. 32, no. 5, pp. 932-940, 2000.

[10] N. Brophy-Williams, M. W. Driller, C. M. Shing, J. W. Fell and S. L. Halson, "Confounding compression: the effects of posture, sizing and garment type on measured interface pressure in sports compression clothing," *Journal of Sports Sciences,* vol. 33, no. 13, pp. 1403-1410, 2015.

[11] B. K. Doan, Y. H. Kwon, R. U. Newton, J. Shim, E. M. Popper, R. A. Rogers, L. R. Bolt, M. Robertson and W. J. Kraemer, "Evaluation of a lower-body compression garment," *Journal of Sports Sciences,* vol. 21, no. 8, pp. 601-610, 2003.

[12] N. Brophy-Williams, M. W. Driller, S. L. Halson, J. W. Fell and C. M. Shing, "Evaluating the Kikuhime pressure monitor for use with sports compression clothing," *Sports Engineering,* vol. 17, no. 1, pp. 55-60, 2014.

[13] K. W. Barazanji, K. S. Rattan and D. W. Repperger, "Design and analysis of a closed-loop controller for an anti-G suit," in *IEEE National Aerospace and Electronics Conference*, Dayton, 1988.

[14] K. S. Rattan and K. Barazanji, "Design of an optimum anti-G suit controller using an adaptive feedforward control scheme," in *IEEE National Aerospace and Electronics Conference*, Dayton, 1990.

[15] M. B. Stenger, A. K. Brown, S. M. Lee, J. P. Locke and S. H. Platts, "Gradient Compression Garments as a Countermeasure to Post-Spacefl ight Orthostatic Intolerance," *Aviation, Space, and Environmental Medicine,* vol. 81, no. 9, pp. 883-887, 2010.

[16] C. A. Latz, K. R. Brown and R. L. Bush, "Compression therapies for chronic venous leg ulcers: interventions and adherence," *Chronic Wound Care Management and Research,* vol. 2, pp. 11-21, 2015.

[17] J. J. Bergan, G. W. Schmid-Schönbein, P. D. Coleridge Smith, A. N. Nicolaides, M. R. Boisseau and B. Eklof, "Chronic Venous Disease," *New England Journal o f Medicine,* vol. 355, no. 3, pp. 488-498, 2006.

[18] S. C. Nicholls, "Sequelae of Untreated Venous Insufficiency," *Seminars in Interventional Radiology,* vol. 22, no. 3, pp. 162-168, 2005.

[19] C. Burrows, R. Miller, D. Townsend, R. Bellefontaine, G. MacKean, H. L. Orsted and D. H. Keast, "Best Practice Recommendations for the Prevention and Treatment of Venous Leg Ulcers: Update 2006," *Advances in Skin & Wound Care,* vol. 20, no. 11, pp. 611-621, 2007.

[20] K. Vowden and P. Vowden, "Effective compression therapy," *Wound Essentials,* vol. 7, no. 2, November 2012.

[21] A. A. Ramelet, "Compression Therapy," *Dermatologic Surgery,* vol. 28, no. 1, pp. 6-10, 2002.

[22] H. Partsch, *Understanding the pathophysiological effects of compression. From: EWMA Position Document; Understanding compression therapy,* London: Medical Education Partnership Ltd, 2003.

[23] "Principles of compression in venous disease: a practitioner's guide to treatment and prevention of venous leg ulcers," Wounds International, London, 2013.

[24] B. Kumar, J. Hu and N. Pan, "Memory Bandage for Functional Compression Management for Venous Ulcers," *Fibers,* vol. 4, no. 1, 2016.

[25] M. Clark, *Compression bandages: principles and definitions. From: EWMA Position Document; Understanding compression therapy,* London: Medical Education Partnership Ltd, 2003.

[26] H. Partsch, M. Clark, S. Bassez, J. P. Benigni, F. Becker, V. Blazek, J. Caprini, A. Cornu-Thénard, J. Hafner, M. Flour, M. Jünger, C. Moffatt and M. Neumann, "Measurement of Lower Leg Compression In Vivo: Recommendations for the Performance of Measurements of Interface Pressure and Stiffness," *Dermatologic Surgery,* vol. 32, no. 2, pp. 224-233, 2006.

[27] P. Flaud, S. Bassez and J. L. Counord, "Comparative In Vitro Study of Three Interface Pressure Sensors Used to Evaluate Medical Compression Hosiery," *Dermatologic Surgery,* vol. 36, no. 12, pp. 1930-1940, 2010.

[28] C. J. Evans, F. G. Fowkes, C. V. Ruckley and A. J. Lee, "Prevalence of varicose veins and chronic venous insufficiency in men and women in the general population: Edinburgh Vein Study," *Epidemiology and Community Health,* vol. 53, no. 3, pp. 149-153, 1999.

[29] R. T. Eberhardt and J. D. Raffetto, "Chronic Venous Insufficiency," *Circulation,* vol. 130, no. 4, pp. 333-346, 2014.

[30] I. C. Valencia, A. Falabella, R. S. Kirsner and W. H. Eaglstein, "Chronic venous insufficiency and venous leg ulceration," *Journal of the American Academy of Dermatology,* vol. 44, no. 3, pp. 401-424, 2001.

[31] R. Kolluri, "Compression Therapy for Treatment of Venous Disease and Limb Swelling," *Current Treatment Options in Cardiovascular Medicine,* vol. 13, pp. 169-178, 2011.

[32] T. Phillips, B. Stanton, A. Provan and R. Lew, "A study of the impact of leg ulcers on quality of life: financial, social, and psychologic implications," *Journal of the American Academy of Dermatology,* vol. 31, no. 1, pp. 49-53, 1994.

[33] C. V. Ruckley, "Socioeconomic Impact of Chronic Venous Insufficiency and Leg Ulcers," *Angiology,* vol. 48, no. 1, pp. 67-69, 1997.

[34] D. L. Lamping, S. Schroter, X. Kurz and S. R. Kahn, "Evaluation of outcomes in chronic venous disorders of the leg: Development of a scientifically rigorous, patient-reported measure of symptoms and quality of life," *Journal of Vascular Surgery,* vol. 37, no. 2, pp. 410-419, 2003.

[35] E. H. Friedberg, M. B. Harrison and I. D. Graham, "Current Home Care Expenditures for Persons with Leg Ulcers," *Journal of Wound, Ostomy and Continence Nursing ,* vol. 29, no. 4, pp. 186-192, 2002.

[36] M. McGuckin, R. Waterman, J. Brooks, G. Cherry, L. Portena, S. Hurley and M. D. Kerstein, "Validation of venous leg ulcer guidelines in the United States and United Kingdom," *The American Journal of Surgery,* vol. 183, no. 2, pp. 132-137, 2002.

[37] R. E. Klabunde, Cardiovascular Physiology Concepts, Baltimore: Lippincott Williams & Wilkins, 2012.

[38] L. B. Rowell, Human Cardiovascular Control, New York: Oxford University Press, 1993.

[39] W. F. Boron and E. L. Boulpaep, Medical physiology: a cellular and molecular approach, Philadelphia: Saunders Elsevier, 2012.

[40] D. E. Mohrman and L. J. Heller, Cardiovascular Physiology, New York: McGraw-Hill, Health Professions Division, 1997.

[41] H. Partsch, "Intermittent pneumatic compression in immobile patients," *International Wound Journal,* vol. 5, no. 3, pp. 389-397, 2008.

[42] B. H. Shaw and V. E. Claydon, "The relationship between orthostatic hypotension and falling in older adults," *Clinical Autonomic Research,* vol. 24, no. 1, pp. 3-13, 2014.

[43] R. Freeman, W. Wieling, F. B. Axelrod, D. G. Benditt, E. Benarroch, I. Biaggioni, W. P. Cheshire, T. Chelimsky, P. Cortelli, C. H. Gibbons, D. S. Goldstein, R. Hainsworth, M. J. Hilz, G. Jacob, H. Kaufmann, J. Jordan, L. A. Lipsitz, B. D. Levine, P. A. Low, C. Mathias, S. Raj, D. Robertson, P. Sandroni, I. J. Schatz, R. Schondorf, J. M. Stewart and J. G. van Dijk, "Consensus statement on the definition of orthostatic hypotension, neurally mediated syncope and the postural tachycardia syndrome," *Clinical Autonomic Research,* vol. 21, pp. 69-72, 2011.

[44] W. F. Ganong, Review of medical physiology, Los Altos: Lang Medical Publications, 1981.

[45] E. Stranden, "Edema in venous insufficiency," *Phlebolymphology,* vol. 18, no. 1, pp. 3-14, 2011.

[46] R. Hainsworth, "Pathophysiology of syncope," *Clinical Autonomic Research,* vol. 14, no. 1, pp. 18-24, 2004.

[47] J. L. Beebe-Dimmer, J. R. Pfeifer, J. S. Engle and D. Schottenfeld, "The Epidemiology of Chronic Venous Insufficiency and Varicose Veins," *Annals of Epidemiology,* vol. 15, no. 3, pp. 175-184, 2005.

[48] P. C. Alguire and B. M. Mathes, "Chronic venous insufficiency and venous ulceration," *Journal of General Internal Medicine,* vol. 12, no. 6, pp. 374-383, 1997.

[49] B. Kumar, A. Das and R. Alagirusamy, Science of Compression Bandages, New Delhi: Woodhead Publishing India, 2014.

[50] J. M. Stewart, "Common Syndromes of Orthostatic Intolerance," *Pediatrics,* vol. 131, no. 5, pp. 968-980, 2013.

[51] M. Helmi, A. Lima, D. Gommers, J. van Bommel and J. Bakker, "Inflatable external leg compression prevents orthostatic hypotension in a patient with a traumatic cervical spinal cord," *Future Cardiology,* vol. 9, no. 5, pp. 645-648, 2013.

[52] S. Houtman, J. J. Thielen, R. A. Binkhorst and M. T. Hopman, "Effect of a pulsating anti-gravity suit on peak exercise performance in individual with spinal cord injuries," *European Journal of Applied Physiology,* vol. 79, no. 2, pp. 202-204, 1999.

[53] D. Rimaud, C. Boissier and P. Calmels, "Evaluation of the Effects of Compression Stockings Using Venous Plethysmography in Persons With Spinal Cord Injury," *Journal of Spinal Cord Medicine,* vol. 31, no. 2, pp. 202-207, 2008.

[54] S. Surhoff, "Compression therapy in sport," *Phlebologie,* vol. 43, no. 3, pp. 144-147, 2014.

[55] B. J. Yates and I. A. Kerman, "Post-spaceflight orthostatic intolerance: possible relationship to microgravity-induced plasticity in the vestibular system," *Brain Research Reviews,* vol. 28, pp. 73-82, 1998.

[56] H. Partsch, "Compression for the management of venous leg ulcers: which material do we have?," *Phlebology,* vol. 29, no. 1, pp. 140-145, 2014.

[57] C. Moffatt, "Variability of pressure provided by sustained compression," *International Wound Journal,* vol. 5, no. 2, pp. 259-265, 2008.

[58] C. S. Lim and A. H. Davies, "Graduated compression stockings," *Canadian Medical Association Journal,* vol. 186, no. 10, pp. E391-E398, 2014.

[59] H. Partsch, "The Static Stiffness Index: A Simple Method to Assess the Elastic Property of Compression Material In Vivo," *Dermatologic Surgery,* vol. 31, no. 6, pp. 625-630, 2005.

[60] W. Marston and K. Vowden, *Compression therapy: a guide to safe practice. From: EWMA Position Document; Understanding compression therapy,* London: Medical Education Partnership Ltd, 2003.

[61] R. K. Spence and E. Cahall, "Inelastic versus elastic leg compression in chronic venous insufficiency: A comparison of limb size and venous hemodynamics," *Journal of Vascular Surgery,* vol. 24, no. 5, pp. 783-787, 1996.

[62] G. Mosti, V. Mattaliano and H. Partsch, "Inelastic compression increases venous ejection fraction more than elastic bandages in patients with superficial venous reflux," *Phlebplogy,* vol. 23, no. 6, pp. 287-294, 2008.

[63] S. O'Meara, N. Cullum, E. A. Nelson and J. C. Dumville, "Compression for venous leg ulcers," *Cochrane Database of Systematic Reviews,* vol. 1, 2009.

[64] H. Partsch, M. Clark, G. Mosti, E. Steinlechner, J. Schuren, M. Abel, J. P. Benigni, P. Smith, A. Cornu-Thénard, M. Flour, J. Hutchinson, J. Gamble, K. Issberner, M. Juenger, C. Moffatt, H. A. M. Neumann, E. Rabe, J. F. Uhl and S. Zimmet, "Classification of Compression Bandages: Practical Aspects," *Dermatologic Surgery,* vol. 34, no. 5, pp. 600-609, 2008.

[65] K. van der Wegen-Franken, B. Tank and M. Neumann, "Correlation between the static and dynamic stiffness indices of medical elastic compression stockings," *Dermatologic Surgery,* vol. 34, no. 11, pp. 1477-1485, 2008.

[66] World Union of Wound Healing Societies, *Principles of best practice: Compression in venous leg ulcers. A consensus document,* London: Medical Education Partnership Ltd, 2008.

[67] J. C. Mayberry, G. L. Moneta, R. D. DeFrang and P. J. M, "The influence of elastic compression stockings on deep venous hemodynamics," *Journal of Vascular Surgery ,* vol. 13, no. 1, pp. 99-100, 1991.

[68] G. Mosti, A. Cavezzi, H. Partsch, S. Urso and F. Campana, "Adjustable Velcro® Compression Devices are More Effective than Inelastic Bandages in Reducing Venous Edema in the Initial Treatment Phase: A Randomized Controlled Trial," *European Journal of Vascular and Endovascular Surgery,* vol. 50, no. 3, pp. 368-374, 2015.

[69] E. Flam, S. Berry, A. Coyle, H. Dardik and L. Raab, "Blood-flow augmentation of intermittent pneumatic compression systems used for prevention of deep vein thrombosis prior to surgery," *American Journal of Surgery,* vol. 171, no. 3, pp. 312-315, 1996.

[70] K. T. Delis, G. Slimani, H. M. Hafez and A. N. Nicolaides, "Enhancing Venous Outflow in the Lower Limb with Intermittent Pneumatic Compression. A Comparative Haemodynamic Analysis on the Effect of Foot vs. Calf vs. Foot and Calf Compression," *European Journal of Vascular and Endovascular Surgery,* vol. 19, pp. 250-260, 2000.

[71] M. Murakami, T. L. McDill, L. Cindrick-Pounds, D. B. Loran, K. J. Woodside, W. J. Mileski, G. C. Hunter and L. A. Killewich, "Deep venous thrombosis prophylaxis in trauma: Improved compliance with a novel miniaturized pneumatic compression device," *Journal of Vascular Surgery,* vol. 38, no. 5, pp. 923-927, 2003.

[72] R. J. Morris, "Intermittent pneumatic compression—systems and applications," *Journal of Medical Engineering & Technology,* vol. 32, no. 3, pp. 179-188, 2008.

[73] A. J. Comerota, "Intermittent pneumatic compression: Physiologic and clinical basis to improve management of venous leg ulcers," *Journal of Vascular Surgery,* vol. 53, no. 4, pp. 1121-1129, 2011.

[74] K. G. Harding, W. Vanscheidt, H. Partsch, J. A. Caprini and A. J. Comerota, "Adaptive compression therapy for venous leg ulcers: a clinically effective, patient-centred approach," *International Wound Journal,* vol. 13, no. 3, pp. 317-325, 2016.

[75] R. J. Damstra, E. R. Brouwer and H. Partsch, "Controlled, comparative study of relation between volume changes and interface pressure under short-stretch bandages in leg lymphedema patients," *Dermatologic Surgery,* vol. 34, no. 6, pp. 773-778, 2008.

[76] H. Partsch and G. Mosti, "Comparison of three portable instruments to measure compression pressure," *International Angiology,* vol. 29, no. 5, pp. 426-430, 2010.

[77] J. P. Bentley, Principles of measurement systems, Longman Scientific & Technical, 1988.

[78] A. Satpathy, S. Hayes and S. Dodds, "Is compression bandaging accurate? The routine use of interface pressure measurements in compression bandaging of venous leg ulcers," *Phlebology,* vol. 21, no. 1, pp. 36-40, 2006.

[79] "Interlink Electronics," March 2016. [Online]. Available: http://www.interlinkelectronics.com/datasheets/Datasheet_FSR.pdf.

[80] S. Pourazadi, S. Ahmadi and C. Menon, "Towards the development of active compression bandages using dielectric elastomer actuators," *Smart Materials and Structures,* vol. 23, no. 6, 2014.

[81] L. Vinckx, W. Boeckx and J. Berghmans, "Analysis of the pressure perturbation due to the introduction of a measuring probe under an elastic garment," *Medical and Biological Engineering and Computing,* vol. 28, no. 2, pp. 133-138, 1990.

[82] K. Tavakolian, G. A. Dumont, G. Houlton and A. P. Blaber, "Precordial vibrations provide noninvasive detection of early-stage hemorrhage," *Shock,* vol. 41, no. 2, pp. 91-96, 2014.

[83] J. J. Smith and J. P. Kampine, Circulatory physiology, the essentials, Baltimore: Williams & Wilkins, 1980.

[84] C. Hinojosa-Laborde, R. E. Shade, G. W. Muniz, C. Bauer, K. A. Goei, H. F. Pidcoke, K. K. Chung, A. P. Cap and V. A. Convertino, "Validation of lower body negative pressure as an experimental model of hemorrhage," *Journal of Applied Physiology,* vol. 116, no. 4, pp. 406-415, 2014.

[85] B. B. Hansen, R. Bouert, H. Bliddal, R. Christensen, T. Bendix, A. Christensen, J. Mehlsen, Z. Rasti and M. Boesen, "External pneumatic compression device prevents fainting in standing weight-bearing MRI: a cohort study," *Skeletal Radiology,* vol. 42, no. 10, pp. 1437-1442, 2013.

[86] W. Vanscheidt, A. Ukat and H. Partsch, "Dose-response of compression therapy for chronic venous edema—higher pressures are associated with greater volume reduction: Two randomized clinical studies," *Journal of Vascular Surgery,* vol. 49, no. 2, pp. 395-402, 2009.

[87] B. Partsch and H. Partsch, "Calf compression pressure required to achieve venous closure from supine to standing positions," *Journal of Vascular Surgery,* vol. 42, no. 4, pp. 734-738, 2005.

[88] J. M. Zanetti and K. Tavakolian, "Seismocardiography: Past, Present and Future," in *35th Annual International Conference of the IEEE Engineering in Medicine and Biology Society (EMBC)*, Osaka, 2013.

[89] W. H. Cooke, K. L. Ryan and V. A. Convertino, "Lower body negative pressure as a model to study progression to acute hemorrhagic shock in humans," *Journal of Applied Physiology,* vol. 96, no. 4, pp. 1249-1261, 2004.

[90] F. M. Melchior, R. S. Srinivasan, P. H. Thullier and J. M. Clère, "Simulation of cardiovascular response to lower body negative pressure from 0 to -40 mmHg," *Journal of Applied Physiology,* vol. 77, no. 2, pp. 630-640, 1994.

[91] C. M. Brown, M. Dütsch, M. J. Hecht, B. Neundörfer and M. J. Hilz, "Assessment of cerebrovascular and cardiovascular responses to lower body negative pressure as a test of cerebral autoregulation," *Journal of the Neurological Sciences,* vol. 208, pp. 71-78, 2003.

[92] G. de Simone and F. Pasanisi, "Systolic, diastolic and pulse pressure: pathophysiology," *Italian Heart Journal,* vol. 2, no. 4, pp. 359-362, 2001.

[93] V. E. Claydon, C. Schroeder, L. J. Norcliffe, J. Jordan and R. Hainsworth, "Water drinking improves orthostatic tolerance in patients with posturally related syncope," *Clinical Science,* vol. 110, no. 3, p. 343–352, 2006.

[94] C. Schroeder, V. E. Bush, L. J. Norcliffe, F. C. Luft, J. Tank, J. Jordan and R. Hainsworth, "Water Drinking Acutely Improves Orthostatic Tolerance in Healthy Subjects," *Circulation,* vol. 106, no. 22, pp. 2806-2811, 2002.

[95] T. Young, N. Connolly and J. Dissemond, "UrgoKTwo Compression Bandage System Made Easy," *Wounds International,* vol. 4, no. 1, 2013.

[96] S. S. Gale, F. Lurie, T. Treadwell, J. Vazquez, T. Carman, H. Partsch, O. Alvarez, D. Langemo, M. E. Posthauer, M. M. Wilkin and M. Bursztynski, "DOMINATE Wounds," *Wounds,* vol. 26, no. 1, pp. 1-12, 2014.

[97] R. A. Wilson, V. S. Bamrah, J. J. Lindsay, M. Schwaiger and J. Morganroth, "Diagnostic accuracy of seismocardiography compared with electrocardiography for the anatomic and physiologic diagnosis of coronary artery disease during exercise testing," *The American Journal of Cardiology,* vol. 71, no. 7, pp. 536-545, 1993.

[98] "Patient Care," SUNY Upstate Medical University, [Online]. Available: http://www.upstate.edu/surgery/healthcare/vascular/cvi.php. [Accessed 16 January 2017].

[99] OpenStax College, "Anatomy & Physiology," OpenStax College, [Online]. Available: http://cnx.org/contents/A4QcTJ6a@3/Blood-Flow-Blood-Pressure-and-. [Accessed 16 January 2017].

[100] Blausen.com, "Medical gallery of Blausen Medical 2014," *WikiJournal of Medicine,* vol. 1, no. 2, 2014.

[101] KingaNBM, "Medical bandage," 21 October 2015. [Online]. Available: https://commons.wikimedia.org/wiki/File:Bandage,_1940s,_First_aid,_second_world_war,_medical_tools.JPG. [Accessed 16 January 2017].

[102] F. C. Müller, "Compression stocking," 26 January 2013. [Online]. Available: https://commons.wikimedia.org/wiki/File:Stuetzstrumpf_03_(fcm).jpg. [Accessed 16 January 2017].

[103] "ACTitouch® Adaptive Compression Therapy System," Tactile Medical, [Online]. Available: http://www.tactilemedical.com/products/actitouch/. [Accessed 16 January 2017].

[104] "Venowave," [Online]. Available: http://venowave.com/. [Accessed 16 January 2017].

[105] CVTC, "Treating Vein Disease," [Online]. Available: http://www.cvtc.net/swollen-and-achy-legs/. [Accessed 16 January 2017].

[106] "Adjustable velcro bandage," [Online]. Available: https://commons.wikimedia.org/wiki/File:Adaptive_Klettbandage_mit_Fu%C3%9Fteil.jpg. [Accessed 16 January 2017].

[107] "Pneumatic Compression Pumps," [Online]. Available: http://encompasshealthcare.com/wound-care-treatment/compression-therapies/pneumatic-compression-pumps/. [Accessed 16 January 2017].

[108] ArjoHuntleigh, "Vascular therapy," [Online]. Available: http://www.arjohuntleigh.com/products/vascular-therapy/. [Accessed 16 January 2017].

[109] InnovaMed Health LLC. [Online]. Available: http://www.innovamedhealth.com/overview/. [Accessed 16 January 2017].

[110] Caremate, "Sphygmomanometer," 21 April 2012. [Online]. Available: https://commons.wikimedia.org/wiki/File:CM-3410-3420.jpg. [Accessed 16 January 2017].

Appendix A.

Mechanical Drawing of Housing[1]

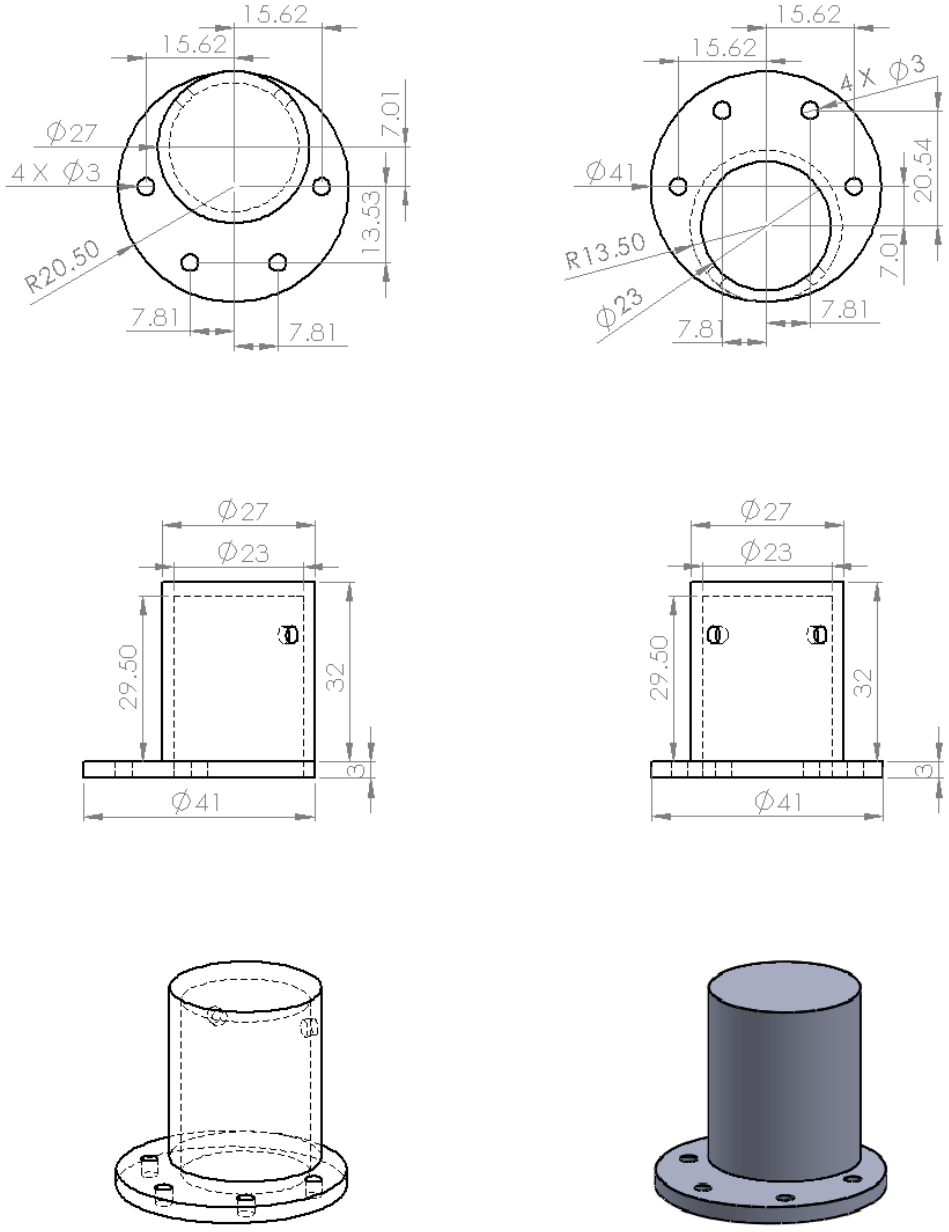

[1] All dimensions are in millimeters.

Appendix B.

Mechanical Drawing of Spool[1]

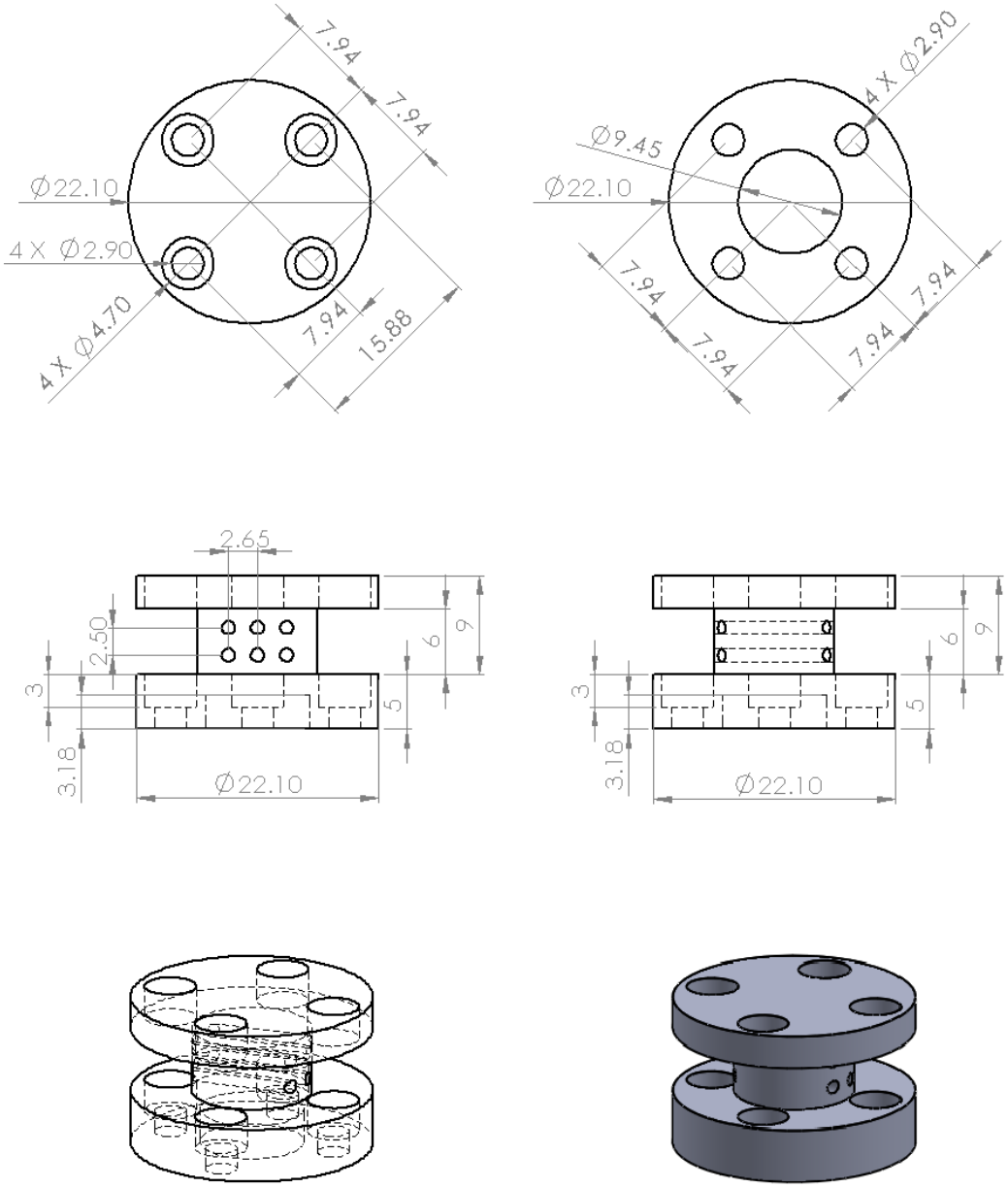

[1] All dimensions are in millimeters.